DECEMBER 2020
BONUS ISSUE

CEP

Chemical Engineering Progress

An **AIChE** Publication

aiche.org/cep

THINKING ABOUT CLIMATE

CEP
DECEMBER 2020 BONUS ISSUE
THINKING ABOUT CLIMATE
VOL.116/NO.13

Precious Metals
Edelmetale
Metale te cmuar
Qiymətli Metallar
Metal preziatuak
Dragoceni metali
Metalls preciosos
Bililhon nga Mga Metals
Zitsulo Zamtengo Wapatali
贵金属
Metalli Preziosi
Dragocjeni metali
Drahé kovy
Værdifulde metaller
Kostbare metalen
Altvaloraj Metaloj
Väärismetallid
Mahalagang Metals
Jalometallit
Métaux Précieux
Edelmetalen
Metais preciosos
Edelmetalle
Metali presye
Karfe mai daraja
Nā Metala kūpono
Lub Neej Zoo Nkauj
Nemesfémek
Dýrmæt málm
Alsdị ọla dị oké ọnụ ahịa
Logam Berharga
Metalli preziosi
貴金属
Metals Logam
귀금속
Metayên hêja
nobilis metalli
Dārgmetāli
Taurieji metalai
Metaly sarobidy
Logam Berharga
Metalli prezzjużi
Metara Raraemi
Edelmetaller
Drogocenne metale
Metais preciosos
Metale prețioase
O Metotia Taua
Meatailtean luachmhor
Metali ea Bohlokoa
Metals anokosha
Drahé kovy
Plemenite kovine
Birta Qaaliga ah
Metales preciosos
Logam lumayan
Vyuma vya Thamani
Ädelmetaller
Değerli Metaller

sabin METAL CORPORATION
Refining • Precious Metals • Recycling

It doesn't matter what you know, until you know what matters.

Sustainability

Platinum Group Metals (PGMs) remain at the forefront, the absolute cutting edge, of Conservation, Energy Production and World Health, and demand for PGMs is expected to increase for decades to come.

Sabin Metal Corp. is dedicated to recycling and refining these valuable metals from industrial by-products and wastes efficiently and sustainably, returning the maximum amount of these assets to our clients for industrial re-use.

If you'd like to learn more about sustainability at Sabin, or any Precious Metal matters, please visit our PM 101 section at sabinmetal.com.

SABIN METAL CORPORATION 75TH ANNIVERSARY 1945-2020

Chemical Engineering Progress
An AIChE Publication
CEP
aiche.org/cep

THINKING ABOUT CLIMATE

December 2020 Bonus Issue • Vol. 116 No. 13

CEP (Publication Number 101-920) (Print ISSN 0360-7275, Online ISSN 1945-0710) is published monthly by the American Institute of Chemical Engineers (AIChE), 120 Wall St., 23rd Floor, New York, NY 10005. All correspondence should be sent to the Editor-in-Chief at the address above, or by email to emilyp@aiche.org. ■ The statements and opinions in this magazine reflect the views of the contributors and not of AIChE, which assumes no responsibility for them. ■ Subscription rates for nonmembers: North America $228/yr; International $410/yr (air service included). Back issues are available from AIChE Customer Service (1-800-AIChemE). Individual copies: AIChE members $25 (plus postage outside North America), Nonmembers $35 (plus postage outside North America). ■ Claims for missing issues must be filed with AIChE Customer Service (customerservice@aiche.org) within three months by North American subscribers, six months by international subscribers. Claims made after that may be fulfilled as supplies permit. ■ Periodicals postage paid at New York, NY, and additional mailing offices.

Postmaster: Please send changes of address to AIChE, 120 Wall Street, 23rd Floor, New York, NY 10005. ■ Return Undeliverable Canadian Addresses to: P.O. Box 1632, Windsor, ON N9A 7C9 ■ Copying restriction and permissions: AIChE authorizes the photocopying of individual articles from CEP for the personal use of nonmembers by libraries and other users registered with the Copyright Clearance Center (CCC) Transactional Reporting Service, provided that a fee of $30 per article is paid directly to CCC, 222 Rosewood Dr., Danvers, MA 01923. Fee code: 0360-7275/00 $30. This consent does not extend to other kinds of copying, such as that for purposes of general distribution, for advertising or promotion, for creating new collective works, or for resale. To request permission, go to www.aiche.org/permissions. ■ To purchase an electronic reprint of an article published after 2001, contact Karen Simpson at kares@aiche.org. ■ Each issue of CEP is indexed regularly by Engineering Village and Applied Science & Technology Index.

institute for **sustainability**
An AIChE Technological Community

AIChE's Institute for Sustainability (IfS) is a member-driven organization that aids in pushing the sustainability profession forward, engaging the community, and defining excellence across the field. With an IfS membership, you have access to resources that will help you be a key partner in driving change.

MEMBER BENEFITS

Technical Resources
Keep apprised of new developments in the chemical engineering profession through our *CEP* magazine, AIChExchange and SmartBrief electronic newsletters, as well as Journals published in partnership with Wiley.

Exclusive Technical Content
Access scientific and technical opportunities and research for sustainability discussions. IfS approaches sustainability from the perspectives of engineering and scientific disciplines to promote the societal, economic, and environmental benefits of sustainable and green engineering. Topics within IfS to interact with:

- Alternative/Renewable Energy
- Circular Economy
- Food-Energy-Water Nexus
- Plastic Lifecycle Management
- Resilience and Adaptation
- Sustainable Development
- Sustainability Education
- Water Initiatives
- Waste Management

Conferences
Get the lowest rates on future conference registrations (both virtual and in-person).

Education
Build new technical knowledge and skills through live and archived webinars, credentials as well as self-paced eLearning courses.

Advance Your Career
Whether you are actively searching or just researching possibilities, CareerEngineer is the leading e-recruitment source for chemical engineers at every level, in every field.

AIChE Engage
Cultivate meaningful professional relationships through AIChE Engage, the mobile-friendly community discussion platform.

Students – funding opportunities
Get all the up-to-date information on Grants and Sponsorship Opportunities to support your registration to present at any of the IfS conferences. Take part in the next dedicated Poster and Short Talk Session to network with leading professionals in your field of study.

Join IfS at aiche.org/ifs

CEP Chemical Engineering Progress

AIChE The Global Home of Chemical Engineers
120 WALL STREET
NEW YORK, NY
10005
aiche.org

Thinking About Climate

I think about climate often. It's hard not to — I doubt a day goes by that I don't see an article, news report, or email that mentions climate.

The most recent item to cross my desk is an article in *Scientific American* entitled "Second Scientists' Warning: The Climate Emergency: 2020 in Review." It is a follow-up to "World Scientists' Warning of a Climate Emergency," by William J. Ripple *et al.*, which appeared in the January 2020 issue of *BioScience*. The authors begin their original article with this statement: "Scientists have a moral obligation to clearly warn humanity of any catastrophic threat and to 'tell it like it is.' On the basis of this obligation …, we declare, with more than 11,000 scientist signatories from around the world, clearly and unequivocally that planet Earth is facing a climate emergency." They then call for transformative change in six areas: energy, short-lived air pollutants, nature, food, economy, and population.

The new article points out that while 2020 brought a few promising developments, we still "need a massive-scale mobilization to address the climate crisis." The authors say that "aggressive transformative change, if framed holistically and equitably, will accelerate broad-based restorative action and avert the worst of the climate emergency. The survival of our society as we know it depends upon this unprecedented change."

Chemical engineers have an important role to play in achieving the necessary transformative change. Climate change is a complex, multidimensional problem that we are well equipped to understand. Our education in chemistry, physics, and math enables us to understand the science, and our knowledge of chemical engineering allows us to address the challenge in a practical and economical manner. But sorting through and keeping up with the climate change literature is a monumental task.

A few years ago, I came up with the idea for a series of short, 1–3-page articles that would explore various chemical-engineering-related aspects of climate and climate change. I thought that breaking this complex subject into many small bits and focusing on chemical engineering concepts would make it easier to understand. I envisioned that the title of this series would be "Thinking About Climate."

When I mentioned my idea to Mark Holtzapple, a professor of chemical engineering at Texas A&M Univ., he told me about his interest in climate and shared with me the slides of a lecture that he gives on the topic. He also helped me realize that we could not do justice to the topic 2,000 words at a time. He liked my idea of looking at climate through a chemical engineering lens, and he offered to write a series of articles that addressed observations, modeling, impacts, and solutions.

This special issue of *CEP* is the fruit of our collaboration. It provides basic information about climate — including numerous figures and reference citations. It is not meant to be a definitive treatment of the subject. Rather, it is intended to provide an overview that helps you to think about climate without getting lost in the claims and counterclaims.

In the interest of minimizing our environmental footprint, we present this as a digital-only issue. And because this topic is of such great importance to society, we are making the issue open access. Please share it widely.

Cynthia F. Mascone, Editor-in-Chief

Setting the Stage to Discuss Climate Change

Mark Holtzapple ▪ Texas A&M Univ.

Let's start our exploration with a look at climate in the public eye — from early scientific reports to energy companies' positions to the treatment of climate change in film.

The World Health Organization (WHO) calls climate change one of the greatest challenges of our time *(1)*. A joint statement signed by 11 national academies of science from major nations states that "there is now strong evidence that significant global warming is occurring. … It is likely that most of the warming in recent decades can be attributed to human activities. … This warming has already led to changes in the Earth's climate" *(2)*. The report states that carbon dioxide emissions — primarily from the combustion of fossil fuels — are responsible for the majority of global warming.

The Global Change Research Act of 1990 mandates that the U.S. government periodically assess the impact of climate change on the U.S. In 2017, the Fourth National Climate Assessment was completed by 13 federal agencies *(3)*. Key findings of that assessment include:

• From 1901 to 2016, global surface air temperatures have increased by about 1.0°C and are now the warmest in the history of modern civilization.

• It is extremely likely that human activities are the dominant cause of the observed warming; there is no convincing alternative explanation.

• Global atmospheric carbon dioxide concentration is now over 400 ppm, a level that last occurred about 3 million years ago, when both global average temperature and sea level were significantly higher than they are today.

• The Earth is warming, which increases the risk of unanticipated changes and impacts, some of which are potentially large and irreversible.

Numerous studies support the often-cited statistic that 97% of climate scientists believe that humans are causing global warming *(4)*, yet a minority of climate scientists from respected universities, including MIT and Georgia Tech, disagree with the scientific consensus *(5)*.

Sorting through the claims and counterclaims about climate change (see sidebar) takes hours and hours, but who has time? If we are not willing to invest the time, should we simply accept the authorities' position? Which authorities should we believe?

For many years, the Pew Research Center has been conducting polls to assess public response to climate change. Interested readers are encouraged to explore the complete survey results, which are available at pewresearch.org. Figures 1–3 highlight a few interesting results from recent polls. Americans report a lower level of concern about climate change than residents of other countries (Figure 1) *(6)*. Concern over global warming has increased over time (Figure 2), but that concern is much greater among Democrats than Republicans (Figure 3) *(7)*.

Climate change is a complex issue that chemical engineers are well equipped to understand. Our education in chemistry, physics, and math enables us to understand the science, and our knowledge of chemical engineering allows us to address the issue in a practical and economical manner.

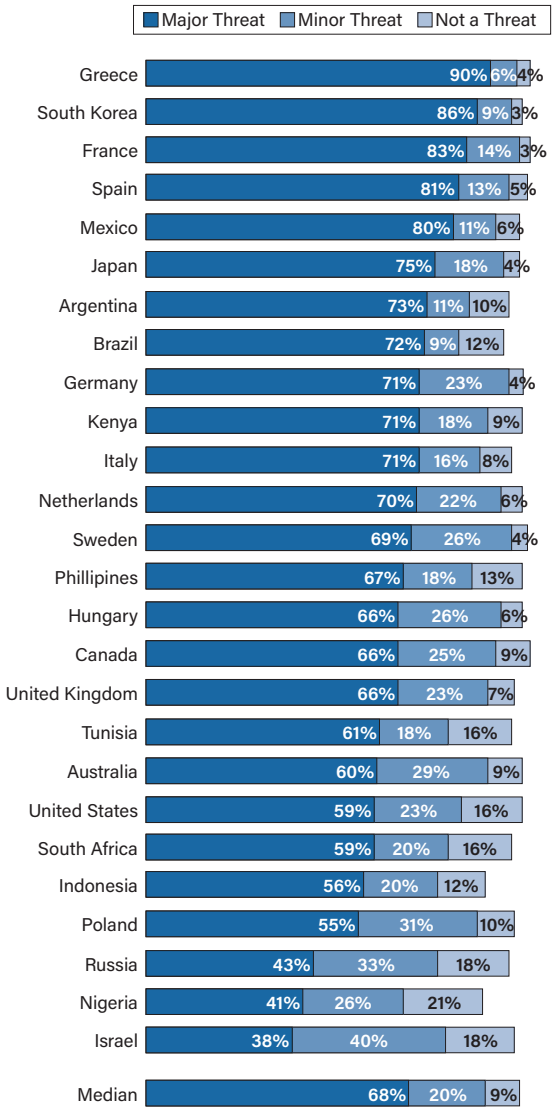

▲ **Figure 1.** Respondents to a Pew Research Center poll (taken in Spring 2018) believe that global climate change is a threat to their country. Source: *(6)*.

Climate Change: Separating Fact from Fiction

A Google keyword search for "climate change hoax" returns hundreds of thousands of results, with numerous arguments, such as:

- The climate has always changed.
- Carbon dioxide is a vital nutrient needed for plants to grow, so adding more is beneficial.
- During the Paleocene era, the earth was much warmer than today.
- Yes, the earth is warming, but it is a natural cycle not caused by humans.
- Global warming is caused by varying solar output.
- In the past, carbon dioxide concentrations were much higher than today, but temperatures were lower.
- Volcanoes release much more carbon dioxide than human activity.
- Global warming will be beneficial.
- Climate models are unreliable.
- There has not been any global warming since 1998.
- The "climategate" scandal disproved global warming.
- Meteorologists cannot predict the weather next week, so they certainly cannot predict the climate 50 years from now.
- Carbon dioxide is too dilute to affect the climate.
- The atmosphere is saturated with carbon dioxide; adding more cannot cause additional warming.

In 2007, Australian cognitive scientist John Cook started the blog *Skeptical Science* to respond to skeptics of human-caused climate change. Scientific responses dispelling nearly 200 climate change and global warming myths raised by skeptics are presented at skepticalscience.com/argument.php. The website has input from many experts and provides much information at beginner, intermediate, and advanced levels. The website posts numerous graphs and tables extracted from the scientific literature and has direct links to papers, making it easy for visitors to read the original scientific literature.

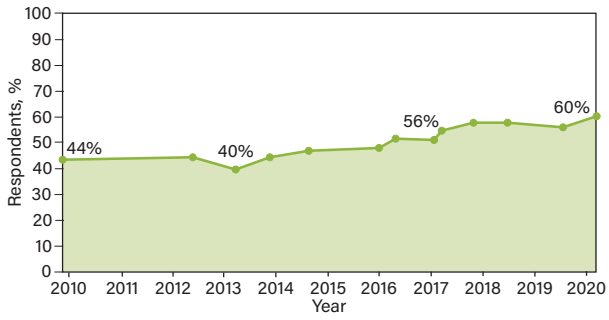

▲ **Figure 2.** According to Pew Reserch Center polling, the percentage of U.S. adults who say global climate change is a major threat to the well-being of the U.S. continues to increase. Source: *(7)*.

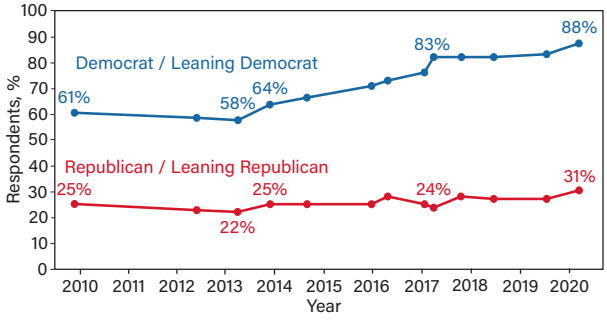

▲ **Figure 3.** The belief that global climate change is a major threat to the well-being of the U.S. is more prevalent among Democrats than Republicans, according to Pew Research Center polling. Source: *(7)*.

This special issue of *CEP* is intended to provide you with basic information about climate change so that you can assess the issue for yourself. It is not meant to be a definitive treatment of the subject. Rather, it is intended to provide an overview that equips you to investigate the subject on your own without getting lost in the claims and counterclaims.

To set the stage, this first article provides an overview of the early scientific reports about global warming and climate change, a few of the international agreements aimed at reducing greenhouse gas (GHG) emissions, public statements made by energy and insurance companies, concerns about the impacts of climate change on the military, and Pope Francis's encyclical on climate change. It also takes a look at the depiction of climate change in film.

Defining key terms

In 1907, English scientist John Henry Poynting coined the term *greenhouse effect* to describe atmospheric heating caused by transmission of short-wavelength solar radiation through the earth's atmosphere and absorption of exiting long-wavelength infrared radiation *(8)*. Although the actual heating mechanism for a greenhouse is different from that of the atmosphere, this simplistic analogy is commonly employed.

In 1956, Gilbert Plass used the term *climatic change* to describe long-term changes in Earth's climate (*e.g.,* melting glaciers, ocean acidification, extreme weather) caused by the greenhouse effect *(9)*.

In 1975, Wallace Broecker used the term *global warming* to describe the increase in average global atmospheric temperature caused by increasing carbon dioxide concentrations *(10)*.

Climate refers to long-term environmental conditions (*e.g.,* temperature, air pressure, humidity, precipitation, sunshine, cloudiness, and winds) on the global scale, whereas *weather* refers to short-term environmental conditions on a local scale.

▲ **Figure 4.** The Mauna Loa Observatory in Hawaii has been measuring the composition of the earth's atmosphere since 1958. Photo by John Bortniak, NOAA.

The scientific history

Because it is discussed so frequently in the news, it is easy to get the impression that global warming is a new topic. In actuality, science has a long history of investigating global warming, including studies by many famous scientists.

In 1827, French physicist and mathematician Joseph Fourier published his observations that the atmosphere readily passes visible light, which heats the Earth's surface upon absorption. The energy is subsequently re-emitted as infrared radiation in accordance with Planck's law *(11)*. Furthermore, Fourier recognized that the atmosphere does not readily transmit infrared radiation, which causes the Earth's surface temperature to be warmer than if there were no atmosphere.

In 1856, Eunice Newton Foote — the second female member of the Association for the Advancement of Science (AAAS) — reported the results of experiments in which she investigated the impact of water vapor and carbon dioxide on the heating of air by the sun *(12)*.

In 1872, British scientist John Tyndall published his measurements of infrared absorption by methane, carbon dioxide, and water *(13)*.

In 1897, Swedish scientist Svante Arrhenius published a paper on the impact of atmospheric water vapor and carbon dioxide on global temperature. He estimated that doubling atmospheric carbon dioxide would increase global temperature by 5–6°C *(14)*.

In 1900, Knut Ångström described an experiment in which infrared radiation passed through a 30-cm tube filled with carbon dioxide. The amount of CO_2 in the tube was only about 12% of the CO_2 found in an equivalent-diameter column of air that reaches from the Earth's surface to the upper atmosphere *(15)*. He reported that the infrared radiation was fully absorbed even when the pressure decreased by a third. His results supported the view that Earth's atmosphere is "saturated" with CO_2, meaning the atmosphere fully blocks infrared radiation and that adding more CO_2 to the atmosphere could not increase global temperature. He concluded that Arrhenius must be wrong.

In 1956, physicist Gilbert Plass published a paper showing that the lower layers of the atmosphere are saturated, as suggested by Ångström, but the upper layers are not *(16)*. Using the latest spectroscopic measurements of low-pressure cold CO_2 taken for the military, he showed that the final radiation emissions that cool the earth occur in the uppermost atmosphere. There, water vapor (a potent greenhouse gas) is negligible and the concentration of CO_2 is much more impactful. He calculated that doubling the CO_2 concentration would raise global temperatures by 3.6°C, which is similar to the modern consensus of about 3°C.

In 1958, chemist Charles David Keeling started

measuring atmospheric gas compositions from his laboratory (Figure 4) on Mauna Loa, a Hawaiian volcano. Surrounded by ocean and free of foliage, this location — isolated from confounding effects — is ideal for taking atmospheric measurements.

In 1965, the President's Science Advisory Committee, which was commissioned by Lyndon Johnson, concluded that the greenhouse effect is a "real concern" *(17)*.

In 1981, James Hansen published results of a climate model in *Science (18)*. He used one-dimensional and three-dimensional modeling and described climate sensitivity, feedbacks (*e.g.,* water vapor, clouds, albedo), effects of solar and volcanic events, uncertainties related to aerosols, and ocean uptake of thermal energy. A commentary on that paper published in 2012 pointed out the close agreement between the predictions of Hansen's model and observed global mean temperatures *(19)*.

In 1984, Exxon scientists Brian Flannery and Andrew Callegari, with Martin Hoffert of New York Univ., published a model showing impacts on climate from changes in CO_2 concentration and solar output *(20)*. This was one of numerous studies on climate change published by Exxon scientists.

In 1988, the United Nations (UN) and the World Meteorological Organization established the Intergovernmental Panel on Climate Change (IPCC) to create a clear scientific view of climate change that could be used by policymakers. The IPCC is currently in its sixth assessment cycle and is scheduled to release the AR6 Synthesis Report in 2022. Previous reports describe the probability that human activity is causing global warming (Table 1).

In 1988, James Hansen testified before Congress and raised public awareness of climate change. He started his career studying radiative transfer in Venus' atmosphere (Figure 5), but later he applied this knowledge to Earth's atmosphere. From 1981 to 2013, he served as head of the NASA Goddard Institute for Space Studies.

International agreements

Since 1995, the UN has held annual meetings — Conferences of the Parties (COP) — to discuss climate change. Some notable highlights include:

COP3 was held in Kyoto, Japan, in 1997 and produced the Kyoto Protocol, which required reductions in GHG emissions from developed countries. Developing nations, which had contributed little to GHG emissions, were exempt from the GHG reduction requirement. To help countries meet their emission targets, the Kyoto Protocol contains flexibility mechanisms such as carbon trading. An Adaptation Fund was established to finance projects in developing countries to adapt to climate change.

During the first commitment period (2008 to 2012), 36 industrialized countries participated. Collectively, these participating countries produced 24% of global GHG emissions in 2010. Although they committed to reduce GHG emissions to an average of 4% below 1990 levels by 2012, they actually reduced emission by 24% below 1990 levels — exceeding their target emission reductions by 2.4×10^9 metric tons (m.t.) CO_2 equivalents (CO2e) per year. Nine of the countries achieved their targets using the flexibility mechanisms *(21)*.

COP18, held in Doha, Qatar, in 2012, extended the Kyoto Protocol by establishing the second commitment period (2012 to 2020). The countries participating in this second commitment period are responsible for only about 15% of global GHG emissions. It does not include many developed nations that opted out of the agreement (*e.g.,* U.S. and Canada), and it excludes developing nations that are major emitters (*e.g.,* China, India, and Brazil).

COP21 was held in Paris, France, in 2015. The resulting Paris Agreement established a goal to limit global temperature increase to 2°C above preindustrial levels, which is considered an achievable temperature rise with moderate environmental impact. For example, at this temperature increase, ocean levels are expected to rise a few feet — which will cause flooding in coastal cities in the U.S. and necessitate migrations from low-lying regions of Bangladesh, India, and Vietnam. Because of pressure from low-lying island states, the agreement includes language to pursue efforts to limit the temperature increase to 1.5°C.

Unlike the Kyoto Protocol, signatories are not committed to specific emissions nor are there penalties for failing to meet goals. Instead, the agreement describes methods for

Table 1. With each successive report, the Intergovernmental Panel on Climate Change (IPCC) reports with greater confidence that human activity causes global warming.

Year	IPCC Report	Degree of Confidence
1995	Second Assessment Report	50%
2001	Third Assessment Report	66%
2007	Fourth Assessment Report	90%
2013	Fifth Assessment Report	95%

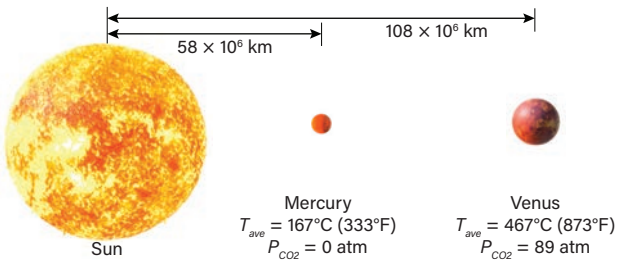

▲ **Figure 5.** Venus is twice as far from the sun as Mercury, but its temperature is much higher because its atmosphere contains a large amount of carbon dioxide.

quantifying emissions and employs a "name-and-shame" system of enforcement. Emission reductions are expected to occur after 2020, when the second commitment period of the Kyoto Protocol expires. Furthermore, the agreement includes a provision to transfer $100 billion per year to developing countries to help them develop renewable energy sources and adapt to the effects of climate change.

On Earth Day (April 22) 2016 in New York, 174 countries and the European Union signed the agreement. On Sept. 3, 2016, the Obama administration agreed to the Paris Accord, which entered into force on Nov. 4, 2016. On June 1, 2017, the Trump administration withdrew the U.S, and that withdrawal took effect on Nov. 4, 2020. Currently, the Paris Agreement has 188 party nations. President-Elect Joseph R. Biden has announced his intention to rejoin the accord, although as this article is being prepared, no specific timetable has been given.

The European Union's energy directive specifies the following legally binding targets for renewable energy as a percentage of total energy demand: 20% by 2020 and 32% by 2030 *(22)*.

Energy industry statements

Numerous energy companies have official positions stating their concern about global warming and climate change. For example:

• *BP:* "The world is not on a sustainable path and needs a rapid transition to lower carbon energy in order to meet the goals of the Paris Agreement" *(23)*.

• *Chevron:* "We proactively consider climate change in our business decisions" *(24)*.

• *ExxonMobil:* "We believe that climate change risks warrant action and it's going to take all of us — business, governments, and consumers — to make meaningful progress" *(25)*.

• *Shell:* "Our lives depend on energy wherever we live. But in order to prosper while tackling climate change, society needs to provide much more energy for a growing global population while finding ways to emit much less CO_2" *(26)*.

In May 2015, six major European energy giants (BG Group, BP, Eni, Shell, Statoil, and Total) sent a joint letter to the UN *(27)* calling on governments to introduce carbon pricing systems and to create an international framework that could connect national systems. The signatories state that climate change is a critical challenge for the world, and "for us to do more, we need governments across the world to provide us with clear, stable, long-term ambitious policy frameworks. … We believe that a price on carbon should be a key element of these frameworks."

Although ExxonMobil was not a signatory to this letter, it also states that a carbon price is needed. "… ExxonMobil believes a revenue-neutral carbon tax would be a more effective policy option than cap-and-trade schemes, regulations, mandates, or standards. A properly designed carbon tax can be predictable, transparent, and comparatively simple to understand and implement" *(28)*.

There is no consensus on the size of the carbon tax; however, ExxonMobil often mentions $80/m.t. carbon dioxide *(29)*. This carbon price corresponds to about $34/bbl oil and about $4/MMBtu of natural gas.

In May 2017, a majority (62.3%) of ExxonMobil shareholders passed a nonbinding resolution that the company prepare open and detailed analyses of risks posed by climate change *(30)*. Their concern is that company valuation may decline should oil and gas reserves become unmarketable if governments pass legislation that constrains the use of fossil fuels.

Major energy companies (*e.g.,* ExxonMobil, Shell, Total, BP) are founding members of the Climate Leader-

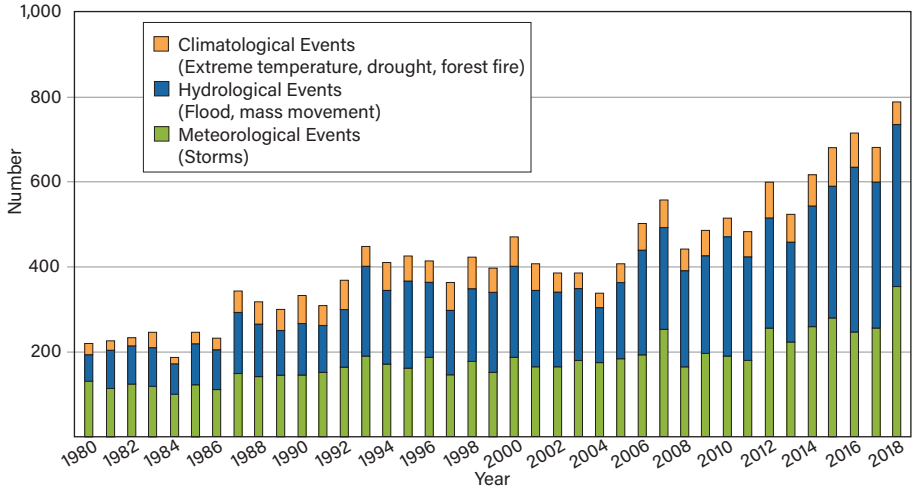

▶ **Figure 6.** Global weather-related natural catastrophes continue to increase. (Counted events had at least one fatality and/or produced normalized economic losses greater than $100,000, $300,000, $1 million, or $3 million, depending on the assigned World Bank income group of the affected country.) Source: *(34);* data from Munich Re, Geo Risks Research, NatCatSERVICE.

ship Council (clcouncil.org), an organization that supports a carbon tax as a means for addressing climate change.

Recently, Shell released its Sky report, which outlines possible scenarios for meeting the objectives of the Paris Agreement (COP21) through carbon pricing, hydrogen fuel, electric cars, biofuels, higher efficiency standards, carbon-neutral energy (*e.g.,* solar, wind, nuclear), replacing coal with natural gas, carbon capture, and reforestation *(31)*.

The Oil and Gas Climate Initiative (oilandgasclimate-initiative.com) is a CEO-led consortium that represents major international energy companies that collectively produce 30% of global oil and gas. Their objective is to accelerate industry response to climate change by explicitly supporting the Paris Agreement and its goals.

In 2012, industry consultant PricewaterhouseCoopers prepared a report entitled *PwC Low Carbon Economy Index*, which contained the following statements *(32)*:

• "Governments' ambitions to limit warming to 2°C appear highly unrealistic."

• "Now one thing is clear: businesses, governments, and communities across the world need to plan for a warming world — not just 2°C, but 4°C, or even 6°C."

• "Any investment in long-term assets or infrastructure, particularly in coastal or low-lying regions, needs to address more pessimistic scenarios."

• "Sectors dependent on food, water, energy, or ecosystem services need to scrutinize the resilience and viability of their supply chains."

• "…business-as-usual is not an option."

Insurance industry perspectives

The insurance industry is directly impacted by increased economic losses from climate change. Mark Carney, Governor of the Bank of England, states that "over time, the adverse effects of climate change could threaten economic resilience and financial stability. Insurers are currently at the forefront" *(33)*.

The insurance industry is concerned about the climate risk protection gap, *i.e.,* the growing difference between total economic losses and insured losses attributed to climate change. ClimateWise (cisl.cam.ac.uk/business-action/sustainable-finance/climatewise) is a consortium of 29 major insurance companies that helps the industry address the climate challenge.

Swiss Re is a leading wholesale provider of reinsurance and other insurance products. It has been studying the impact of climate change on the insurance industry for the past 20 years. The Insurance Information Institute reports that the number of global weather-related natural catastrophes since 1980 (Figure 6) and the economic impacts of those events (Figure 7) are growing *(34)*.

Several leading insurance companies have issued statements on climate change:

• *Allianz:* "Our climate change strategy and our environmental management help us in anticipating climate risks, caring for the climate-vulnerable, and enabling a low-carbon economy …" *(35)*.

• *Allstate:* "The increased frequency and severity of weather events and natural catastrophes affect the cost and number of claims submitted by our customers … Our success depends, in part, on our ability to properly model, price, and manage climate-related risks, as well as develop products and services to address climate change" *(36)*.

• *Lloyds:* "The threats posed by climate change, unclean air, water scarcity, and related food insecurity are already well documented. For example, disruptions to the production and delivery of goods and services due to environmental disasters are up by 29% since 2012" *(37)*.

Mott MacDonald and the Global Sustainability Institute estimate that within 20 years, $200 billion/yr of investment

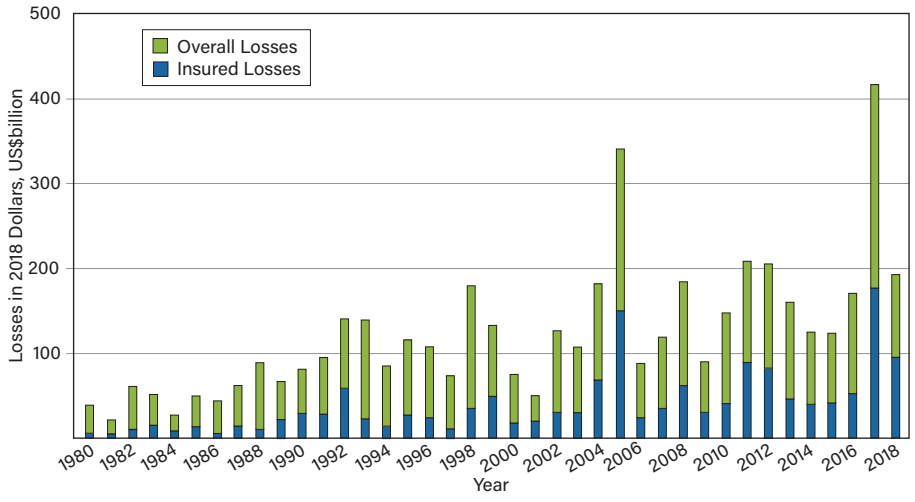

◀ **Figure 7.** Global economic losses from weather-related natural catastrophes include a significant portion of uninsured losses. (Inflation-adjusted losses are based on country-specific consumer price indexes and exchange rates to U.S. dollars.) Source: *(34);* data from Munich Re, Geo Risks Research, NatCatSERVICE.

will be required to address losses from climate change *(38)*.

Congress established the National Flood Insurance Program (NFIP) in 1968 because flood insurance was not profitable for private insurers. Currently, the program has a $20.5 billion deficit *(39)*. CoreLogic estimates that 6.9 million homes along the Atlantic and Gulf coasts are at risk of damage from hurricane storm surge — homes that could cost more than $1.6 trillion to replace *(40)*. Should NFIP be privatized, insurance premiums are likely to be so high that development in flood-prone regions will be prohibitively expensive *(41)*.

Military concerns

The Center for Climate and Security (CCS; climateandsecurity.org) is a nonpartisan policy institute comprising security and military experts who focus on the intersection of climate and security. Its analysis indicates that climate change impacts the U.S. military in several ways:

- many military facilities are located along the coast and are at risk from flooding events
- the military is mobilized to help the U.S. populace recover from flooding events
- disruptions to food and water cause mass migrations that exacerbate global conflicts.

The military considers climate change a threat multiplier — *i.e.,* it can exacerbate political instability in unstable regions.

Ahead of the COP21 negotiations in Paris in 2015, the NATO Parliamentary Assembly passed a resolution urging countries to make ambitious commitments to tackling climate change and encouraging NATO to do more on the issue. The resolution states that "climate change-related risks are significant threat multipliers that will shape the security environment in areas of concern to the Alliance and have the potential to significantly affect NATO planning and operations" *(42)*.

Pope Francis's encyclical

In May 2015, about seven months before the Paris climate talks, Pope Francis released his second encyclical, entitled *Laudato si* ("Praise be to you") and subtitled "On Care for our Common Home" *(43)*. After consulting with Hans Joachim Schellnhuber (Director of the Potsdam Institute for Climate Impact Research), the pope fully accepts the scientific consensus that climate change is predominantly caused by human activity and states that "climate change is a global problem with grave implications: environmental, social, economic, political, and for the distribution of goods. It represents one of the principal challenges facing humanity in our day." He is particularly concerned with social justice and that the brunt of the impacts of climate change will be felt by the poor, who did little to create the problem and do not have the resources to respond.

The pope counsels society to develop technologies that serve humanity rather than simply produce a short-term profit: "We have the freedom needed to limit and direct technology; we can put it at the service of another type of progress, one which is healthier, more human, more social, more integral."

He even presents short- and long-term strategies for supplying our energy needs: "We know that technology based on the use of highly polluting fossil fuels — especially coal, but also oil and, to a lesser degree, gas — needs to be progressively replaced without delay. Until greater progress is made in developing widely accessible sources of renewable energy, it is legitimate to choose the less harmful alternative or to find short-term solutions."

Climate change in cinema

Climate change has been popularized in movies — documentaries as well as fictional films.

- *The Unchained Goddess*. In 1958, chemical engineer Frank Capra — famous for *It's a Wonderful Life* — produced a documentary film on weather and global warming for the Bell Telephone Science Hour.
- *Soylent Green.* This 1973 science fiction thriller is set in a future (2022) dystopia in which the planet is severely damaged from global warming and can no longer supply food via conventional means. Instead, food such as Soylent Green is supplied from "novel" sources. The movie starred prominent actors Charlton Heston and Edward G. Robinson.
- *Waterworld.* This 1995 movie, and notable box-office flop, featured an earth that is underwater because polar ice caps have melted and very little land remains. Some humans mutate by growing fins and gills that allow them to adapt to their new environment.
- *The Day After Tomorrow.* In 2004, this science fiction disaster film depicted disruptions to the North Atlantic

Ocean circulation caused by climate change. Because warm tropical water no longer circulated to northern latitudes, New York City was thrust into a catastrophic cooling event.

• *An Inconvenient Truth*. Former Vice President Al Gore starred in this 2006 documentary, which included scenes from his public lectures, to describe climate science to the lay public.

• *The 11th Hour.* Leonardo DiCaprio's 2007 documentary explained global environment problems and potential solutions.

• *Chasing Ice*. National Geographic photographer James Balog recorded the multiyear loss of glaciers in this 2012 documentary.

• *Snowpiercer.* This 2013 Korean science fiction movie takes place on a frozen Earth after a climate engineering experiment that attempted to address global warming failed.

• *Merchants of Doubt.* In 2014, the book of the same name was translated into a documentary that showed the parallels between the global warming controversy and earlier controversies (*e.g.,* the link between tobacco smoking and cancer) where contrarian media consultants and representatives are hired by commercial interests to purposely spread doubt even when scientific consensus is strong.

• *Before the Flood.* Another Leonardo DiCaprio documentary, this 2016 film reexamines global warming and its potential impacts on the planet.

• *An Inconvenient Sequel: Truth to Power*. Al Gore stars in this 2017 sequel documentary, which describes efforts to persuade governmental leaders to invest in renewable energy.

• *Chasing Coral.* This 2017 video documented the bleaching of coral from climate change.

• *Downsizing.* Matt Damon starred in this 2017 science fiction movie, in which a portion of humanity decides to shrink themselves to just a few inches tall to reduce their consumption of resources and thereby address climate change.

• *Geostorm.* This 2017 science fiction adventure film featured a satellite designer who tried to correct malfunctioning climate-controlling satellites that are threatening the world with major floods.

Closing thoughts

Among climate scientists, there is strong consensus (97%) that human activity is causing climate change *(4)*. The UN has responded by forming the IPCC, which summarizes scientific understanding and helps coordinate government response through protocols and accords. The pope has responded by emphasizing the moral component of the problem. The energy and insurance industries are working on strategies to minimize the impact of climate change on their profitability. The military views climate change as a threat multiplier and includes it in their security planning. And through cinema, global warming and climate change have entered popular culture.

Concern over climate change varies strongly with political affiliation, gender, and age. With each passing year, public concern over climate change increases.

To limit potential negative impacts — such as extreme weather events or coastal flooding — 36 countries successfully implemented the Kyoto Protocol, which limited CO_2 emissions to 24% below 1990 levels. The most recent international agreement to address climate change is the Paris Agreement (COP 21), which has 188 party nations and entered into force on Nov. 4, 2016.

In the future, the industries served by chemical engineers are likely to be subjected to regulations that restrict or penalize carbon dioxide emissions. Chemical engineers have the intellectual skills to respond to these challenges. Therefore, it is incumbent on us to educate ourselves about climate change so we can adapt and help shape a sustainable future. CEP

Acknowledgments

The author is grateful for the suggestions provided by John Nielsen-Gammon, Regents Professor of Texas A&M Univ. and Texas State Climatologist, and Liz Fisher, a chemical engineer with Citizens Climate Lobby.

Literature Cited

1. **Chan, M.,** "Message from WHO Director-General," who.int/world-health-day/dg_message/en (accessed Sept. 7, 2020).
2. "Joint Science Academies' Statement: Global Response to Climate Change," nationalacademies.org/documents/link/LF5F46A0F4D8D3765F6DBFFA9DD3EA606B9CCD57CD98/file/DD545DB2BB17731A876DF838087FC19943CADEE27AFA (2005).
3. **Wuebbles, D. J., *et al.,* eds.,** "Climate Science Special Report: Fourth National Climate Assessment (NCA4), Vol. I," U.S. Global Change Research Program, Washington, DC, doi: 10.7930/J0J964J6, science2017.globalchange.gov (2017).
4. **Cook, J., *et al.,*** "Consensus on Consensus: A Synthesis of Consensus Estimates on Human-Caused Global Warming," *Environmental Research Letters,* **11** (4), 048002 (Apr. 2016).
5. **Barnham, J. A.,** "The Top 15 Climate-Change Scientists: Consensus and Skeptics," TheBestSchools.org, thebestschools.org/features/top-climate-change-scientists (Mar. 23, 2020).
6. **Fagan, M., and C. Huang,** "A Look at How People around the World View Climate Change," Pew Research Center, pewresearch.org/fact-tank/2019/04/18/a-look-at-how-people-around-the-world-view-climate-change (Apr. 18, 2019).

Literature Cited continues on next page

Literature Cited (continued)

7. **Kennedy, B.,** "U.S. Concern About Climate Change is Rising, But Mainly Among Democrats," Pew Research Center, pewresearch.org/fact-tank/2020/04/16/u-s-concern-about-climate-change-is-rising-but-mainly-among-democrats (Apr. 16, 2020).
8. **Easterbrook, S.,** "Who First Coined the Term 'Greenhouse Effect'?," *Serendipity,* easterbrook.ca/steve/2015/08/who-first-coined-the-term-greenhouse-effect (Aug. 18, 2020).
9. **Plass, G.,** "The Carbon Dioxide Theory of Climatic Change," *Tellus,* **8** (2), pp. 140–154 (1956).
10. **Broecker, W. S.,** "Climatic Change: Are We on the Brink of a Pronounced Global Warming?," *Science,* **189** (4201), pp. 460–463 (Aug. 8, 1975).
11. **Fourier, J.-B. J.,** "Mémoire sur les Températures du Globe Terrestre et des Espaces Planétaires," *Mémoires d l'Académie Royale des Sciences de l'Institute de France,* VII, pp. 569–604 (1827).
12. **Foote, E.,** "Circumstances Affecting the Heat of the Sun's Rays," *The American Journal of Science and Arts,* **22** (66), pp. 383–384 (Nov. 1856).
13. **Tyndall, J.,** "Contribution to Molecular Physics in the Domain of Radiant Heat," Longmans, Green, and Co., London, U.K. (1872).
14. **Arrhenius, S.,** "On the Influence of Carbonic Acid in the Air upon the Temperature of the Earth," *Publications of the Astronomical Society of the Pacific*, **9** (54), pp.14–24 (1897).
15. **Ångström, K.,** "Ueber die Bedeutung des Wasserdampfes und der Kohlensäure bei der Absorption der Erdatmosphäre" *Annalen der Physik*, **308** (12), pp. 720–732 (1900).
16. **Plass, G. N.,** "Infrared Radiation in the Atmosphere," *American Journal of Physics,* **24** (5), pp. 303–321 (1956).
17. **President's Science Advisory Committee, Environmental Pollution Panel,** "Restoring the Quality of our Environment," The White House, Washington, DC (Nov. 1965).
18. **Hansen, J., *et al.,*** "Climate Impact of Increasing Atmospheric Carbon Dioxide," *Science*, **213** (4511), pp. 957–966 (Aug. 28, 1981).
19. **van Oldenborgh, G. J., and R. Haarsma,** "Evaluating a 1981 Temperature Projection," RealClimate, realclimate.org/index.php/archives/2012/04/evaluating-a-1981-temperature-projection (Apr. 2, 2012).
20. **Flannery, B. P., *et al.,*** "Energy Balance Models Incorporating Evaporative Buffering of Equatorial Thermal Response," in Hansen, J. E., and T. Takahashi, eds., "Climate Processes and Climate Sensitivity," *Geophysical Monograph Series,* Vol. 29, pp. 108–117 (Jan. 1984).
21. **Shishlov, I., *et al.,*** Compliance of the Parties to the Kyoto Protocol in the First Commitment Period, *Climate Policy*, **16** (6), pp. 768–782 (2016).
22. **European Commission,** "Renewable Energy Directive," ec.europa.eu/energy/topics/renewable-energy/renewable-energy-directive/overview_en (July 16, 2014, updated Aug. 4, 2020).
23. **BP,** "Climate Change and the Energy Transition," bp.com/en/global/corporate/sustainability/climate-change.html (accessed Sept. 7, 2020).
24. **Chevron,** "We Proactively Consider Climate Change in Our Business Decisions," chevron.com/corporate-responsibility/climate-change (accessed Sept. 7, 2020).
25. **ExxonMobil,** "Climate Change," corporate.exxonmobil.com/en/current-issues/climate-policy/climate-perspectives/our-position (accessed Sept. 7, 2020).
26. **Shell,** "Climate Change and Energy Transitions," shell.com/sustainability/environment/climate-change.html (accessed Sept. 7, 2020).
27. **Shell,** "Oil and Gas Majors Call for Carbon Pricing," shell.com/media/news-and-media-releases/2015/oil-and-gas-majors-call-for-carbon-pricing.html (June 1, 2015).
28. **Union of Concerned Scientists,** "The Climate Accountability Scorecard, Appendix: Supporting Fair and Effective Climate Policies," ucsusa.org/sites/default/files/attach/2016/10/climate-accountability-scorecard-appendix-fair-effective-climate-policies.pdf (Oct. 2016).
29. **Institute for Energy Research,** "Exxon Forecasts Growth in Global Energy Demand," instituteforenergyresearch.org/analysis/exxon-forecasts-growth-in-global-energy-demand (Jan. 3, 2014).
30. **Cardwell, D.,** "Exxon Mobil Shareholders Demand Accounting of Climate Change Policy Risks," *The New York Times,* nytimes.com/2017/05/31/business/energy-environment/exxon-shareholders-climate-change.html (May 31, 2017).
31. **Shell,** "Shell Scenarios: Sky, Meeting the Goals of the Paris Agreement," shell.com/promos/business-customers-promos/download-latest-scenario-sky/_jcr_content.stream/1530643931055/eca19f7fc-0d20adbe830d3b0b27bcc9ef72198f5/shell-scenario-sky.pdf (2018).
32. **Johnson, L.,** "Too Late for Two Degrees? Low Carbon Economy Index 2012," PwC, pwc.com/gx/en/sustainability/publications/low-carbon-economy-index/assets/pwc-low-carbon-economy-index-2012.pdf (2012).
33. **Johns, M., *et al.,*** "Closing the Protection Gap: ClimateWise Principles Independent Review 2016," Univ. of Cambridge Institute for Sustainability Leadership (Dec. 2016).
34. **Insurance Information Institute,** "Facts + Statistics: Global Catastrophes," iii.org/fact-statistic/facts-statistics-global-catastrophes (accessed Sept. 7, 2020).
35. **Allianz,** "Climate Change," allianz.com/en/sustainability/low-carbon-economy/climate-change.html (accessed Sept. 7, 2020).
36. **Allstate,** "Sustainability Report," allstatesustainability.com/wp-content/uploads/materials/downloads/Allstate_ClimateChangeStatement2018.pdf (accessed Sept. 7, 2020).
37. **Lloyd's,** "ClimateWise," lloyds.com/lloyds/corporate-responsibility/environment/climatewise (accessed Sept. 7, 2020).
38. **Jones, A.,** "Climate Change and Business Survival: The Need for Innovation in Delivering Climate Resilience," Mott MacDonald and the Global Sustainability Institute, mottmac.com/download/file/127/6772/climate change and business survival.pdf (June 2015).
39. **Congressional Research Service,** "Introduction to the National Flood Insurance Program (NFIP)," fas.org/sgp/crs/homesec/R44593.pdf (updated Dec. 23, 2019).
40. **CoreLogic,** "CoreLogic Report Finds 6.9 Million Homes at Risk of Hurricane Storm Surge Damage with $1.6 Trillion in Potential Reconstruction Costs at Stake," corelogic.com/news/corelogic-report-finds-6.9-million-homes-at-risk-of-hurricane-storm-surge-damage-with-1.6-trillion-in-potential-reconstruction.aspx (May 31, 2018).
41. **Kowitt, B.,** "Climate Change Is About to Remake the Insurance Industry," *Fortune,* fortune.com/2017/07/25/climate-change-insurance-industry (July 25, 2017).
42. **Fetzek, S.,** "The Alliance in a Changing Climate: Bolstering the NATO Mission Through Climate Preparedness," *Briefer,* No. 37, climateandsecurity.files.wordpress.com/2012/04/the-alliance-in-a-changing-climate_bolstering-the-nato-mission-through-climate-preparedness_briefer-37.pdf (May 22, 2017).
43. **Francis,** "Encyclical Letter, Laudato Si′, of the Holy Father Francis on Care for Our Common Home," w2.vatican.va/content/francesco/en/encyclicals/documents/papa-francesco_20150524_enciclica-laudato-si.html (May 24, 2015).

AIChE ACADEMY

Coming Soon

Climate Change & Carbon Management eLearning Course

Learn proven techniques and methodologies for identifying the reward and reputation opportunities that come from carbon mitigation, including new revenue sources and improved standing among prospective employees, shareholders, stakeholders, and society. Discover the most credible ways to approach carbon management.

What You'll Learn:

- **Assess** the impact of climate change on your organization's upstream and downstream supply chain
- **Apply** lessons learned from other organizations that are addressing these impacts
- **Establish** and continually improve a credible carbon accounting system for your organization
- **Build** a business case for a scalable carbon mitigation program with achievable targets consistent with the Fourth National Climate Assessment

Climate Change and Carbon Management

Source: Institute for Sustainability (IfS)

Course ID: ELA123
Skill Level: Intermediate
Type: eLearning
Duration: 5 hours
CEUs: .5
PDHs: 5.0

Who Should Attend:
Any professional with an interest in systems thinking will benefit from this course, whether they have little or no experience in or knowledge of climate change.

This course may be taken as part of the AIChE Credential for Sustainability Professionals (ACSP).

aiche.org/academy | academy@aiche.org

institute for sustainability
An AIChE Technological Community

AIChE INSTITUTE FOR LEARNING & INNOVATION

Climate Observations

Mark Holtzapple ▪ Texas A&M Univ.

This article focuses on observations of phenomena that impact the climate, including energy, greenhouse gases, and temperature.

The Earth is a complex system involving chemical and physical interactions driven by the flow of energy. In this regard, the Earth is like a chemical plant (Figure 1) and chemical engineers can use their skills to understand processes that impact the Earth and result in climate change.

This article examines observations of phenomena that affect the climate, including energy, greenhouse gases (GHGs), and temperature. It does not address modeling of the underlying phenomena, which is covered in Part 3 of this special issue.

Energy flows

The temperature of deep space is 2.73 K, which is determined by measuring the cosmic microwave background *(1)*. The wavelength distribution of this background radiation exactly matches that of a blackbody radiator at that temperature.

▲ **Figure 1.** The Earth can be thought of as a process, with inputs and outputs.

The core temperature of the sun is estimated to be 15,710,000 K *(2)*. Through fusion nuclear reactions, matter is destroyed at a rate of 4.260×10^9 kg/sec. According to Einstein's mass-energy equivalence equation $E = mc^2$, energy is produced at a rate of 3.828×10^{26} W. Through conduction, convection, and radiation, this energy flows to the surface of the sun. Because the sun is surrounded by a vacuum, conduction and convection can no longer operate, so radiation is the only heat-transfer mechanism for the sun's energy. Solar radiant energy is emitted with a spectrum that closely corresponds to that of a blackbody radiator at 5,772 K.

The average distance from the sun to the Earth is 1 astronomical unit (1 AU = 149,597,870,700 m). At this

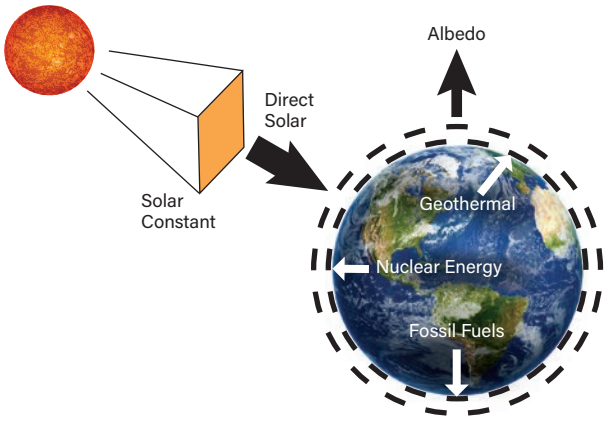

▲ **Figure 2.** Solar irradiation is the largest contributor to the Earth's energy flows.

distance, the surface area of a sphere is 2.812×10^{23} m^2 and the solar energy flux through the sphere is 1,361 W/m^2, which is referred to as the solar constant or the total solar irradiance (Figure 2).

Is the solar constant actually constant? As shown in Figure 3 *(3),* the solar constant is not exactly constant; it varies slightly during the solar cycle, which has a period of about 11 years. Data in Figure 3 for the years after and including 1978 are based on direct satellite observations. The pre-1978 data are based on a solar model that used sunspots as the measured variable. The number of sunspots observed within a month strongly correlates with solar output and serves as a proxy. Since 1610, solar astronomers have observed and recorded sunspots, so solar output can be known with a fair degree of certainty from that point onward. The period from 1645 to 1715 is known as the Maunder Minimum or the prolonged sunspot minimum.

The satellite data in Figure 3 show three completed solar cycles and part of a fourth. During the three completed cycles, the average solar constant is essentially unchanged (1,361.1 W/m^2) and the peak-to-valley difference is about 1.1 W/m^2.

When the solar energy flux hits the Earth, it is intercepted by the projected area of the Earth, a nearly circular

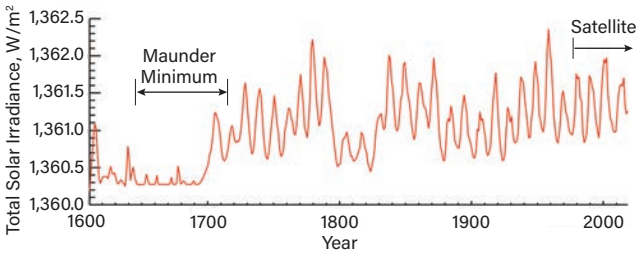

▲ **Figure 3.** The solar constant, or total solar irradiance, varies during the solar cycle, with a period of about 11 years. Source: *(3).*

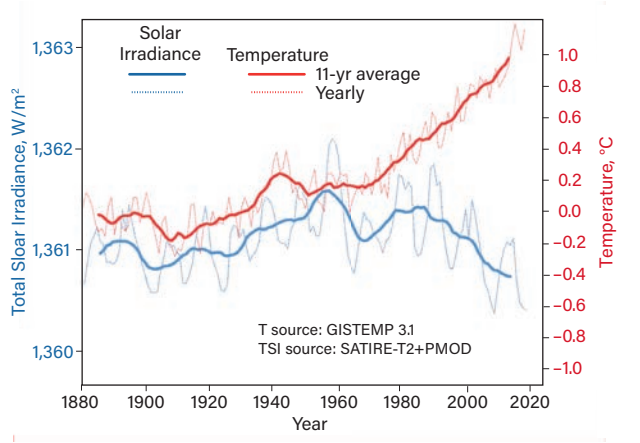

▲ **Figure 4.** Since 1960, average global temperature (red) and total solar irradiance (blue) are anticorrelated. Source: *(4).*

disk (with an area $A = \pi r^2$). As the Earth rotates, this intercepted solar energy is distributed over the Earth's surface, essentially a sphere (with a surface area $A = 4\pi r^2$). Based on these considerations, the average solar energy input to the Earth's surface is one-fourth the solar constant (340.3 W/m^2) with a peak-to-valley difference of 0.28 W/m^2.

Figure 4 *(4)* shows the historical (1880–2020) total solar irradiance and change in average global surface temperature. Until 1960, the datasets were well correlated — as total solar irradiance increased, average global temperature increased as well. This is expected because total solar irradiance is well recognized as a climate forcing. A climate forcing, as defined by the United Nations Intergovernmental Panel on Climate Change (IPCC), is "an externally imposed perturbation in the radiative energy budget of the Earth climate system, *e.g.,* through changes in solar radiation, changes in the Earth albedo, or changes in atmospheric gases and aerosol particles."

However, after 1960, average global temperature and total solar irradiance are anticorrelated — *i.e.,* as total solar irradiance decreased, average global temperature increased. Clearly, total solar irradiance is not the sole climate forcing; other factors are also important.

Earth's energy balance. Table 1 *(3, 5–9)* shows that the solar energy intercepted by Earth (173,500 TW) is by far the dominant energy flow. Geothermal energy (47 TW), which results primarily from the natural fission of radioactive elements in the Earth, is small. Direct heat released from combustion of fossil fuels (14.8 TW) and nuclear fission reactors (1.18 TW) is even smaller.

Not all of the solar energy that intercepts the Earth is absorbed; instead, much of it is reflected. Bond albedo (or simply albedo) is the fraction of shortwave solar energy — at all frequencies and angles incident on an astronomical body — that is scattered into space. The average albedo of the moon is 0.11 and the average albedo

Table 1. Solar energy is the largest component of the Earth's energy balance.

	Power, TW	Reference
Direct Solar[a]	173,500	*(3)*
Albedo[b]	−53,091	*(5)*
Geothermal	47	*(6)*
Nuclear Energy[c]	1.18	*(7, 8)*
Fossil Fuels[d]	14.8	*(9)*
Total	120,472	—

a. Direct solar = 1,361 W/m^2(π)(6,371,000 m)^2 TW/10^{12}W = 173,500 TW

b. Albedo = 0.306 × 173,500 TW = 53,091 TW

c. Nuclear = 390,000 MWe (1/0.33) = 1,180,000 MWt

d. Fossil fuels = 130,000 TWh/yr × (1 yr/8,760 hr) = 14.8 TW

of Earth is 0.306 *(5)*. The albedo of the Earth depends on the surface materials and the amount and kind of clouds (Figure 5) *(10)*. Fresh snow is particularly reflective. As Arctic sea ice (albedo ≈ 0.7) melts, it is replaced by water (albedo ≈ 0.08). Because water is less reflective, the Arctic temperature is greatly affected by the quantity of sea ice.

NASA's Clouds and the Earth's Radiant Energy System (CERES) provides satellite data for the Earth. Figure 6 presents changes in shortwave radiant energy reflected from Earth. Figure 6a shows that the clear-sky flux has decreased by about 1.2 W/m^2 since 2000, while Figure 6b shows that the all-sky flux, which includes the effects of clouds, has decreased by about 1.7 W/m^2 over the same period. These decreases suggest that a larger fraction of the incident solar radiation is absorbed by the Earth, which leads to greater warming.

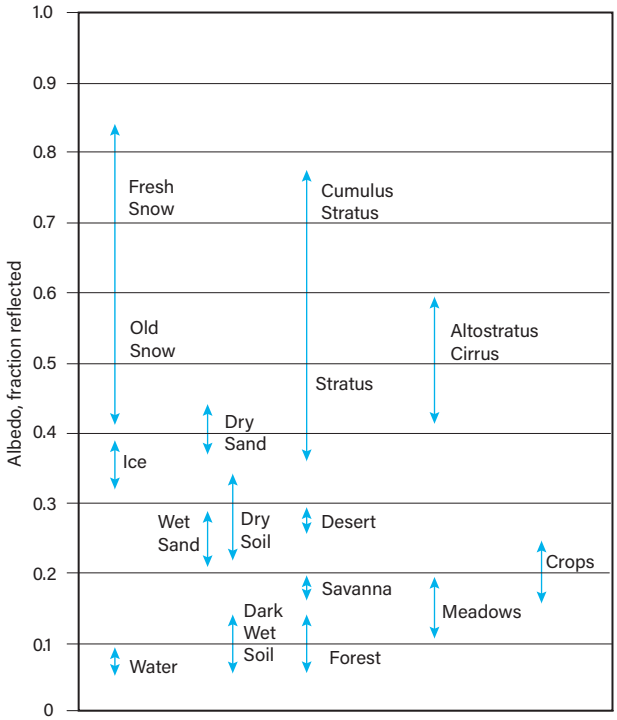

▲ **Figure 5.** The albedo of the Earth depends on the materials covering the surface and the cloud cover in the atmosphere. Source: *(10)*.

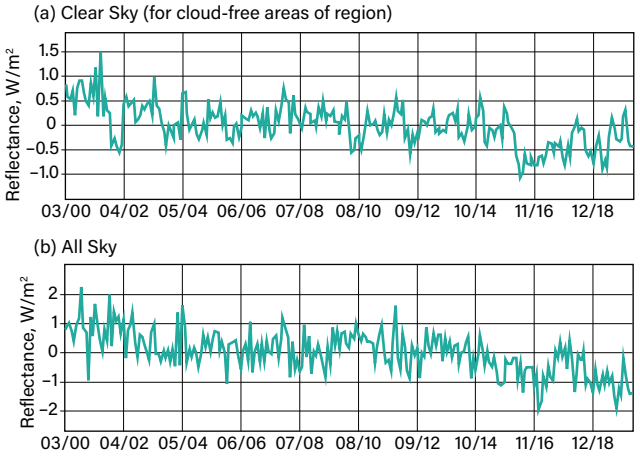

▲ **Figure 6.** Top-of-atmosphere (TOA) reflectance of shortwave radiation from Earth has decreased since 2000. Source: Doelling, D. R., CERES, NASA, based on ceres.larc.nasa.gov.

Table 2. Common greenhouse gases found in the Earth's atmosphere *(11)*.

Gas	Pre-1750 Tropospheric Concentration	Recent Tropospheric Concentration	Global Warming Potential (100-yr horizon)	Atmospheric Lifetime	Increased Radiative Forcing
Carbon Dioxide (CO_2)	~280 ppm	399.5 ppm	1	~100–300 yr	1.94 W/m^2
Methane (CH_4)	722 ppb	1,834 ppb	28	12.4 yr	0.50 W/m^2
Nitrous Oxide (N_2O)	270 ppb	328 ppb	265	121 yr	0.20 W/m^2
Tropospheric Ozone (O_3)	—	—	N/A	hours-days	0.40 W/m^2
CFC-11 (CCl_3F)	0	232 ppt	4,660	45 yr	0.060 W/m^2
CFC-12 (CCl_2F_2)	0	516 ppt	10,200	100 yr	0.166 W/m^2
CFC-113 (CCl_2CClF_2)	0	72 ppt	5,820	85 yr	0.022 W/m^2
HCFC-22 ($CHClF_2$)	0	233 ppt	1,760	11.9 yr	0.049 W/m^2
HCFC-141b (CH_3CCl_2F)	0	24 ppt	782	9.2 yr	0.0039 W/m^2
HCFC-142b (CH_3CClF_2)	0	22 ppt	1,980	17.2 yr	0.0041 W/m^2
Halon 1211 ($CBrClF_2$)	0	3.6 ppt	1,750	16 yr	0.0010 W/m^2
Halon 1301 ($CBrClF_3$)	0	3.3 ppt	6,290	65 yr	0.0010 W/m^2
HFC-134a (CH_2FCF_3)	0	84 ppt	1,300	13.4 yr	0.0134 W/m^2
Carbon tetrachloride (CCl_4)	0	82 ppt	1,730	26 yr	0.0140 W/m^2
Sulfur hexafluoride (SF_6)	0	8.6 ppt	23,500	3,200 yr	0.0049 W/m^2
Total					3.3793 W/m^2

Greenhouse gases

Greenhouse gases are transparent to most shortwave radiation, but they absorb and emit longwave (infrared) radiation. Table 2 *(11)* lists the most common GHGs. The second column presents the natural preindustrial concentrations of these gases in the atmosphere, whereas the third column lists today's concentrations. The global warming potential (Column 4) characterizes the impact of a given mass of gas released into the atmosphere relative to the impact of carbon dioxide, the reference gas. For example, over a 100-yr time horizon, 1 kg of methane has the same impact as 28 kg of carbon dioxide. The last two columns indicate the persistence of each gas in the atmosphere and the increased radiative forcing caused by the gas at modern concentrations compared to preindustrial concentrations.

The most impactful GHG, which is not shown in Table 2, is water vapor. Its concentration in the atmosphere varies greatly depending on temperature and the local presence of water (*e.g.,* desert vs. ocean). In addition, water vapor readily condenses, forming clouds that can yield rain, hail, or snow, all of which interact with climate in a more complex manner than the gases listed in Table 2. For these reasons, it is not possible to assign a single radiative forcing value to water vapor. Furthermore, because water vapor pressure is determined by surface temperature, it affects climate as a feedback mechanism that interacts in a different manner than the other gases.

Of the gases listed in Table 2, carbon dioxide has the greatest radiative forcing (1.94 W/m^2). Most carbon dioxide emissions into the atmosphere are produced by the combustion of fossil fuels, which transfers carbon that was previously stored below the Earth's surface to the atmosphere. In modern times, about 10% of carbon dioxide emissions result from changes in land use. For example, as rainforest is burned to clear land for agriculture, carbon that was previously sequestered in the wood is released to the atmosphere.

Carbon emissions. Figure 7 *(9)* plots the historical global consumption of coal, oil, and natural gas. Figure 8 *(12)* breaks down the historical carbon dioxide emissions by region of the world.

Before 1850, the emissions were virtually indistinguishable from zero, so prior to 1850 may be viewed as preindustrial. Since 1980, emissions from China have increased greatly as it has industrialized. During this same time, emissions from the U.S. have remained roughly constant even though real gross domestic product (GDP) increased by about 2.6 times *(13),* in large part due to improvements in energy efficiency, a shift from coal to less-carbon-intense natural gas, and a shift from a manufacturing economy to a service economy. During this same time, Europe has significantly reduced its carbon dioxide emissions as it embraces renewable energy. For example, Germany now produces

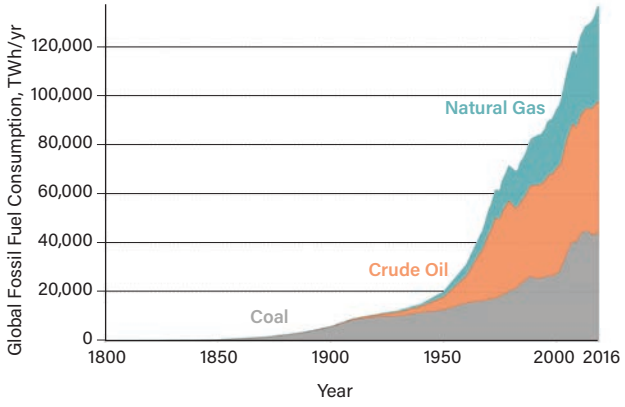

▲ **Figure 7.** Global fossil fuel consumption has increased dramatically since the middle of the 20th century. Source: *(9).*

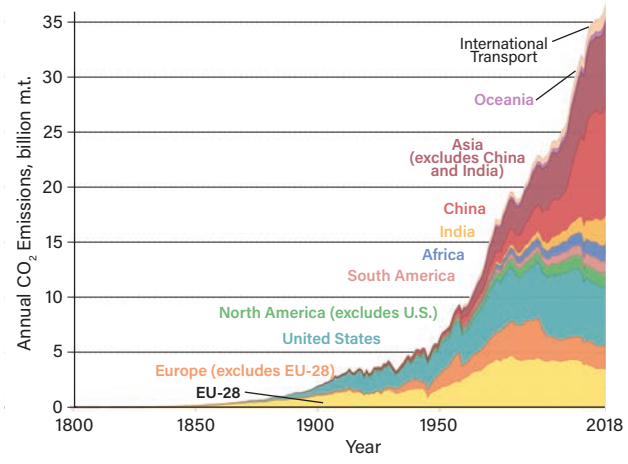

▲ **Figure 8.** Carbon dioxide emissions from fossil fuel combustion and cement manufacturing continue to increase in some regions of the world. Source: *(12).*

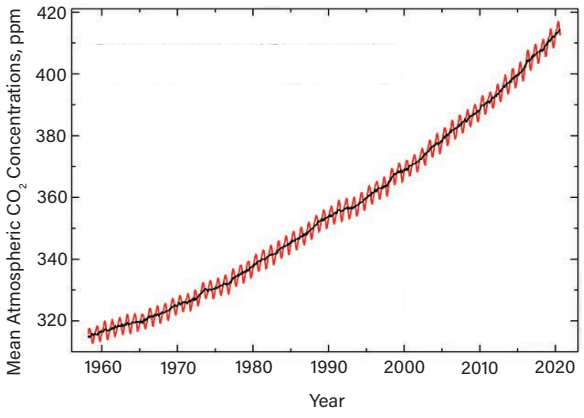

▲ **Figure 9.** Monthly mean atmospheric carbon dioxide molar concentrations are measured by the Mauna Loa Observatory in Hawaii. Source: *(14).*

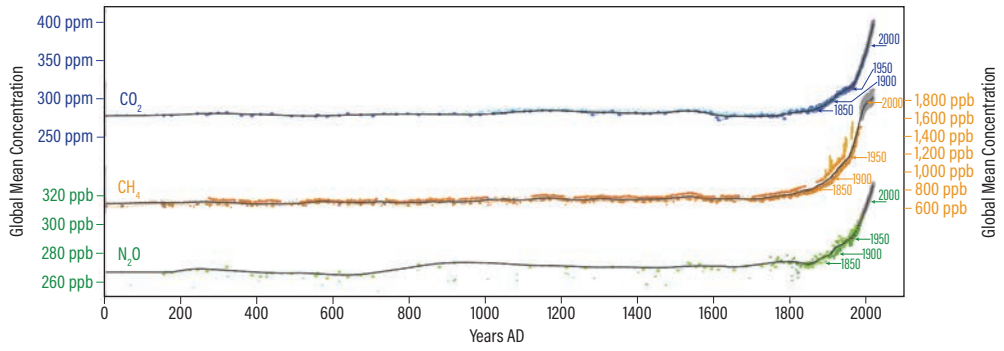

◀ **Figure 10.** The impact of industrialization is evident in the increases in atmospheric greenhouse gas concentrations starting around the time of the Industrial Revolution. Source: *(15)*.

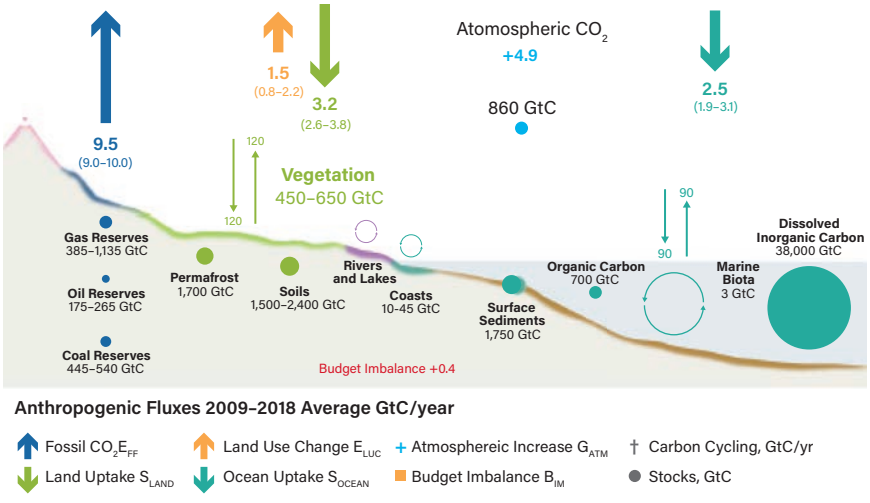

▲ **Figure 11.** This schematic represents the overall perturbation of the global carbon cycle caused by anthropogenic activities, averaged globally for the decade 2009–2018. Source: *(16)*.

about one-third of its electricity from renewable resources.

As carbon dioxide is released into the atmosphere from the combustion of fossil fuels and changes in land use, it accumulates in the atmosphere and thereby its concentration increases. Figure 9 *(14)* shows the carbon dioxide concentration in the atmosphere as measured by the observatory in Mauna Loa, Hawaii.

Figure 10 *(15)* places the recent carbon dioxide concentrations, as well as those of methane and nitrous oxide, into historical context. Before 1850, the concentrations of these gases were constant. The impact of industrialization is readily apparent based on the significant increases in the concentrations of all three GHGs since 1850. On a percentage basis, the largest increase is in methane concentrations, in the form of fugitive emissions from the fossil fuel industry, ruminant animal digestive tracts (mostly domestic cattle), and anaerobic decomposition of biomass in the soil (mostly wet rice agriculture).

Of the carbon dioxide released by the combustion of fossil fuels and land use changes, about 44% accumulates in the atmosphere (Figure 11) *(16)*. The remainder enters the soil and the ocean. Carbon dioxide that enters the ocean increases the concentration of carbonic acid, which reduces seawater pH. Detailed accounting of the carbon budget is available online at globalcarbonproject.org/carbonbudget/19/data.htm.

Temperature

The temperature of the Earth is a critical driver of climate change. This section examines historical global temperatures, the current global average temperature, and the difficulties involved in measuring temperature accurately

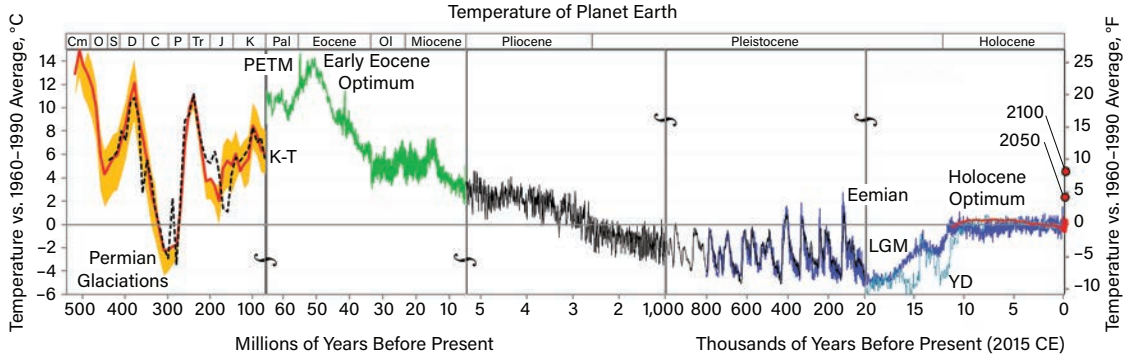

◀ **Figure 12.** The average temperature of the Earth during the past 542 million years ranged from 6°C colder to 14°C warmer than current temperatures. Source: *(17)*.

and proving the reliability of past measurements.

Geological temperatures. Figure 12 *(17)* presents the estimated temperature of Earth during the past 542 million years. These temperatures are determined based on proxies, such as the ratio of ^{18}O to ^{16}O, both of which are stable isotopes. The natural occurrences of ^{16}O and ^{18}O are 99.76% and 0.20%, respectively. Carbonate-forming sea creatures incorporate these isotopes into their shells in a temperature-dependent manner; thus, the ratio of these isotopes is a proxy for temperature.

The parameter $\delta^{18}O$ (delta-O-18) is defined as:

$$\delta^{18}\mathrm{O} \equiv \left(\frac{\left(\frac{^{18}\mathrm{O}}{^{16}\mathrm{O}}\right)_{\text{sample}}}{\left(\frac{^{18}\mathrm{O}}{^{16}\mathrm{O}}\right)_{\text{standard}}} - 1 \right) \times 1{,}000‰ \qquad (1)$$

where the standard is Vienna standard mean ocean water (VSMOW). In the formation of calcium carbonate shells, $\delta^{18}O$ correlates with temperature *(18)*:

$$T = 16.5 - 4.3\left(\delta^{18}\mathrm{O}\right) + 0.14\left(\delta^{18}\mathrm{O}\right)^2 \qquad (2)$$

over the range 9°C < T < 29°C.

Figure 12 shows that historical global temperatures have been as much as 6°C colder and 14°C warmer than modern temperatures. The colder temperatures resulted in glaciation and the warmer temperatures produced a world much different than today. For example, during the Early Eocene Epoch (54–48 million years ago), the CO_2 concentration was estimated to be 1,000–2,000 ppm and the poles were tropical in nature *(19)*.

Ice core data. Figure 13 *(20–22)* presents a more recent history of Earth's climate based on ice cores, which provide insights into Earth's climate during the past 800,000 years. In the Arctic and Antarctic, ice has accumulated for hundreds of thousands of years. Snow does not fall at a uniform rate, but rather forms layers. Thus, time can be correlated with depth by counting the number of layers in ice core samples.

To estimate geological temperature, since the 1960s, scientists have been measuring $\delta^{18}O$ in ice cores. Water-^{18}O is less volatile than water-^{16}O, so at a given equilibrium temperature, liquid is enriched in water-^{18}O whereas vapors are enriched in water-^{16}O. As atmospheric water vapor from the tropics flows to the poles, water-^{18}O selectively precipitates; thus, the snow at the poles is enriched in water-^{16}O. This enrichment is more pronounced at colder temperatures; thus, $\delta^{18}O$ in ice cores serves as a proxy for temperature (Figure 14) *(23, 24)*.

When snow falls and accumulates at the poles, air is trapped between the snowflakes. As layers of snow build up, the older layers are compacted into ice. The trapped air accumulates in small bubbles, which can be sampled to determine the geological composition of the atmosphere. Figure 13 shows the measured carbon dioxide conentration in the bubbles. Other GHGs, such as methane and nitrous oxide, can be measured as well (Figure 10).

Figure 13 shows that temperatures are highly periodic as a result of the following periodic changes in Earth's movements: ellipse eccentricity, 100,000 years; axial tilt, 41,000 years; and axial precession, 26,000 years. The collective effects of these changes in Earth's movements on climate over thousands of years are know as Milankovitch cycles.

As shown in Figure 13, global temperatures and carbon dioxide concentrations are highly correlated, with carbon dioxide changes lagging temperature changes by hundreds of years. A recent study concluded that this lag is an artifact of the manner in which bubbles form *(25)*. Until a depth of 50–120 m, the snow does not become compacted enough to form ice with trapped bubbles. Prior to ice formation, gases are free to diffuse from one layer of snow to another;

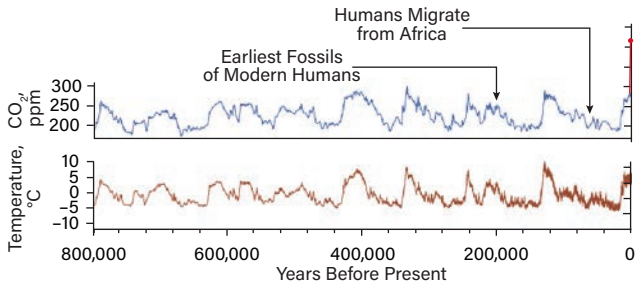

▲ **Figure 13.** Global temperatures and carbon dioxide concentrations can be obtained from ice core data. The current carbon dioxide concentration is shown in red. Source: *(20)* based on data in *(21, 22)*.

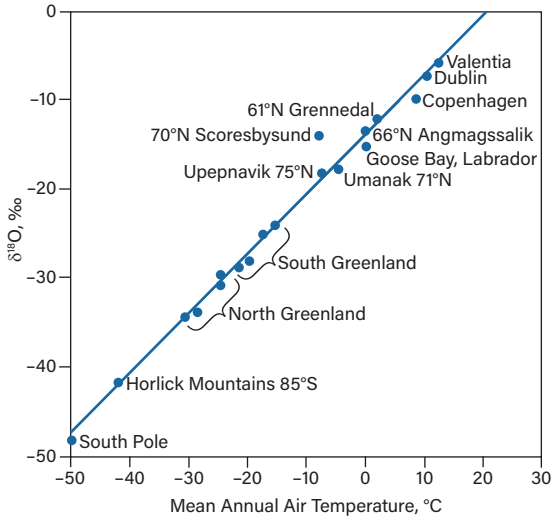

▲ **Figure 14.** The parameter $\delta^{18}O$ (the ratio of oxygen isotopes ^{18}O to ^{16}O) correlates with temperature. Source: *(23, 24)*.

thus, the carbon dioxide concentration and temperature are partly decoupled. When diffusion is considered, the apparent lag disappears.

Temperature and carbon dioxide concentration interact in a complex manner. As temperatures decrease in response to changing solar radiation distribution as a result of Milankovitch cycles, the solubility of carbon dioxide in the ocean increases, which removes carbon dioxide from the atmosphere and accentuates the cooling. Similarly, as temperatures increase, the solubility of carbon dioxide in the ocean decreases, which adds carbon dioxide to the atmosphere and accentuates the warming. During historic time periods, the Milankovitch cycle is the independent variable and carbon dioxide is a feedback mechanism that enhances the warming or cooling.

The hockey stick graph. Figure 15 *(26, 27),* known as the hockey stick graph, plots Earth temperature data for the past 1,500 years. The temperatures measured by thermometers are shown in red, and the temperatures measured by proxies are shown in blue. The proxies (tree rings, coral, ice cores, cave formations, marine sediment, lake sediment, and historical records) were obtained from 1,209 datasets. The green line represents the average global temperature from 500 to 1850, which may be viewed as the preindustrial temperature. (Note that because industrialization took place over many years, there is no universal agreement on the definition of the "preindustrial period" *(28).*) The data show that recent warming trends are unusual compared to historical records.

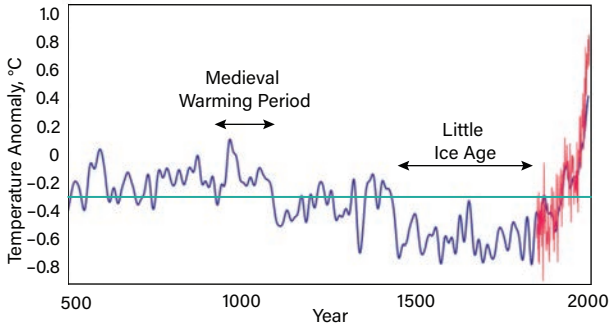

▲ **Figure 15.** The hockey stick graph depicts the climate record in terms of the temperature anomaly compared to the global average temperature during 1960–1990, which was 14.1°C. Temperatures reconstructed from multiple proxies, such as tree rings, coral data, and cave deposits, are shown in blue. The red line is the CRUTEM4 (Climatic Research Unit Temperature, version 4) instrumental record, which started in 1850. The horizontal green line is the average global temperature from 500 to 1850 (13.8°C), which may be viewed as the preindustrial temperature. Source: *(26, 27).*

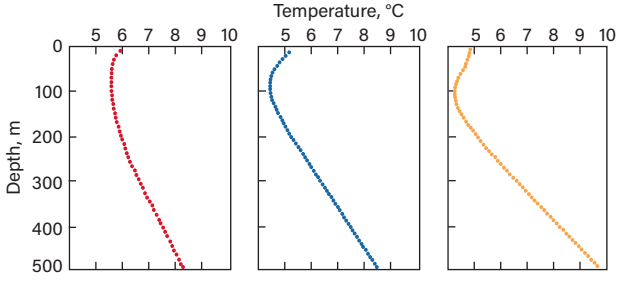

▲ **Figure 16.** These three borehole temperature profiles were taken at three sites in Canada. Source: *(29, 30).*

Figure 16 *(29, 30)* shows borehole temperature measurements taken at three sites in Canada. As mentioned previously, the Earth produces geothermal energy from fission. If the thermal conductivity of the rock is constant and the atmospheric temperature is constant, then the temperature profile with respect to depth should be a straight line. In Figure 16, at depths greater than 200 m, the temperature profiles are straight, but at shallower depths, they curve back toward warmer temperatures. The surface temperature is about 2°C warmer than the temperature obtained by extrapolation of the straight portion of the curve to the surface.

Using a nonsteady-state model of heat transfer, historical surface temperatures can be determined from the borehole temperature profiles. Figure 17 *(26, 29, 31)* overlays the surface temperatures estimated from borehole temperature profiles on the hockey stick graph. The fact that the two datasets agree provides confirmation of the historical temperatures.

Instrumental records. Since the mid-1800s, instrumental records are sufficient to estimate global temperatures without the need for proxies. Four government agencies focus on maintaining the instrumental records of temperature: NASA Goddard Institute for Space Studies (U.S.), NOAA National Climatic Data Center (U.S.), Met Office Hadley Centre/Univ. of East Anglia Climatic Research Unit (U.K.), and Japanese Meteorological Agency (Japan).

It can be difficult to accurately determine average global temperatures for a few key reasons: weather stations are not

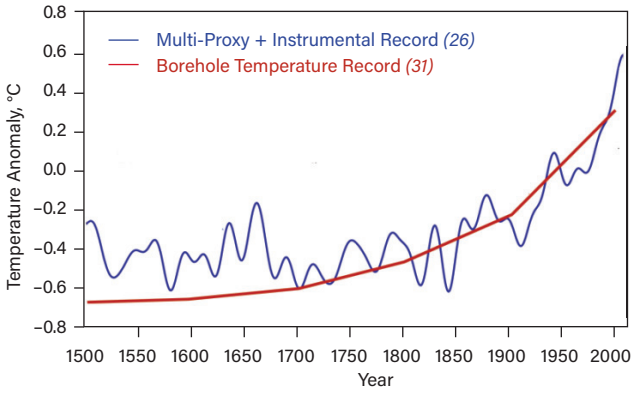

▲ **Figure 17.** Surface temperatures estimated from borehole temperature profiles (red) are overlaid on the hockey stick graph (blue) — showing agreement between the datasets. Source: *(26, 29, 31).*

evenly distributed around the Earth, so some regions have a paucity of data; the environment around weather stations may change; the quality of some thermometers is poor; it is necessary to determine appropriate methods to modify data to account for confounding effects; methods for sampling data change; and methods for measuring temperature change. Some specific issues include the following *(32)*:

• urban heat island effect — as urban structures encroach on a formerly rural weather station, the local temperature increases because buildings and roads hold thermal energy more than rural environments

• averaging methods — a region has multiple weather stations, each with time-varying temperatures, so an acceptable method is developed to process the spatial and temporal data to calculate an appropriate average for the region

• changes in the way ocean temperatures are measured — historically, ships would dip a bucket into the ocean to obtain a sample for measuring the ocean's temperature; now, ocean temperatures are obtained by measuring the temperature of the intake water to the ships' engines

• satellites — since 1982, satellites have provided temperature data with broader coverage and higher spatial resolution than weather stations, but they introduce their own sources of uncertainty

• ice — the presence of sea ice prevents changes in water temperature because of phase change.

Because of the importance of the temperature record and claims by climate change skeptics that the temperature data were being manipulated, Berkeley Earth Surface Temperature (BEST) — an academic initiative — was formed to evaluate the temperature data. They concluded that the temperature record is not unduly biased *(33)*.

Despite the numerous challenges associated with measuring average global temperature, the various sources report very similar findings (Figure 18) *(34)*. Similarly, Figure 19 *(35)* shows that surface temperature measurements are consistent with satellite temperature measurements.

The NASA Goddard Institute for Space Studies (GISS) temperature data are conveniently available online *(36)* and allow for customized graphics. Figure 20 indicates that the record temperatures in 2016 have a temperature anomaly of 1.0°C (*i.e.,* they were 1.0°C higher than the baseline global average temperature from 1951 to 1980, which is estimated to be 14.0°C); this is 1.2°C warmer than the preindusrial temperatures represented by the green line in Figure 15.

Figure 21 is notable because it shows extreme Arctic warming in February 2018 (with an anomaly of 12.3°C). Similar extreme warming occurred in February 2016, 2019, and 2020. Climate scientists expect greater warming of the

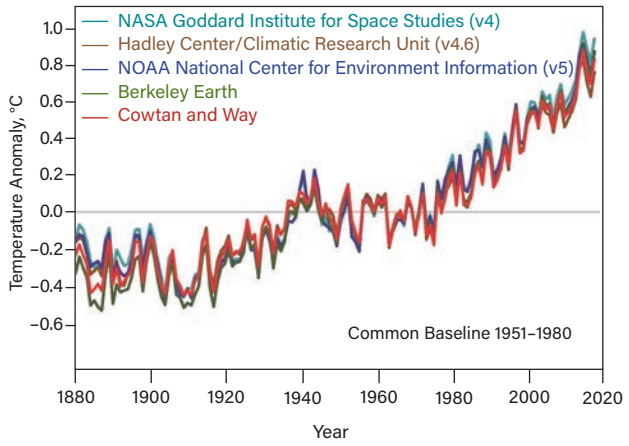

▲ **Figure 18.** Data on the global average temperature anomaly are consistent among multiple datasets. Source: *(34)*.

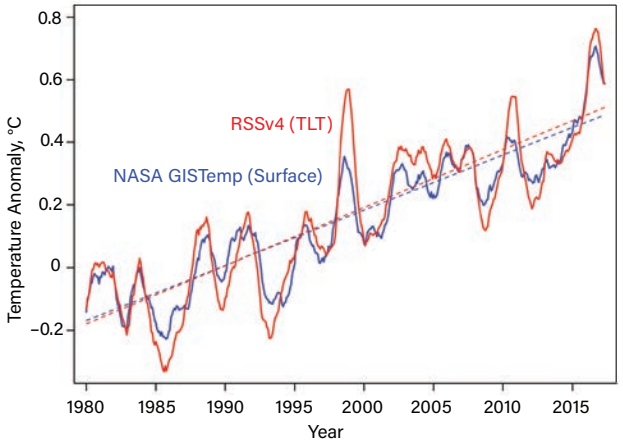

▲ **Figure 19.** Surface temperature measurements (blue) are consistent with satellite temperature measurements (red). Source: *(35)*.

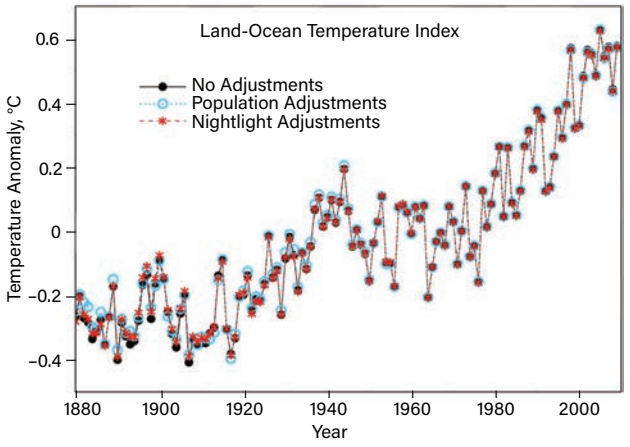

▲ **Figure 20.** The warmest year on record was 2016, when the global average temperature over land and sea was 15.0°C. This was 1.0°C warmer than the reference temperature, the global average temperature from 1951 to 1980, which is estimated to be 14.0°C. Source: Data from *(36)*.

Arctic because melting sea ice greatly reduces the albedo; lower albedo provides a strong positive feedback that accentuates warming.

Energy storage. Temperature data in the vertical dimension can be used to calculate the enthalpy content between two depths. For example, the areal enthalpy content H of the ocean can be determined by:

$$H = \rho C_p \int_{z_1}^{z_2} T(z)\,dz \qquad (3)$$

where ρ is seawater density (kg/m^3), C_p is the specific heat (J/kg-K), T is temperature (K), z is depth (m), and H is areal enthalpy (J/m^2). Multiplying the areal enthalpy by the area of the ocean gives the total enthalpy content of the ocean. Similar calculations can be performed for the air and soil. Figure 22 *(37)* shows that the vast majority of global enthalpy change occurs in the ocean.

If only a small fraction of ocean energy is exchanged with the atmosphere, it can drastically change atmospheric temperatures. For example, El Niño (warm anomaly) and La Niña (cold anomaly) are fluctuations in Pacific Ocean surface temperatures resulting from interactions with the atmosphere. An El Niño or La Niña episode typically lasts 9–12 months. Their frequency is irregular, but El Niño and La Niña events typically occur every two to seven years, with El Niño more frequent than La Niña. These temperature fluctuations can have large impacts on global

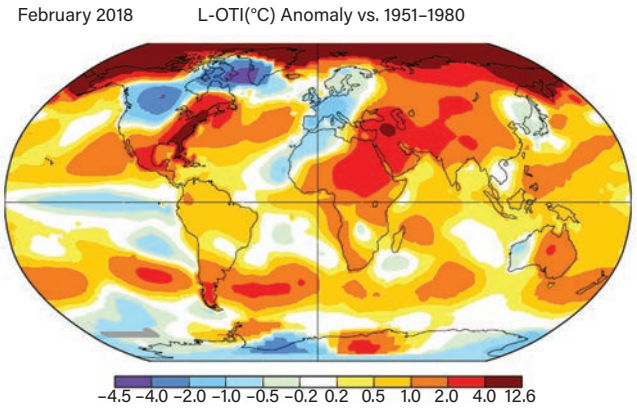

▲ **Figure 21.** Global ocean and land temperature anomalies in February 2018 reveal extreme Arctic warming. The temperature anomaly is compared to the global average temperature from 1951 to 1980, which is estimated to be 14.0°C. Source: Data from *(36).*

Literature Cited

1. **Noterdaeme, P., *et al.,*** "The Evolution of the Cosmic Microwave Background Temperature. Measurements of TCMB at High Redshift from Carbon Monoxide Excitation," *Astronomy and Astrophysics,* **526,** p. L7, doi: 10.1051/0004-6361/201016140 (2011).
2. **Williams, D. R.,** "Sun Fact Sheet," NASA, nssdc.gsfc.nasa.gov/planetary/factsheet/sunfact.html (accessed Sept. 7, 2020).
3. **Kopp, G.,** "Total Solar Irradiance Data," Laboratory for Atmospheric and Space Physics, Univ. of Colorado Boulder, lasp.colorado.edu/home/sorce/data/tsi-data (July 18, 2019).
4. "Graphic: Temperature vs Solar Activity," NASA, Jet Propulsion Laboratory, California Institute of Technology, climate.nasa.gov/climate_resources/189/graphic-temperature-vs-solar-activity (July 10, 2020).
5. **Williams, D. R.,** "Moon Fact Sheet," NASA, nssdc.gsfc.nasa.gov/planetary/factsheet/moonfact.html (accessed Sept. 7, 2020).
6. **Davies, J. H., and D. R. Davies,** "Earth's Surface Heat Flux," *Solid Earth*, **1,** pp. 5–24, (2010).
7. "Nuclear Power in the World Today," World Nuclear Association, world-nuclear.org/information-library/current-and-future-generation/nuclear-power-in-the-world-today.aspx (accessed Sept. 7, 2020).
8. **Nuclear Power for Everybody,** "Thermal Efficiency of Nuclear Power Plants," nuclear-power.net/nuclear-engineering/thermodynamics/laws-of-thermodynamics/thermal-efficiency/thermal-efficiency-of-nuclear-power-plants (accessed Sept. 7, 2020).
9. **Ritchie, H., and M. Roser,** "Fossil Fuels," ourworldindata.org/fossil-fuels (accessed Sept. 7, 2020).
10. **Grobe, H.,** "Albedo," simple.wikipedia.org/wiki/Albedo#/media/File:Albedo-e_hg.svg, Creative Commons Attribution-ShareAlike 2.5 Generic license (CC BY-SA 2.5) (accessed Sept. 7, 2020).
11. **Blasing, T. J.,** "Recent Greenhouse Gas Concentrations," Carbon Dioxide Analysis Center, U.S. Dept. of Energy, doi: 10.3334/CDIAC/atg.032, cdiac.ess-dive.lbl.gov/pns/current_ghg.html (accessed Sept. 7, 2020).
12. **Ritchie, H., and M. Roser,** "CO_2 and Greenhouse Gas Emissions," ourworldindata.org/co2-and-other-greenhouse-gas-emissions (accessed Sept. 7, 2020).
13. **Amadeo, K.,** "U.S. GDP by Year Compared to Recessions and Events," The Balance, thebalance.com/us-gdp-by-year-3305543 (accessed Sept. 7, 2020).
14. **Global Monitoring Laboratory,** "Monthly Average Mauna Loa CO_2," National Oceanic and Atmospheric Administration, Earth System Research Laboratories, esrl.noaa.gov/gmd/ccgg/trends (accessed Sept. 7, 2020).
15. **Meinshausen, M., *et al.,*** "Historical Greenhouse Gas Concentrations for Climate Modelling (CMIP6)," *Geoscientific Model Development*, **10,** pp. 2057–2116, doi: 10.5194/gmd-10-2057-2017 (2017).
16. **Le Quéré, C., *et al,*** "Global Carbon Budget 2019," *Earth System Science Data,* **11,** pp. 1783–1838, doi: 10.5194/essd-11-1783-2019 (2019).
17. **Fergus, G.,** "All Paleotemps," en.wikipedia.org/wiki/File:All_palaeotemps.png, Creative Commons Attribution-ShareAlike 3.0 Unported license (CC BY-SA 3.0) (accessed Sept. 7, 2020).
18. **Epstein, S., *et al.,*** "Revised Carbonate-Water Isotopic Temperature Scale," *Geological Society of America Bulletin,* **64** (11), pp. 1315–1325, doi: 10.1130/0016-7606(1953)64[1315:RCITS]2.0.CO;2 (1953).
19. **National Centers for Environmental Information,** "Early Eocene Period – 54 to 48 Million Years Ago," National Oceanic and Atmospheric Administration, ncdc.noaa.gov/global-warming/early-eocene-period (accessed Sept. 7, 2020).

Literature Cited continues on next page

weather and climate. For example, the most recent El Niño, superimposed onto baseline warming trends, contributed to 2016 being by far the warmest year on record.

Closing thoughts

As global population increases and standards of living improve, fossil fuel combustion is increasing. Approximately half of the resulting carbon dioxide accumulates in the atmosphere, causing its concentration to increase above levels not observed within the past 800,000 years. Since 1960, global temperatures have increased substantially, which coincides with large increases in carbon dioxide emissions. The recent warming trends cannot be explained by changing solar output, which on average has been constant since 1950. The warmest year on record, 2016, had a global average temperature that was 1.2°C warmer than preindustrial temperatures. CEP

Acknowledgments

The author expresses gratitude to climate scientists Andrew Dessler, Gunnar Schade, and John Nielsen-Gammon of Texas A&M Univ. for reviewing the manuscript for accuracy.

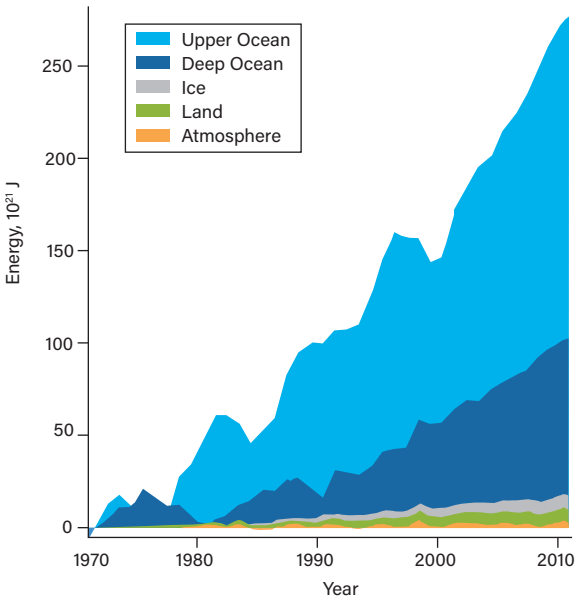

▲ **Figure 22.** Most of the global enthalpy change occurs in the ocean. The upper ocean is defined as a depth of less than 700 m, whereas the deep ocean is at a depth greater than 700 m. Source: *(37).*

Literature Cited (continued)

20. **Simmon, R.,** "Levels of Carbon Dioxide in the Atmosphere …," in "Changes in the Carbon Cycle," NASA Goddard Space Flight Center, earthobservatory.nasa.gov/features/CarbonCycle/page4.php (June 16, 2011).
21. **Luthi, D. M., *et al.,*** "High-Resolution Carbon Dioxide Concentration Record 650,000–800,000 Years Before Present," *Nature*, **453,** pp. 379–382, doi:10.1038/nature06949 (May 15, 2008).
22. **Jouzel, J., *et al.,*** "Orbital and Millennial Antarctic Climate Variability over the Past 800,000 Years," *Science*, **317** (5839), pp. 793–797 (2007).
23. **Broecker, W. S., and V. M. Oversby,** "Chemical Equilibria in the Earth," McGraw-Hill, New York, NY (1971).
24. **Dansgaard, W.,** "Stable Isotopes in Precipitation," *Tellus,* **16** (4), pp. 436–468, doi: 10.1111/j.2153-3490.1964.tb00181.x (1964).
25. **Parrenin, F., *et al.,*** "Synchronous Change of Atmospheric CO_2 and Antarctic Temperature During the Last Deglacial Warming," *Science,* **339** (6123), pp. 1060–1063, doi: 10.1126/science.1226368 (Mar. 1, 2013).
26. **Mann, M. E., *et al.,*** "Proxy-Based Reconstructions of Hemispheric and Global Surface Temperature Variations over the Past Two Millennia," *Proceedings of the National Academy of Sciences of the United States of America*, **105** (36), pp. 13252–13257, doi: 10.1073/pnas.0805721105 (2008).
27. **Bralower, T., and D. Bice,** "Recent Climate Change," Module 2 of Earth 103: Earth in the Future, Penn State Univ., College of Earth and Mineral Sciences, e-education.psu.edu/earth103/node/6 (accessed Sept. 7, 2020).
28. **Hawkins, E., *et al.,*** "Estimating Changes in Global Temperature since the Preindustrial Period," *Bulletin of the American Meteorological Society*, **98** (9), pp. 1841–1856, doi: 10.1175/BAMS-D-16-0007.1 (2017).
29. **Bralower, T., and D. Bice,** "Temperature: Borehole Temperatures," Module 2 of Earth 103: Earth in the Future, Penn State Univ., College of Earth and Mineral Sciences, e-education.psu.edu/earth103/node/752 (accessed Sept. 7, 2020).
30. **Pollack, H. N., and S. Huang,** "Climate Reconstruction for Subsurface Temperatures," *Annual Review of Earth and Planetary Sciences,* **28,** pp. 339–365 (2000).
31. **Huang, S., *et al.,*** "Temperature Trends over the Past Five Centuries Reconstructed from Borehole Temperatures," *Nature,* **403,** pp. 756–758 (Feb. 17, 2000).
32. **Hansen, J., *et al.,*** "Global Surface Temperature Change," *Reviews of Geophysics,* **48** (4), Paper No. 2010RG000345, doi: 10.1029/2010RG000345 (Dec. 2010).
33. **Berkeley Earth,** "About Berkeley Earth — Our History," berkeleyearth.org/about (accessed Sept. 7, 2020).
34. **NASA Jet Propulsion Laboratory,** "Scientific Consensus: Earth's Climate is Warming," NASA, climate.nasa.gov/scientific-consensus (accessed Sept. 7, 2020).
35. **Hausfather, Z.,** "Major Correction to Satellite Data Shows 140% Faster Warming Since 1998," Carbon Brief, carbonbrief.org/major-correction-to-satellite-data-shows-140-faster-warming-since-1998 (June 30, 2017).
36. **NASA Goddard Institute for Space Studies,** "GISS Surface Temperature Analysis (GISTEMP v4)," data.giss.nasa.gov/gistemp (accessed Sept. 7, 2020).
37. **Rhein, M., *et al.,*** "Observations: Ocean," Chapter 3 in Stocker, T. F., *et al.,* eds., "Climate Change 2013: The Physical Science Basis," Contribution of Working Group I to the Fifth Assessment Report of the Intergovernmental Panel on Climate Change, Cambridge Univ. Press, Cambridge, U.K. and New York, NY (2013).

Climate Modeling

Mark Holtzapple ▪ Texas A&M Univ.

Climate models provide insight into the fundamental principles that underlie global warming.

Measurements taken during the last 140 years show that global temperature and carbon dioxide concentrations are correlated (Figure 1) *(1)* — a relationship that has also been observed in ice core data spanning the past 800,000 years (see Figure 13 in the previous article, p. 19). However, correlation does not imply causation. Identifying causation requires a deeper understanding of the underlying phenomena that link the correlated variables. With regard to climate, we seek to answer the question: Are human activities — particularly those related to the release of carbon dioxide — causing the currently observed rapid global warming?

When attempting to answer a scientific question, engineers and scientists typically perform a controlled experiment. In the context of global warming, this would require two Earths orbiting the sun at the same distance. One Earth — the control — would operate without human intervention, while the other Earth would be subjected to human activity, such as combustion of fossil fuels, land use changes, etc. During the experiment, measurements (*e.g.,* temperature, ocean pH, sea ice) of properties of the two Earths would be taken. The impact of human activities would be reported as the difference between the measurements taken of the experimental Earth's properties and those of the control Earth.

Clearly, the above experiment is fanciful — we do not have a second Earth to serve as the control. The only available tool for discerning the impacts of human activity is modeling. Climate models are based on the laws of physics and include scientific measurements (*e.g.,* heat capacity, density, thermal conductivity, reflectivity) that are incorporated into computer simulations of the Earth. In some cases, the models are extremely simple, whereas in other cases, the models are exceedingly complex.

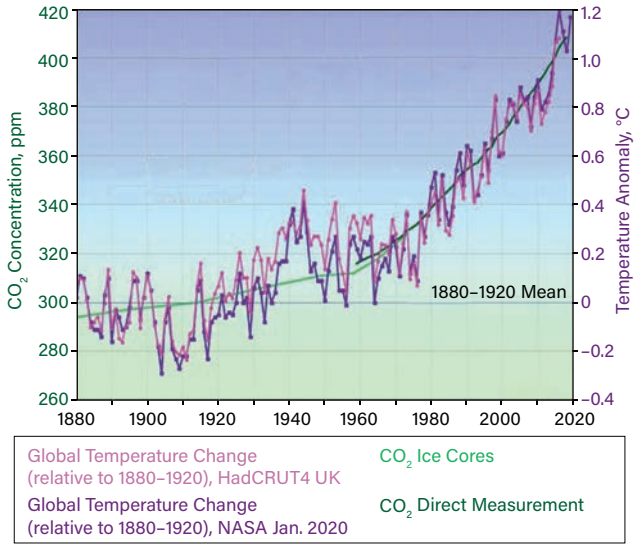

▲ **Figure 1.** Global temperature and carbon dioxide concentration are correlated. Plotted temperatures are measurements by instruments. Carbon dioxide concentrations prior to 1959 were determined from ice core samples; after 1959, carbon dioxide concentrations were directly measured by the observatory at Mauna Loa, HI. Source: *(1).*

The famous aphorism "all models are wrong … but some are useful" is attributed to statistician George Box. This quip is particularly relevant in the context of global warming. All models are imperfect, but often they contain useful information that allows decisions to be made. Imperfect models are not uncommon in chemical engineering. For example, managers must decide whether to construct a new chemical plant based on imperfect models of the chemistry, physics, market, safety, etc.

Global climate is exceedingly complex, chaotic, and highly coupled. For example, one can ask the question "Is carbon dioxide concentration a cause or an effect?" Arguments can be made for both positions. As carbon dioxide is added to the atmosphere (cause), more radiation is absorbed by the atmosphere, which causes warming (effect). On the other hand, as global temperature cools from varying solar output or Earth's orbital patterns (cause), more carbon dioxide dissolves in the ocean, lowering the atmospheric concentration (effect). Differentiating cause and effect requires a fundamental understanding of the chemistry and physics of climate.

Atmosphere

The total mass of the atmosphere is easily calculated from the average atmospheric pressure (14.7 $lb_f/in.^2$). This pressure is caused by the air mass in the vertical column above the Earth's surface (14.7 $lb_m/in.^2$ or 10,300 kg/m^2). From the radius of the earth (6,371 km) and the area of a sphere ($4\pi r^2$), the mass of air in the atmosphere is 5.27×10^{18} kg. From the average atomic mass of air (28.97 g/mol), the total moles in the atmosphere are calculated to be 1.82×10^{20} mol. From this known quantity of air and measured concentrations of gases, it is possible to calculate the total quantity of a given gas in the atmosphere.

As altitude increases, air pressure decreases monotonically in an exponential manner (Figure 2) *(2)*. The pressure under a column of fluid is:

$$dP = -\rho g dz \tag{1}$$

where P is the absolute pressure (Pa), ρ is the fluid density (kg/m^3), g is the local acceleration due to gravity (9.81 m/sec^2), and z is the height (m). Assuming the gas is ideal and at constant temperature allows for a simple substitution for density:

$$dP = -\left(\frac{MP}{RT}\right) g dz \tag{2}$$

where M is the atomic mass (kg/mol), T is the absolute temperature (K), and R is the ideal gas constant (8.314 Pa-m^3/mol-K). Equation 2 can be integrated to obtain:

$$P = P_0 \exp\left(-\frac{Mgh}{RT}\right) \tag{3}$$

where h is the elevation and P_0 is the pressure at the Earth's surface.

The relationship between pressure and elevation becomes

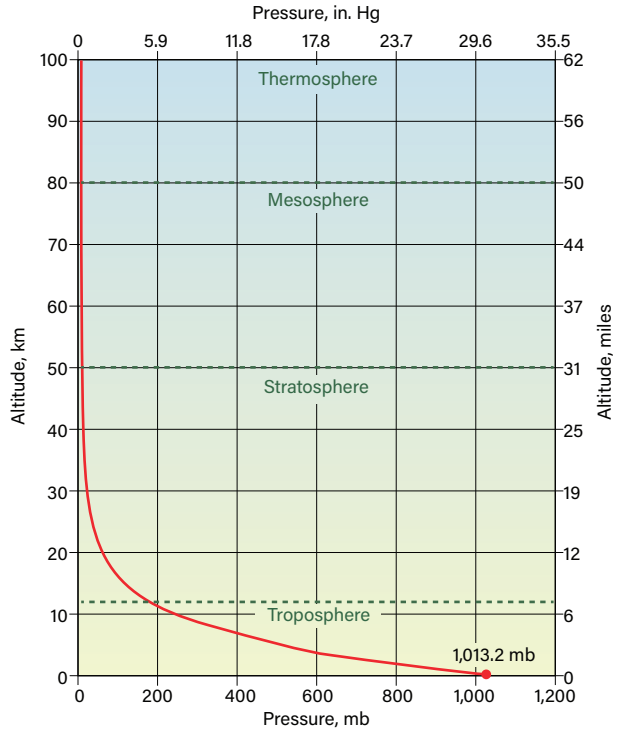

▲ **Figure 2.** Atmospheric pressure decreases with increasing altitude. Source: *(2)*.

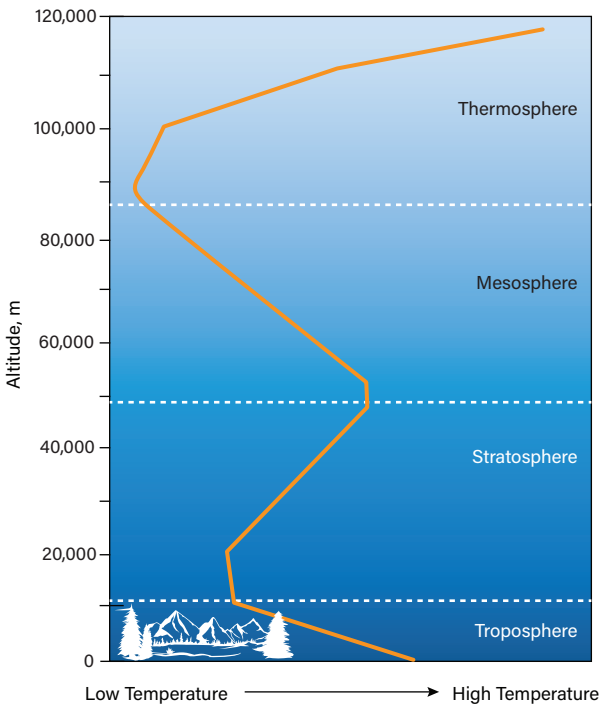

▲ **Figure 3.** Atmospheric temperature varies with altitude in a complex way. Source: *(3)*.

more complex if temperature is not held constant. It should be noted that atmospheric pressure changes on a daily basis and is an important parameter used to predict weather. In contrast, at the time scales of climate modeling, the daily changes in pressure can be neglected and the average pressure distribution can be used.

Atmospheric temperature is related to altitude in a complex manner (Figure 3) *(3)*. At lower altitudes (troposphere), air temperature decreases with increasing elevation. Convection currents cause air to flow from the Earth's surface to higher elevations. At higher elevations, the air pressure decreases, causing volume to expand and exert adiabatic work on the surroundings, thereby cooling the air. From simple thermodynamic calculations, this rate of cooling — the lapse rate — is 9.8°C/km for dry air. For wet air, the lapse rate is less (about 5°C/km) because the latent heat of the condensing water can provide some of the adiabatic work.

At higher altitudes, the temperature can increase with height. Some solar wavelengths are absorbed directly by water vapor, oxygen, and ozone, so the atmosphere is directly heated by sunlight. Temperatures in the stratosphere, which contains approximately 10% of the atmosphere's mass, typically range from 200 K to 270 K.

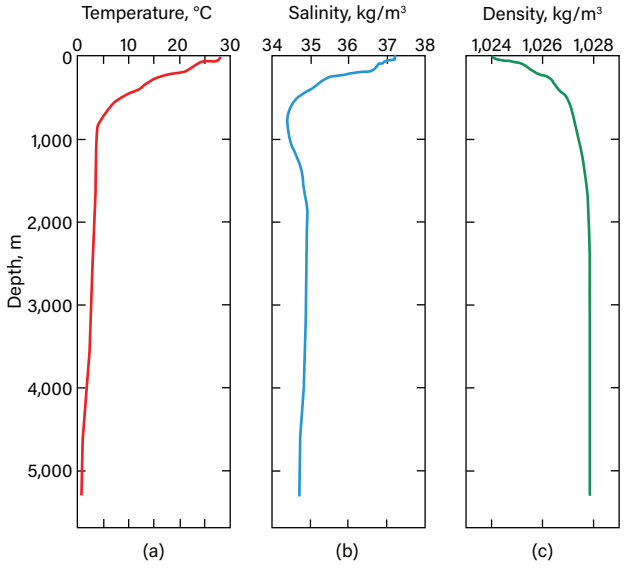

▲ **Figure 4.** The physical properties of seawater vary with ocean depth. These curves are for the Atlantic Ocean at a latitude of 20 deg. south. Source: *(4)*.

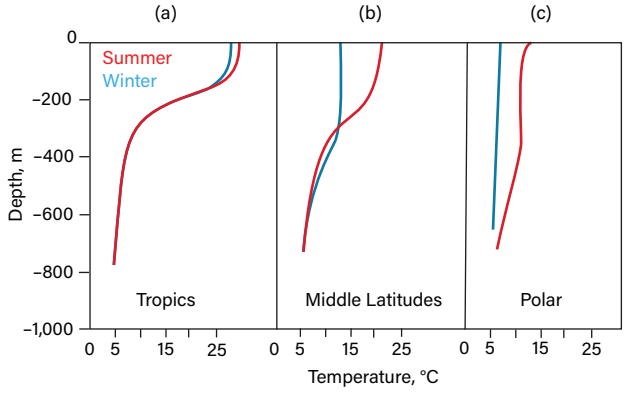

▲ **Figure 5.** (a) Ocean temperatures at the equator vary little with the season; (b) temperatures vary more at middle latitudes of 45-deg. north or south, and (c) still more at the poles. Source: *(5)*.

Oceans

Figure 4 *(4)* shows typical seawater properties (temperature, salinity, density) as a function of depth. The upper 1,000 m are the most dynamic, whereas depths below that are much more stable. The surface seawater is warmer and has lower density, which reduces the tendency for the surface water to mix with deep waters. The surface is more saline than the depths, because water evaporates from the surface, thereby concentrating the salt.

Figure 5 *(5)* shows the impact of seasons on the temperature profile of the ocean at different latitudes. The temperatures in the tropics do not vary significantly with seasons, whereas temperatures at middle latitudes and the poles vary more. Warm surface waters provide energy that drives cyclones (*e.g.*, hurricanes, typhoons).

Blackbody radiation

A blackbody is an object (solid, liquid, gas) that absorbs all radiation of all wavelengths falling on it. A good approximation to a blackbody is graphite or lampblack. An ideal blackbody is a hohlraum, a hollow cavity with a small hole (Figure 6). Any radiation that passes through the hole will be reflected multiple times within the cavity until it eventually is absorbed by the walls.

A blackbody is reversible. Not only does it absorb radiation, but it emits radiation as well. The molecules that comprise the walls of the hohlraum vibrate because they contain thermal energy. A fundamental principle of physics is that

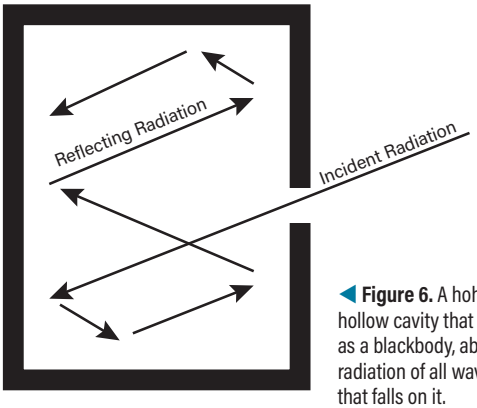

◀ **Figure 6.** A hohlraum is a hollow cavity that behaves as a blackbody, absorbing radiation of all wavelengths that falls on it.

an accelerating charge emits photons; thus, the charged particles (electrons, protons) that comprise the wall emit photons as they accelerate during thermal vibrations. The distribution of thermal vibrational frequencies is affected by temperature; at high temperatures, the charged particles vibrate more rapidly, while at low temperatures, they vibrate more slowly. The distribution of emitted photons is affected by the distribution of thermal vibrational frequencies, which is determined by temperature.

For a blackbody at a uniform temperature, the emission of photons has a characteristic temperature-dependent wavelength distribution, *i.e.,* the number of photons emitted at a particular wavelength during a unit of time. Each photon carries energy ($E = hc/\lambda$), so the distribution of photon wavelengths also describes the amount of power emitted at each wavelength.

According to Planck's law, the spectral radiance B per unit wavelength is:

$$B = \frac{2hc^2}{\lambda^5}\frac{1}{\exp\left(\frac{hc}{\lambda kT}\right)-1} \qquad (4)$$

where h is Planck's constant (6.6260700×10^{-34} J-sec), c is the speed of light (299,792,458 m/sec), k is Boltzmann's constant (1.380648×10^{-23} J/K), λ is wavelength (m), and B has units of W/m^2-sr-m where sr is a steradian, a measure of solid angle.

Planck's law can be integrated over all wavelengths to give the Stefan-Boltzmann equation:

$$J = \sigma T^4 \qquad (5)$$

where J is the energy flux (J/sec-m^2 or W/m^2), σ is the Stefan-Boltzmann constant (5.670373×10^{-8} W/m^2-K^4), and T is the absolute temperature (K). Real materials do not follow the idealized Stefan-Boltzmann equation, so an empirical emissivity ε is introduced:

$$J = \varepsilon\sigma T^4 \qquad (6)$$

where $0 < \varepsilon < 1$. The emissivity depends on the wavelength and also the material. For example, polished silver has an emissivity of 0.02 whereas the emissivity of graphite is 0.98. Most of the Earth's surface is ocean, which has an emissivity of 0.984 *(6)*; thus, much of Earth's surface is well approximated as a blackbody.

As explained in the previous article (p. 15), the solar constant — the energy flux above Earth's atmosphere — is 1,361 W/m^2. When the solar energy flux hits the Earth, it is intercepted by the projected area of the Earth, a circular disk ($A = \pi r^2$). As the Earth rotates, this intercepted solar energy is distributed over the Earth's surface, a sphere ($A = 4\pi r^2$). Thus, the average energy flux hitting the outer atmosphere is one-fourth, or 340 W/m^2. The Earth's albedo — the fraction of the energy that is reflected from the Earth — is about 0.306, so about 104 W/m^2 is reflected into space. Based on these considerations, the net solar energy flux on the Earth's surface is 236 W/m^2 (Figure 7).

If the atmosphere were transparent to infrared radiation (Figure 7a), the average temperature of the Earth would be easily calculated by rearranging Eq. 6:

$$T = \left(\frac{J}{\varepsilon\sigma}\right)^{1/4}$$

$$= \left(\frac{236.1\ \text{W/m}^2}{(0.984)\left(5.670373\times10^{-8}\ \text{W/m}^2\text{-K}^4\right)}\right)^{1/4}$$

$$= 255\ \text{K} = -18°\text{C}$$

As described in the previous article, the current average global temperature is 15°C (288 K), or 33 K warmer. Clearly, the absorption of infrared radiation by greenhouse gases plays a significant role in warming the planet.

Using the known average temperature of the Earth, the average energy flux emanating from the Earth's surface can be calculated from Eq. 6:

$$J = \varepsilon\sigma T^4$$

$$= (0.984)\left(5.670373\times10^{-8}\ \text{W/m}^2\text{-K}^4\right)(288\ \text{K})^4$$

$$= 384\ \text{W/m}^2$$

This energy flux emanating from the Earth's surface (384 W/m^2) is substantially greater than the average solar energy flux reaching earth (236 W/m^2). The difference, 148 W/m^2, is energy recycled from the atmosphere to the Earth's surface (Figure 7b).

Spectroscopy

Spectroscopy is the study of the interaction of matter with particular wavelengths of radiation through absorption and emission. This field has particular relevance to

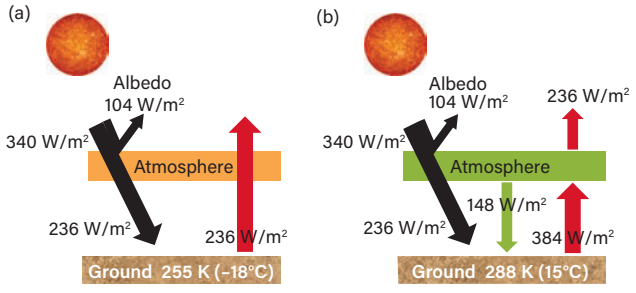

▲ **Figure 7.** Solar energy impinging on Earth is reemitted as infrared radiation. (a) If the atmosphere were transparent to infrared radiation, all of the incident radiation would be reemitted. (b) However, the atmosphere contains greenhouse gases and recycles some radiation back toward the Earth's surface.

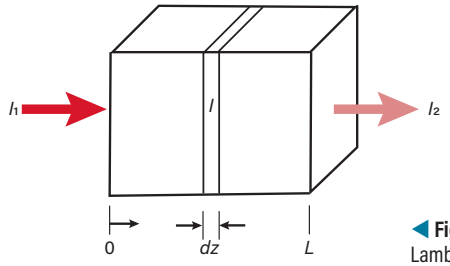

Figure 8. The Beer-Lambert Law describes the absorption of light.

global warming because radiation is the only heat transfer mechanism that warms or cools the Earth; conduction and convection do not operate in the vacuum of space. Furthermore, the incoming and outgoing radiation interact with Earth's atmosphere in complex ways that affect global temperature.

In conventional ultraviolet-visible (UV-VIS) spectroscopy, a liquid sample is placed in a cuvette and a beam of single-wavelength light is passed through the sample. As molecules absorb light, photon energy is converted to internal energy irreversibly, *i.e.,* the internal energy cannot be converted back into UV-VIS photons. The energy levels of the incoming high-energy photons are very different from those of the outgoing low-energy thermal photons; therefore, interconversion is not possible. In contrast, in the infrared (IR) region, the energy levels of the incoming and outgoing photons are very similar, so the process is partially reversible — some of the outgoing low-energy thermal photons are reabsorbed by neighboring molecules. In this discussion, only the initial absorption is described, not the reabsorption of low-energy emitted thermal photons.

The Beer-Lambert Law relates the attenuation of light to the properties of the material through which the light is traveling (Figure 8).

In conventional UV-VIS spectroscopy, the change in light intensity I per length z is first-order in the concentration c (mol/m^3) of the molecule and first-order in the light intensity at a given position in the cuvette of total length L:

$$\frac{dI}{dz} = kcI$$

$$\frac{dI}{I} = kcdz$$

$$\int_{I_1}^{I_2} \frac{dI}{I} = kc\int_0^L dz$$

$$\ln\frac{I_2}{I_1} = kcL \qquad (7)$$

where k is a proportionality constant.

It is traditional to use common logarithms rather than natural logarithms:

$$2.303\log_{10}\frac{I_2}{I_1} = kcL$$

$$\log_{10}\frac{I_2}{I_1} = \frac{1}{2.303}kcL \qquad (8)$$

and make the following term-by-term substitution:

$$A = \varepsilon cL \qquad (9)$$

where A is the absorbance and ε is the molar extinction coefficient (a measure of how strongly a chemical species absorbs light at a particular wavelength). (Note that the molar extinction coefficient is different from the emissivity discussed earlier; traditionally, both quantities are represented by ε.)

Although this relationship is usually applied to liquids, it is also valid for gases:

$$A = \varepsilon\left(\frac{P_A}{RT}\right)L \qquad (10)$$

where P_A is the partial pressure of Species A, R is the universal gas constant, and T is the absolute temperature.

Equation 10 indicates that as the partial pressure of Species A increases in a gas mixture, a greater fraction of light intensity is absorbed. At high partial pressures of Species A, nearly all of the light is absorbed in length L; at low partial pressures of Species A, only a small portion of light is absorbed in length L.

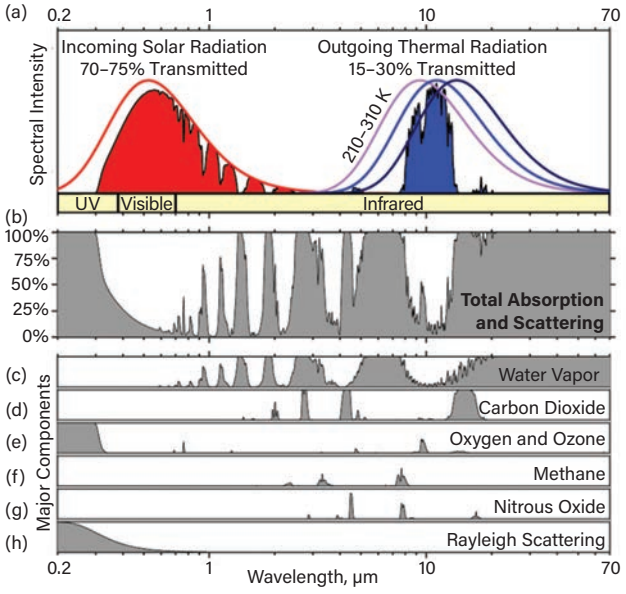

Figure 9. Radiation transmitted through the atmosphere. (a) Incoming solar radiation measured at the Earth's surface; outgoing infrared radiation measured above the atmosphere. (b) Total adsorption from gases and scattering. (c–h) Contributions of each component of the atmosphere. Source: *(8).*

When a gas molecule absorbs radiation, its internal energy increases according to the following transitions:

- electronic — generally UV radiation (<0.4 μm)
- vibrational — near-IR radiation (0.7–20 μm)
- rotational — far-IR radiation (>20 μm).

Photon absorption is quantized, *i.e.,* only certain frequencies resonate with a particular molecule. In Earth's atmosphere, very little absorption occurs in the visible range (0.4–0.7 mm), which is in the gap of most electronic and vibrational transitions of gases *(7)*. Gases that absorb where most terrestrial radiation is emitted (5–50 mm) are called greenhouse gases (GHGs). Figure 9 *(8)* shows the absorption spectra for the most important greenhouse gases.

Incoming solar radiation

Figure 9a shows the distribution of visible wavelengths of solar energy above the atmosphere. Figure 10 *(9)* shows the distribution of solar energy wavelengths at a higher resolution. Although the sun's surface temperature is not uniform, the distribution is well represented by a blackbody at 5,778 K. Most of the solar radiation (70–75%) reaches the Earth's surface unimpeded, except for some absorption primarily by water vapor but also by oxygen, carbon dioxide, and ozone. Figure 9h shows the amount of solar energy affected by Rayleigh scattering from air molecules, which is responsible for the blue color of the sky. Figure 9b shows the combined impact of absorption by greenhouse gases (Figures 9c–g) and scattering (Figure 9h).

Outgoing infrared radiation

In Figure 11 *(7, 10),* the jagged green line shows the emission spectrum measured by a satellite looking down on Earth. Superposed on this emission spectrum is a series of smooth dashed-line curves, each corresponding to the emission spectrum of blackbodies at a specific temperature. Depending on the wavenumber, the green emission spectrum overlays closely with a particular blackbody temperature. For example, water vapor (400–550 cm^{-1}) overlays with T_1 = ~270 K and carbon dioxide (630–700 cm^{-1}) overlays with T_2 = ~215 K.

The concentration of carbon dioxide is uniform throughout the atmosphere. At very high elevations, the partial pressure of carbon dioxide is so miniscule that it has negligible impact on radiation. At low elevations, its partial pressure is so large that the atmosphere is essentially opaque at wavelengths where carbon dioxide absorbs. An idealized effective opaque height can be defined as the height below which the atmosphere is opaque and above which it is transparent. The blue bar in Figure 11b represents the height of the opaque layer for carbon dioxide. According to the lapse rate graph, this height corresponds to the tropopause and a temperature of T_2 = ~215 K.

Unlike carbon dioxide and other greenhouse gases, the concentration of water vapor is not uniform throughout the atmosphere. Water readily condenses to form clouds, so at very high elevations, its partial pressure is miniscule. For this reason, the effective opaque height for water vapor, depicted by the blue bar in Figure 11a, is much less than that of other greenhouse gases and corresponds to a temperature of T_1 = ~270 K.

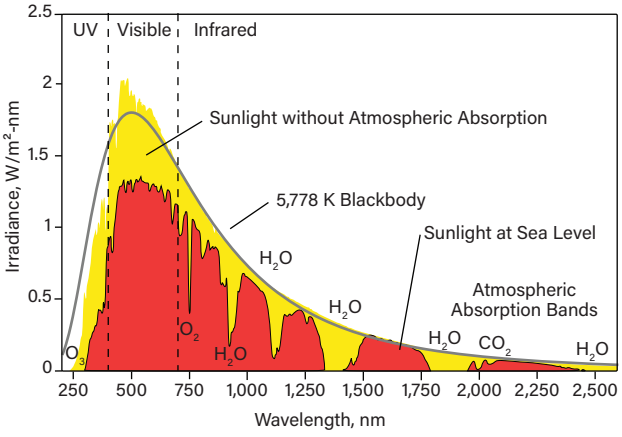

▲ **Figure 10.** Solar energy above the atmosphere (yellow) and at sea level (red). Source: *(9)*.

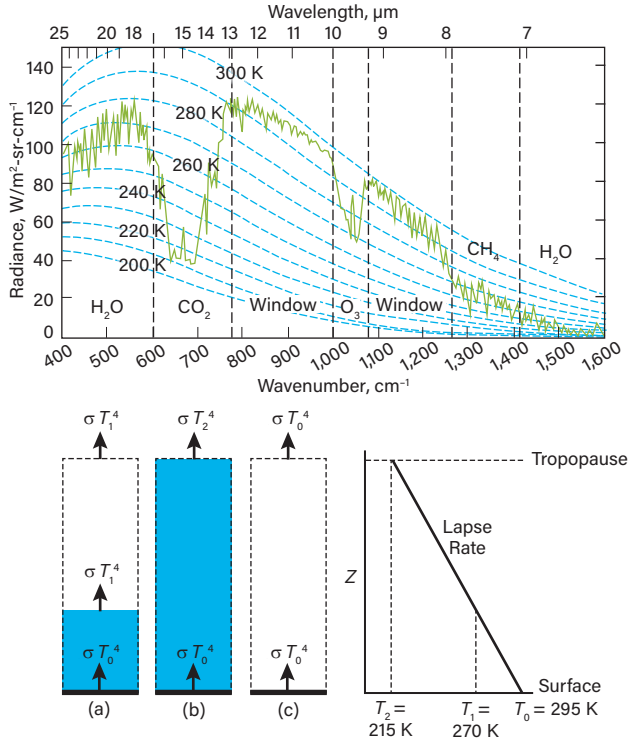

▲ **Figure 11.** Infrared radiation measured at the top of the atmosphere via Nimbus 4 satellite looking down on the tropical Pacific Ocean. Source: *(7, 10)*.

Article continues on next page

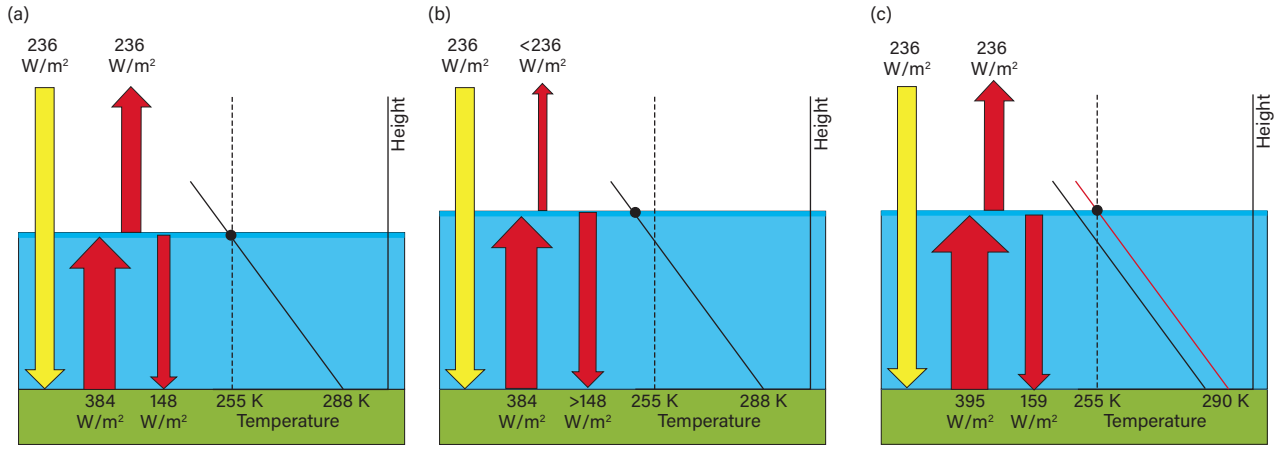

▲ **Figure 12.** This simple radiative model describes global warming. (a) Current temperature and emitted energy assuming thermal balance. (b) The addition of greenhouse gases increases the effective opaque height and causes the system to go out of thermal balance. (c) New temperature and emitted energy assuming thermal balance.

The spectrum has two atmospheric windows (780–1,000 cm^{-1} and 1,080–1,275 cm^{-1}, which overlay with T_0 = ~295 K) where very little infrared radiation is absorbed by the atmosphere, so the effective opaque height is zero. The measured emission spectrum corresponds to blackbody radiation emitted at the Earth's surface temperature of T_0 = ~295 K. The two atmospheric windows are graphically illustrated by Figure 11c.

Simple conceptual model of global warming

Figure 12 illustrates a simple conceptual model that describes radiative transfer in the atmosphere. Above the effective opaque height, the atmosphere is modeled as completely transparent. Below the effective opaque height, a portion of the infrared radiation emitted from the Earth's surface is recycled back to the Earth. The upper surface of the opaque atmosphere is modeled as a blackbody that radiates outwardly into space. As previously described, the net amount of energy that reaches and leaves the Earth-atmosphere system is 236 W/m^2.

Figure 12a depicts the current situation assuming the Earth is thermally balanced. The net solar energy input is balanced by the same amount of infrared radiation emitted from the surface of the opaque atmosphere, which is at 255 K. The current surface temperature of the Earth is 288 K; at this temperature, the Earth radiates 384 W/m^2, of which 148 W/m^2 is recycled.

Figure 12b shows the situation when the partial pressure of greenhouse gases increases, which increases the effective opaque height. The lapse rate is the same as in Figure 12a, so the surface temperature of the opaque atmosphere is lower. This reduces the infrared radiation emitted from the surface of the opaque atmosphere below the incoming solar energy — thus, the system is not in energy balance. Thermal energy is stored within the opaque atmosphere causing the temperatures of the atmosphere and Earth's surface to increase.

Figure 12c shows the system after a new thermal equilibrium is established. The temperatures of the atmosphere and the Earth's surface have both increased by 2 K. The surface of the opaque atmosphere has returned to 255 K, which emits infrared radiation that matches the incoming solar energy.

Figure 12 illustrates the fundamental mechanism behind global warming. As greenhouse gases are emitted into the atmosphere, the effective opaque height increases. At greater heights, the Earth's atmosphere is colder, which reduces infrared radiation from the surface of the opaque atmosphere, thus throwing the system out of balance. As thermal energy is stored within the atmosphere, the temperature of

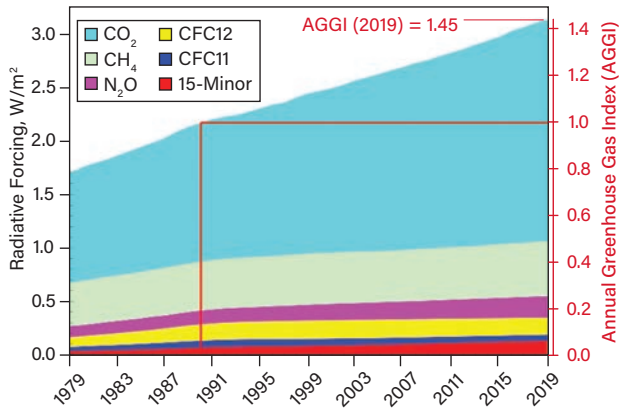

▲ **Figure 13.** Radiative forcing due to greenhouse gases in the atmosphere can be estimated by radiative transfer computer models *(13)*. The forcing (on the left vertical axis) is expressed relative to the year 1750, which is defined as preindustrial. The annual greenhouse gas index (AGGI) (right vertical axis) is the total direct radiative forcing from long-lived greenhouse gases relative to 1990. Source: *(13)*.

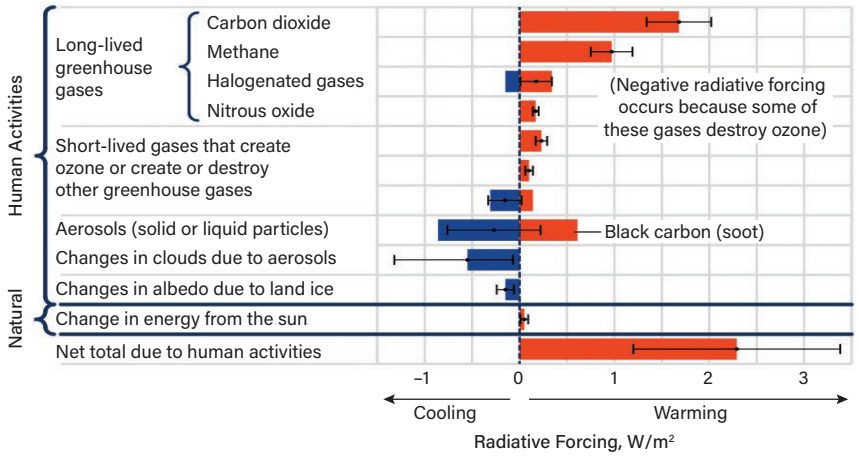

▶ **Figure 14.** In 2011, net total radiative forcings due to human activity relative to 1750 (which is defined as preindustrial) are estimated to be 2.3 W/m^2. Source: *(14)*.

the opaque atmosphere increases until infrared emissions match the incoming solar energy. In this process, the Earth's surface temperature increases as well.

Atmospheric radiative transfer modeling

Although the physics of radiant absorption and emission are conceptually simple, the detailed interactions between radiation and multiple greenhouse gases at elevations within the atmosphere are very complex. As described by Eq. 10, the absorption characteristics depend on the temperature and partial pressure of each greenhouse gas at each point in the atmosphere. When a gas molecule absorbs radiation, the radiation is converted to internal energy that is transferred to neighboring molecules. Those warmed molecules, in turn, reemit radiation, which other gas molecules absorb, and so on.

Because of the importance of atmospheric radiative transfer, numerous sophisticated computer models have been developed *(11)*. Of these, one of the most popular for climate modeling is MODTRAN, which has been validated against satellite data and is available free *(12)*.

Using measured concentrations of greenhouses gases averaged over the Earth's atmosphere, MODTRAN can determine the radiant forcing caused by greenhouse gases (Figure 13) *(13)*. The United Nations Intergovernmental Panel on Climate Change (IPCC) defines climate forcing as an externally imposed perturbation in the radiative energy budget of the Earth climate system, *e.g.,* through changes in solar radiation, changes in the Earth's albedo, or changes in atmospheric gases and aerosol particles. Since 1979, radiant forcing has been increasing nearly linearly.

Figure 14 *(14)* places the greenhouse gas forcings in the context of other forcings that warm or cool the planet. Overall, the radiative forcing in 2011 is estimated to be 2.3 W/m^2 higher than in 1750, which the IPCC defines as preindustrial.

The expected temperature rise F from this added net radiative forcing can be calculated by differentiating the Stefan-Boltzmann equation:

$$F = \varepsilon\sigma T^4$$

$$\frac{dF}{dT} = 4\varepsilon\sigma T^3$$

$$\frac{dT}{dF} = \frac{1}{4\varepsilon\sigma T^3}$$

$$dT = \frac{dF}{4\varepsilon\sigma T^3}$$

$$= \frac{2.3\ \text{W/m}^2}{4(0.984)\left(5.670373\times10^{-8}\ \text{W/m}^2\text{-K}^4\right)(273.15+15\ \text{K})}$$

$$= 0.64\ \text{K}$$

According to this calculation, an additional 2.3 W/m^2 of forcing should increase the global average temperature by 0.64 K.

Feedback

The addition of greenhouse gases to the atmosphere is a forcing that acts directly on Earth's climate. Numerous feedback mechanisms can either accentuate (positive feedback) or mitigate (negative feedback) the forcing. For example, rising temperatures melt sea ice, thereby allowing the underlying ocean water to absorb more sunlight, which reduces the albedo (positive feedback). On the

Table 1. Positive feedback mechanisms increase global warming, while negative feedback mechanisms reduce global warming.

Positive Feedback Increases Global Warming	Negative Feedback Reduces Global Warming
Atmospheric water vapor	Increased plant growth
Melted ice	Biosequestration
Methane release	Ocean sequestration
More-frequent forest fires	Formation of seashells
Release of CO_2 from oceans	Blackbody radiation
Increase in high, thin clouds	Increase in low, thick clouds

other hand, higher carbon dioxide concentrations enhance plant growth, which sequesters more carbon (negative feedback). Table 1 lists various positive and negative feedback mechanisms.

Feedback can be quantified by:

$$\Delta T_{measured} = \frac{\Delta T_{calc}}{1-f}$$

$$f = 1 - \frac{\Delta T_{calc}}{\Delta T_{measured}} \qquad (11)$$

where $\Delta T_{measured}$ is the actual global temperature change, ΔT_{calc} is the calculated temperature increase from the additional radiant forcing, and f is the feedback factor ($f > 1$ for positive feedback, $f < 1$ for negative feedback). As reported in the preceding article, the average global temperature was 13.6°C in 1750 and 14.6°C in 2011 — an increase of 1.0°C. So:

$$f = 1 - \frac{\Delta T_{calc}}{\Delta T_{measured}} = 1 - \frac{0.64°C}{1.0°C} = 0.36$$

According to this calculation, the feedback is positive, so the warming trends are accentuated by feedback mechanisms.

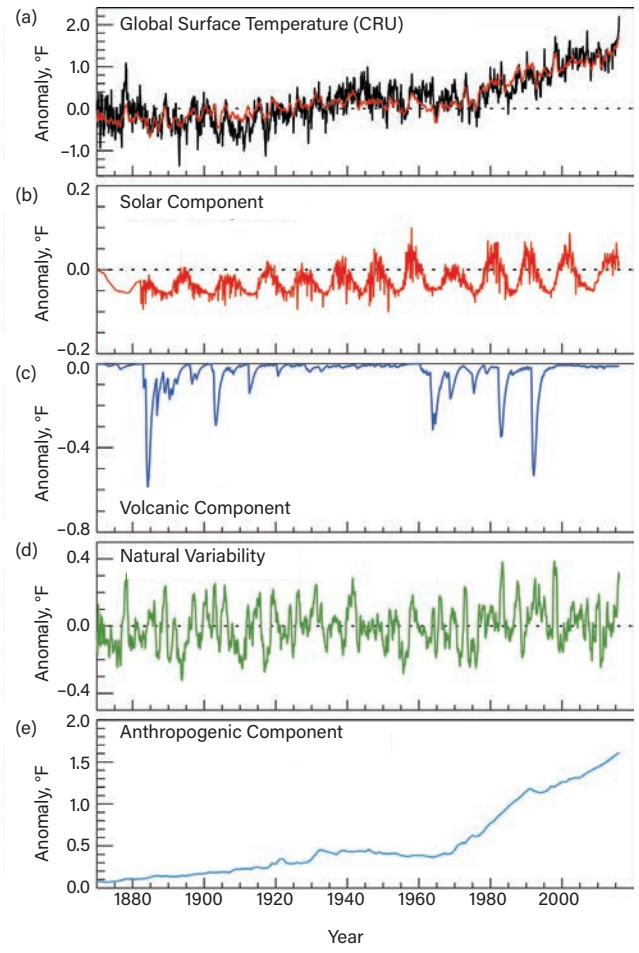

▲ **Figure 15.** Effect of forcing on global temperature. (a) Observed temperature data are shown in black, and the combined effects of all forcings are shown in red. (b) The total forcings include contributions by variations in solar output, (c) aerosols from volcanic eruptions, and (d) natural variability related to El Niño/Southern Oscillation. (e) Anthropogenic activities that produce greenhouse gases contribute to warming and anthropogenic aerosols contribute to cooling. Source: *(7)*.

General circulation models

General circulation models (GCMs), sometimes called global climate models, simulate the various processes that affect climate. They include factors such as solar radiation, albedo, atmospheric radiative transfer, circulation patterns in the oceans and atmosphere, water vapor pressure, temperature, cloud formation, ice formation, greenhouse gas emissions, aerosols, vegetation, and soot deposition onto ice. GCMs were first created in the 1950s. Since then, dozens have been created by various research groups.

The GCM numerical simulations solve the Navier-Stokes equations in the atmosphere and oceans coupled with energy flows. Obviously, these models are enormously complex and require supercomputers to run the code. To solve the equations, the Earth is divided into three-dimensional grids and finite-element techniques are used. Horizontal grid dimensions are typically between 250 km and 600 km. The atmosphere is simulated using 10 to 20 vertical layers and the oceans are sometimes represented by as many as 30 layers.

The models describe well-known physical and chemical processes without the use of fudge factors. However, because some processes — such as cloud formation and convection patterns — occur at a length scale less than the grid size, a technique called parameterization is employed. For example, rather than operate at a grid scale that allows each individual cloud to be resolved, a typical or average value of cloud cover would be used to describe the clouds within the large grid. Modeling clouds is one of the largest sources of uncertainty in GCMs and remains a vibrant research topic.

Figure 15a *(7)* compares climate models (red) to historical temperature data (black). Contributions of the dominant forcings are shown in Figure 15b–e. Temperature variations from the solar constant (Figure 15b) are very small. Volcanic activity (Figure 15c) has a dramatic cooling effect, but is short-lived. Natural variability (Figure 15d) results from El Niño/Southern Oscillation. Anthropogenic activity (Figure 15e) has a dominant warming effect with an inflection that occurred in 1970.

Based on GCMs, Figure 16 *(15)* summarizes our current understanding of the energy flows in Earth's climate. A portion of the incoming solar radiation is reflected by clouds and the surface. The remaining solar energy is absorbed by

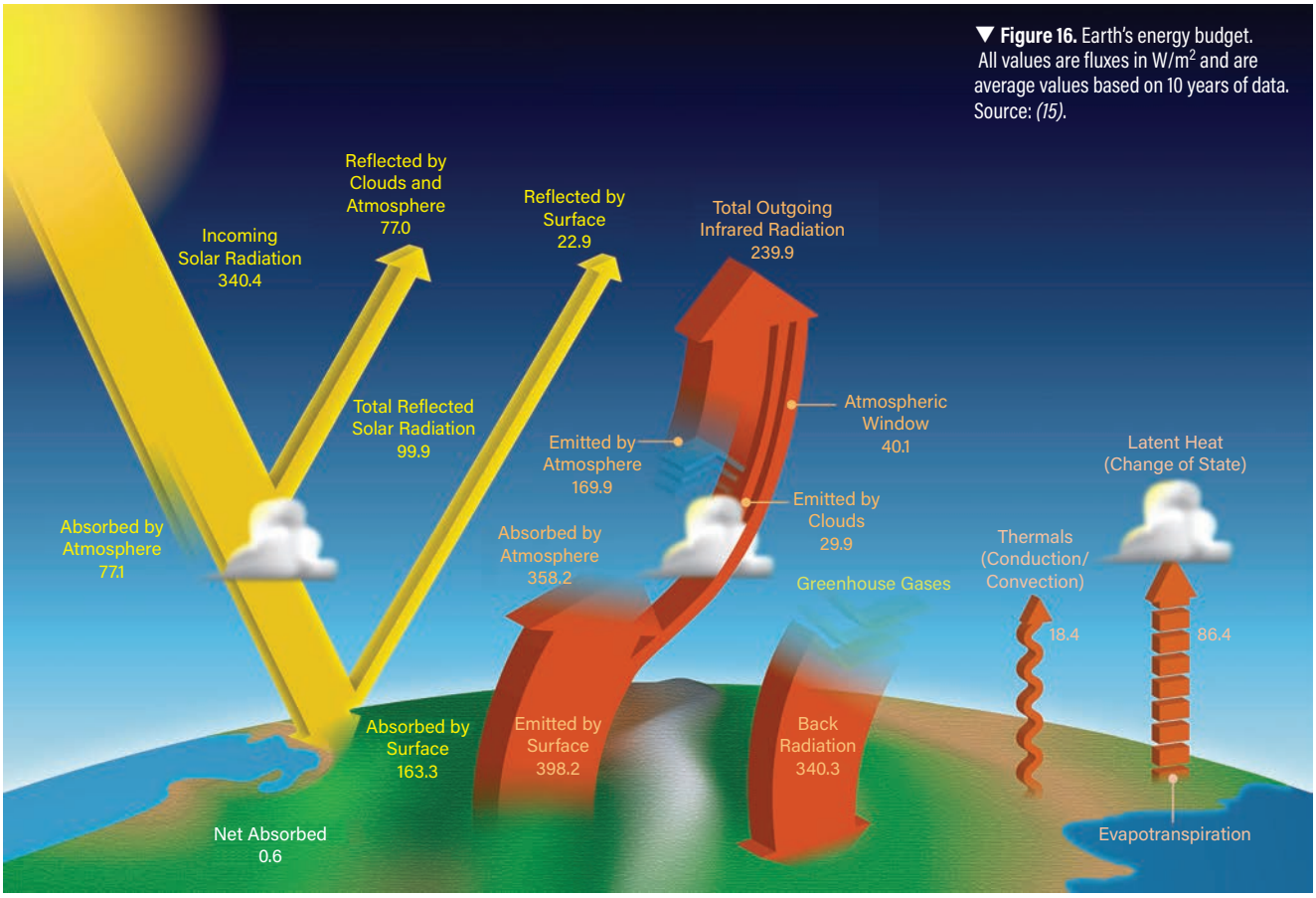

▼ **Figure 16.** Earth's energy budget. All values are fluxes in W/m^2 and are average values based on 10 years of data. Source: *(15)*.

the Earth. Of the energy that is absorbed, a small portion is transferred to higher elevations by convection currents and phase changes. The majority of the absorbed energy is transferred as infrared radiation. A portion is emitted directly to space through the atmospheric window. The remaining portion of the emitted infrared radiation is absorbed by the atmosphere and is recycled. The recycled energy impinges on the Earth, which raises the surface temperature until it is sufficiently high enough to emit to space. Increasing concentrations of greenhouse gases impede radiative transfer through the atmosphere, causing more energy to recycle, which raises the surface temperature.

Because the soil and oceans have heat capacity, some energy must be retained within the system. The current estimate is that 0.6 W/m^2 is the net retention of thermal energy, which increases the Earth's temperature.

To validate and tune the models, researchers hindcast to back-predict historical data. The validated models are used to forecast into the future using various scenarios that depend on the assumed utilization of fossil fuels, changes in land use, etc.

GCMs are highly nonlinear and highly coupled, which makes them behave chaotically. Chaotic systems do not

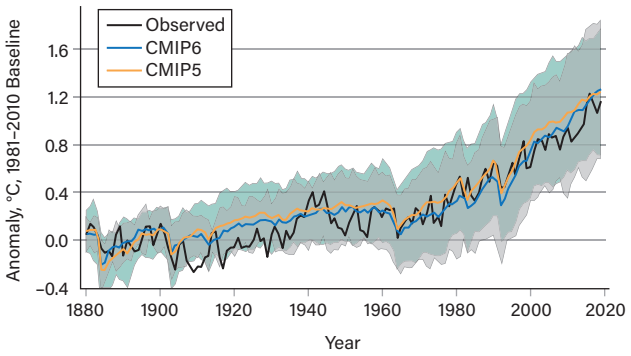

▲ **Figure 17.** Measured global average surface temperature (black line) compares favorably with model simulations. The Coupled Model Intercomparison Project (CMIP) uses about 100 models from 49 different modeling groups. CMIP5 supported the 2013 IPCC fifth assessment report and CMIP6 will support the 2021 IPCC sixth assessment report. Solid lines represent the multimodel mean, whereas the shaded areas represent ±2 standard deviations. Source: *(16, 17)*.

behave randomly; rather, they are very sensitive to the choice of initial conditions, boundary conditions, and parameters. By running multiple models multiple times, the average performance does a good job of describing the data (Figure 17) *(16, 17)*. Although the focus of GCMs is to describe average global temperatures, they describe many

Table 2. Predictions of global climate models that agree with data.
More warming over land than ocean
More warming in winter than in summer
Cooling of the stratosphere
Warming in the upper troposphere
Increased water vapor
Large warming in the Arctic and less warming in the Antarctic

other features of climate as well (Table 2).

Figure 18 *(18)* shows the GCM simulations with (Figure 18a) and without (Figure 18b) human influences. With human influences, the models describe the historical temperature data very well. However, when the models are run without human influences, they describe the historical temperature data very well only until about 1960. After 1960, the model without human influences can no longer describe the data. This result is easily understood. Before 1960, the net human influence on average atmospheric temperature was small and remained below natural variability. However, after 1960, human activity has been powerful enough to increase average atmospheric temperature above natural variability. (The pivotal significance of 1960 is also illustrated in Figure 4, p. 15, of the preceding article, on climate observations. Prior to 1960, temperature and total solar irradiance were well correlated; however, after 1960, they were no longer correlated.)

Let's look at carbon dioxide as a driver of climate change. The preindustrial carbon dioxide concentration in the atmosphere was 280 ppm (5.10×10^{16} mol). In 1960, it was 317 ppm (5.77×10^{16} mol), and in 2020 it was 415 ppm (7.55×10^{16} mol). Of total carbon dioxide emissions, only 27% occurred before 1960. Seventy-three percent of emissions have occurred since then, and have been sufficiently large to affect the climate.

The GCM simulations with and without human influ-

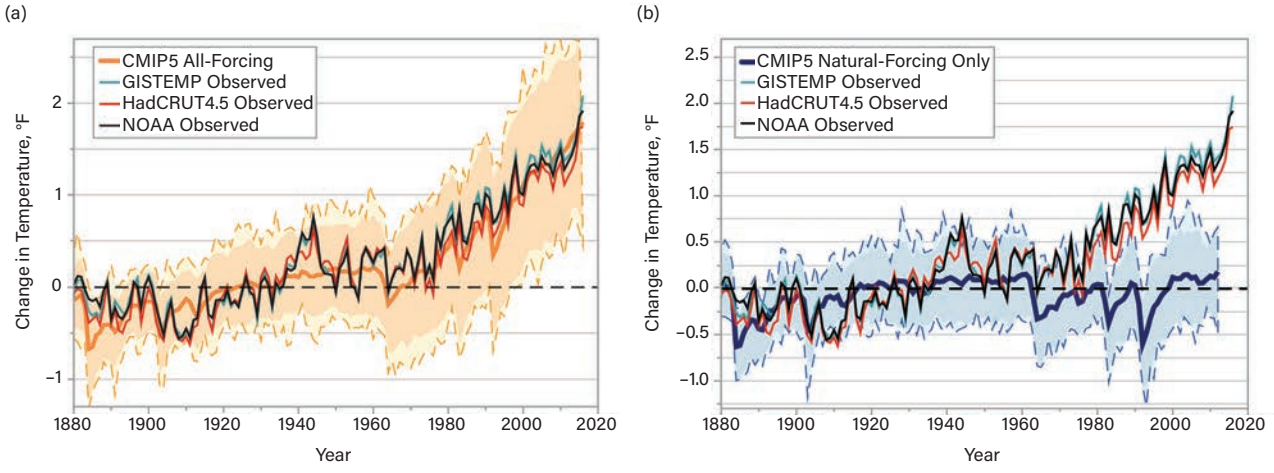

▲ **Figure 18.** Global climate model simulations with (a) natural and human forcings and (b) only natural forcings. Source: *(18)*.

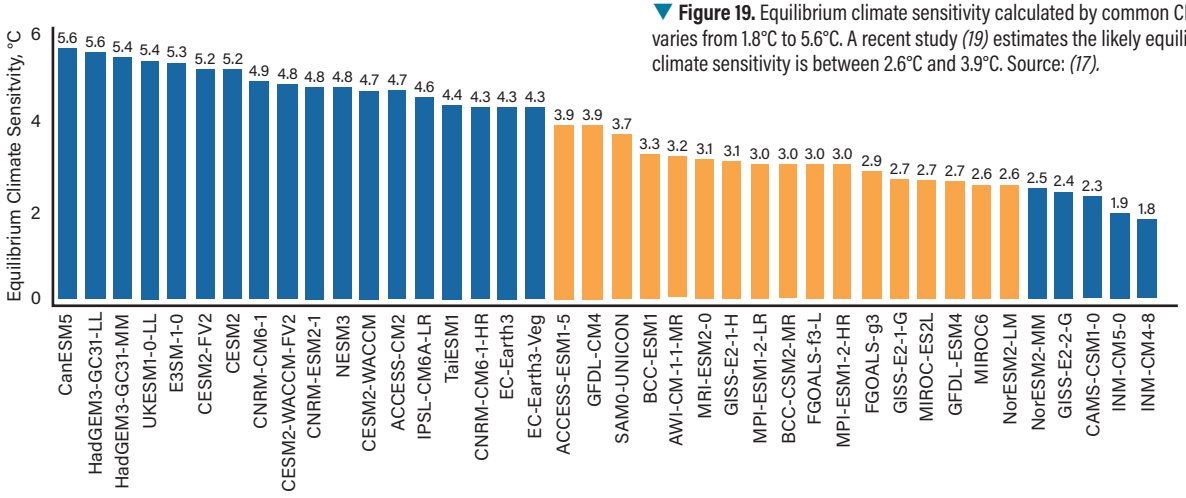

▼ **Figure 19.** Equilibrium climate sensitivity calculated by common CMIP models varies from 1.8°C to 5.6°C. A recent study *(19)* estimates the likely equilibrium climate sensitivity is between 2.6°C and 3.9°C. Source: *(17)*.

ences provide strong evidence that human emissions of carbon dioxide and other greenhouse gases are causing global warming. In the absence of a controlled experiment, this is the best information available. No other hypothesis has been able to explain the data.

In climate modeling, an important parameter is the equilibrium climate sensitivity — *i.e.,* the equilibrium temperature increase that results from doubling the CO_2 concentration. A recent study estimates the likely equilibrium climate sensitivity is between 2.6°C and 3.9°C *(19)*, a range that includes 17 of 40 models used in IPCC projections (Figure 19) *(17)*. The wide variation in equilibrium climate sensitivity indicates that the wide error bands in Figure 17 are only partly attributed to the inherently chaotic nature of climate models. In addition, some of the variation can be attributed to fundamental differences in the physics represented within each model. Compared to the likely equilibrium climate sensitivity of 2.6–3.9°C, more models predict warmer values than cooler values. In making projections, the IPCC uses a large number of models, which reduces the impact of outliers on the mean value; however, the outliers do impact the reported standard deviation.

Closing thoughts

Climate science is a well-established scientific field that has benefitted from enormous resources devoted to understanding the planet's climate system. Although the state of knowledge is not perfect, the state of knowledge is quite advanced.

The data clearly show that the Earth is warming, which can be explained both by simple algebraic and complex GCM models. Fundamentally, it is quite simple. The addition of greenhouse gases impedes radiative heat transfer, causing radiant energy to be recycled back to the Earth's surface. Ultimately, to transfer this recycled energy to the universe, the surface temperature must increase.

Experimental evidence indicates that the Earth-atmosphere system responds in a positive feedback — temperature increases directly attributed to additional radiant forcings will be amplified and enhance the warming further. CEP

Acknowledgments

The author expresses gratitude to climate scientists Gunnar Schade and John Nielsen-Gammon of Texas A&M Univ. for reviewing this document for accuracy.

Literature Cited

1. **Burrows, K.,** "Is Our Climate Changing? And Why?," Climate Science for Skeptics, cs4s.net/climate-2.html (accessed Sept. 7, 2020).
2. **Pidwirny, M.,** "Atmospheric Pressure," in "Fundamentals of Physical Geography," 2nd Ed., physicalgeography.net/fundamentals/7d.html (2006) (accessed Sept. 7, 2020).
3. **University Corporation for Atmospheric Research,** "Change in the Atmosphere with Altitude," UCAR, Boulder, CO, scied.ucar.edu/learning-zone/how-weather-works/change-atmosphere-altitude (accessed Sept. 7, 2020).
4. **Brandon, M.,** "The Oceans," adapted extract from Course S206 Environmental Science, the Open University, open.edu/openlearn/ocw/mod/oucontent/view.php?id=20129&printable=1 (accessed Sept. 7, 2020).
5. **Inouye, B.,** "Compare-Contrast-Connect: Seasonal Variation in Ocean Temperature Vertical Profiles," Exploring Our Fluid Earth, Univ. of Hawaii, manoa.hawaii.edu/exploringourfluidearth/physical/density-effects/ocean-temperature-profiles/compare-contrast-connect-vertical-profiles-ocean (accessed Sept. 7, 2020).
6. **Konda, M., *et al.,*** "Measurement of the Sea Surface Emissivity," *Journal of Oceanography*, **50,** pp. 17–30 (1994).
7. **Jacob, D. J.,** "The Greenhouse Effect," Chapter 7 in "Introduction to Atmospheric Chemistry" Princeton Univ. Press, Princeton, NJ, acmg.seas.harvard.edu/people/faculty/djj/book/bookchap7.html (1999) (accessed Sept. 7, 2020).
8. **Rohde, R. A.,** "Atmospheric Transmission," commons.wikimedia.org/wiki/File:Atmospheric_Transmission.png (accessed Sept. 7, 2020).
9. "Solar Spectrum," commons.wikimedia.org/wiki/File:Solar_spectrum_en.svg (accessed Sept. 7, 2020).
10. **Petty, G. W.,** "A First Course in Atmospheric Radiation," 2nd Ed., Sundog Publishing, Madison, WI (2006).
11. "Atmospheric Radiative Transfer Codes," en.wikipedia.org/wiki/Atmospheric_radiative_transfer_codes (accessed Sept. 7, 2020).
12. "MODTRAN Infrared Light in the Atmosphere," climatemodels.uchicago.edu/modtran/modtran.doc.html (accessed Sept. 7, 2020).
13. **Butler, J. H., and S. A. Montzka,** "The NOAA Annual Greenhouse Gas Index (AGGI)," esrl.noaa.gov/gmd/aggi/aggi.html (accessed Sept. 7, 2020).
14. **U.S. Environmental Protection Agency,** "Climate Change Indicators: Climate Forcing," epa.gov/climate-indicators/climate-change-indicators-climate-forcing (accessed Sept. 7, 2020).
15. **Loeb, N.,** "What is Earth's Energy Budget? Five Questions with a Guy Who Knows," Atkinson, J., ed., National Aeronautics and Space Administration, nasa.gov/feature/langley/what-is-earth-s-energy-budget-five-questions-with-a-guy-who-knows (Aug. 6, 2017).
16. "Institutions Participating in WCRP-CMIP CMIP6_CVs version: 6.2.54.7," wcrp-cmip.github.io/CMIP6_CVs/docs/CMIP6_institution_id.html (accessed Sept. 7, 2020).
17. **Hausfather, Z.,** "CMIP6: The Next Generation of Climate Models Explained," carbonbrief.org/cmip6-the-next-generation-of-climate-models-explained (Dec. 2, 2019) (accessed Sept. 7, 2020).
18. **Wuebbles, D. J., *et al.,* eds.,** "Climate Science Special Report: Fourth National Climate Assessment, Volume 1," U.S. Global Change Research Program, Washington, DC, science2017.globalchange.gov/chapter/3 (2017) (accessed Sept. 7, 2020).
19. **Voosen, P.,** "After 40 Years, Researchers Finally See Earth's Climate Destiny More Clearly," *Science,* doi:10.1126/science.abd9184 (July 22, 2020).

Impacts of Climate Change

Mark Holtzapple ▪ Texas A&M Univ.

Climate change has far-reaching impacts now and into the future.

The preceding articles in this issue provide evidence that global warming is occurring and review the theoretical basis for its mechanisms. This article describes current and future impacts of this change in climate.

CURRENT IMPACTS

Plant growth

Carbon dioxide concentration has a major impact on the growth rates of C3 and C4 plants, as shown in (Figure 1) *(1)*. C3 plants conduct photosynthesis directly by introducing carbon dioxide into the Calvin cycle, the initial product of which is a three-carbon compound (3-phosphoglycerate). In contrast, C4 plants conduct photosynthesis indirectly using a so-called "carbon dioxide pump" that first produces a four-carbon compound (malate), which then releases carbon dioxide that enters the Calvin cycle. C4 plants — such as corn, sorghum, and sugarcane — expend "pump energy" to concentrate carbon dioxide from the atmosphere into their cells. At low carbon dioxide concentrations, the carbon dioxide pump increases plant growth rates. C3 plants — such as rice, wheat, and potatoes — do not have a carbon dioxide pump, so they have slower growth rates than C4 plants at lower carbon dioxide concentrations. At low carbon dioxide concentrations, both types of plants grow more rapidly as carbon dioxide concentrations increase; therefore, plants help dampen increases in carbon dioxide concentrations by removing it from the atmosphere.

During preindustrial times (prior to 1750), the concentration of carbon dioxide in the atmosphere was about 280 ppm, and C4 plants grew about 1.4 times faster than C3 plants. At current carbon dioxide concentrations of approximately 400 ppm, C4 plants grow about 1.1 times faster than C3 plants. At higher carbon dioxide concentrations (~450 ppm), C4 plants lose their competitive advantage, because the

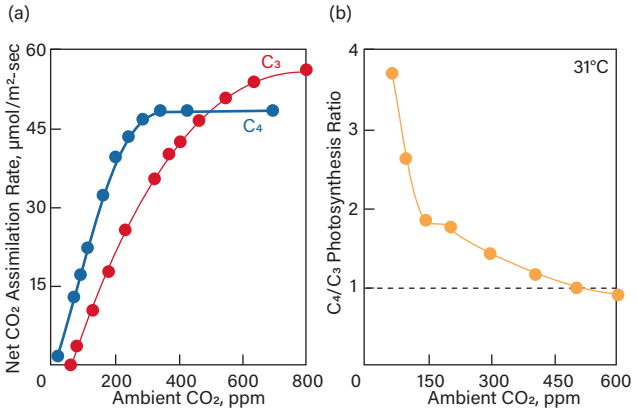

▲ **Figure 1.** Carbon dioxide concentration has a major impact on the growth rate of C3 and C4 plants. (a) Measured rate of carbon dioxide assimilation for each type of plant. (b) Growth rate of C4 plants relative to C3 plants. Source: *(1)*.

energy required to pump carbon dioxide does not return sufficient dividends.

Figure 2 *(2)* shows the change in leaf-covered land area from 1982 to 2015 as measured by NASA's moderate-resolution imaging spectrometer and the National Oceanic and Atmospheric Administration's (NOAA) advanced very-high-resolution radiometer satellite instruments. At current carbon dioxide concentrations, photosynthesis is not saturated; therefore, higher carbon dioxide concentrations have the effect of fertilizing plants, allowing them to grow more abundantly. More extensive plant growth is a negative feedback mechanism that mitigates global warming.

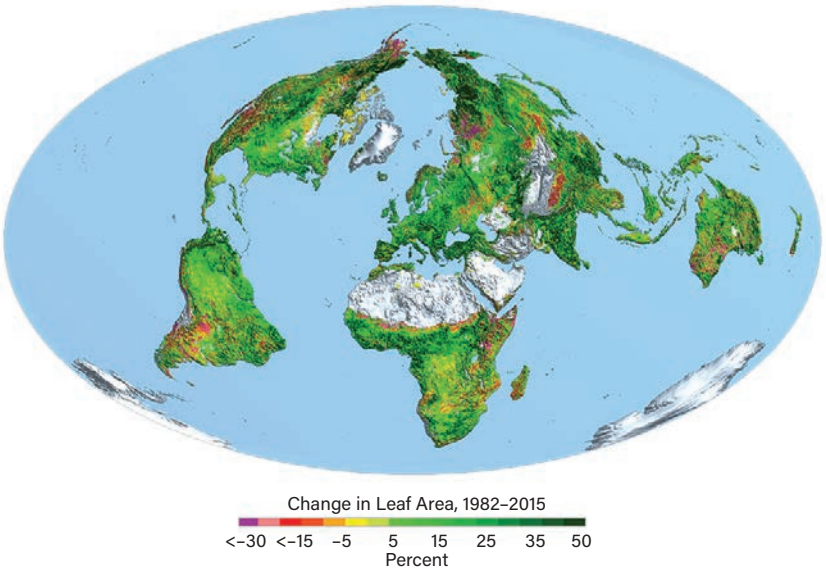

▲ **Figure 2.** Satellite imaging reveals the change in leaf area from 1982 to 2015. Credit: Boston Univ. / R. Myneni. Source: *(2).*

Permafrost

Permafrost is ground that is at or below the freezing point of water for two or more successive years. Permafrost potential is defined by the decadal air temperature — if the annual average temperature during a 10-year period was 0°C or below, that area was regarded as permafrost *(3)*. Figure 3 *(3)* shows the estimated decline in permafrost potential across the northern hemisphere from 1850 to 2013. Since 1900, approximately 4 million km^2 of permafrost has thawed.

The permafrost contains enormous quantities of biomass that is normally frozen, and hence biologically inactive. When the permafrost thaws, biological activity resumes. Because the biomass is submerged, oxygen is not readily available and anaerobic decomposition occurs, releasing carbon dioxide and methane — both potent greenhouse gases. Figure 4 *(4)* shows the tundra landscape changing as thermokarst lakes form from thawing tundra.

Loss of permafrost is a positive feedback mechanism that enhances global warming.

Ice

In regions with persistent ice — sea ice, land ice, or glaciers — atmospheric temperatures above 0°C will cause the ice to melt.

Sea ice. Figure 5 *(5)* shows the average amount of Arctic sea ice measured by satellite each September, when coverage is at its minimum. Sea ice coverage has been declining at a rate of 12.9% per decade. These satellite

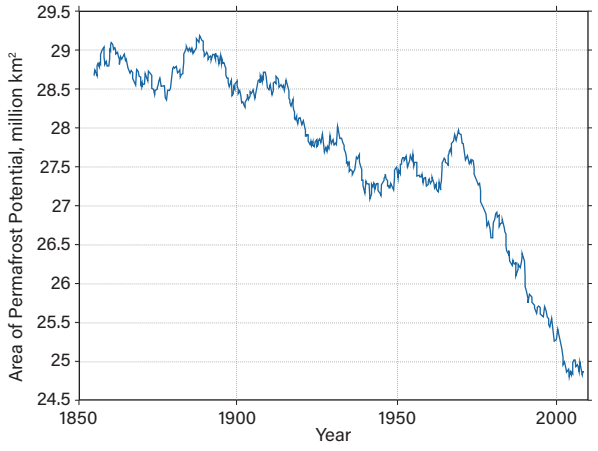

▲ **Figure 3.** Since 1900, approximately 4.5 million km^2 of northern hemisphere permafrost potential has been lost. Source: *(3).*

▲ **Figure 4.** Thermokarst lakes formed from thawing tundra in Hudson Bay, Canada. Source: *(4).*

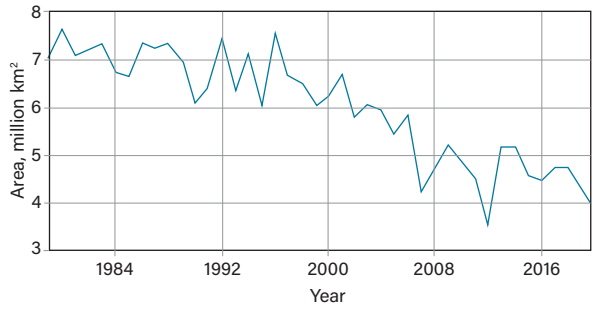

▲ **Figure 5.** Arctic sea ice coverage, measured at its minimum each September, has been declining by about 13% per decade. Source: *(5)*.

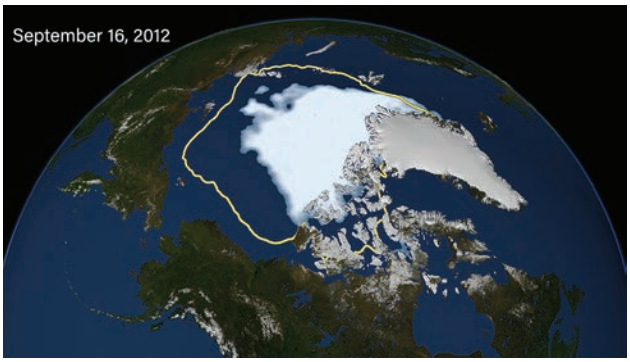

▲ **Figure 6.** Arctic sea ice coverage was at a record minimum in September 2012. The yellow line represents the average sea ice minimum for 1979–2010. Source: *(6)*.

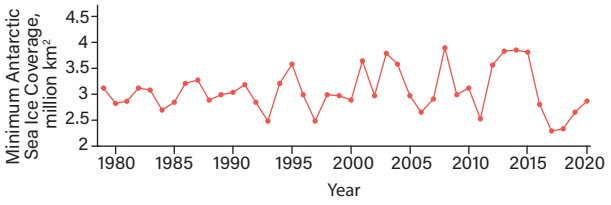

▲ **Figure 7.** Antarctic sea ice coverage, measured at its minimum in February, has been fluctuating. Source: *(7)*.

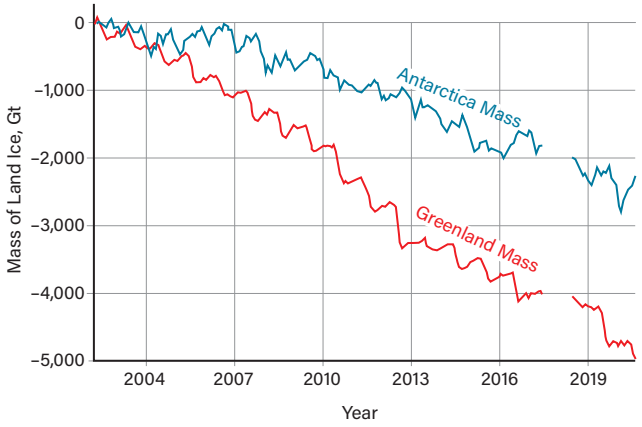

▲ **Figure 8.** The mass of land ice in Greenland (red) and Antarctica (blue) has been steadily decreasing. (Data for 2017–2018 were not included.) Source: *(9)*.

measurements are consistent with visual observations of Arctic sea ice.

Figure 6 *(6)* shows the extent of sea ice in September 2012, when it was at its all-time minimum. For comparison, the yellow outline indicates the average minimum ice coverage over the period of 1979–2010. Visual observations clearly reveal that Arctic sea ice is declining.

The consequence of this decline is a dramatic local change in albedo. As noted in the article on climate observations previously in this issue, ice is much more reflective than seawater (Part 2, Figure 5, p. 16), so melting sea ice is a positive feedback that exacerbates global warming. The impact of this positive feedback mechanism is dramatically illustrated by the abnormally high Arctic temperatures in February 2018, which were 12.3°C warmer than the average temperatures from 1951 to 1980 (Part 2, Figure 21, p. 22). Unlike in the Arctic, the extent of sea ice around Antarctica has fluctuated and has not displayed a long-term downward or upward trend (Figure 7) *(7)*.

According to Archimedes' principle, the mass of ice

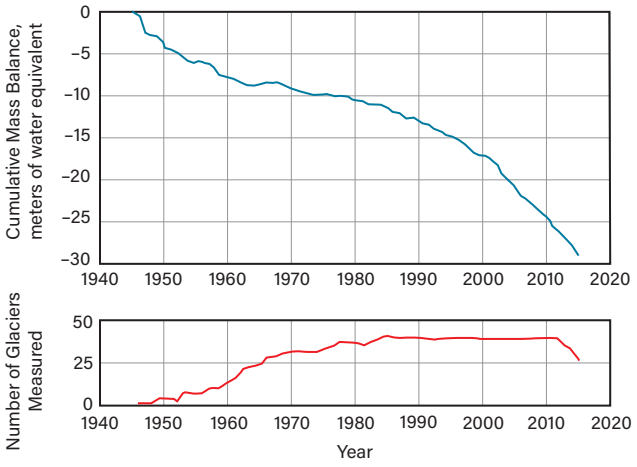

▲ **Figure 9.** The balance between snow accumulation and melting indicates how glaciers around the world are shrinking, shown here relative to the base year of 1945. Source: *(10)*.

▲ **Figure 10.** The Muir Glacier in Alaska, photographed from the same vantage point on August 13, 1941, and August 31, 2004. Source: *(11)*.

equals the mass of water displaced by the ice. In the case of a drinking glass filled with ice and freshwater, as the ice melts, there is no change in the water level. Because the compositions of ice and freshwater are identical, there is no volume change when the melted ice mixes with the water. In contrast, in the case of ice floating in seawater, the salt concentrations in ice and seawater are not identical. When the melted ice dissolves into the seawater, there is a volume change of mixing, which results in a change in sea level. It is estimated that if all existing floating shelf ice melted, the global sea level would rise by about 4 cm. Because it takes time to mix melted ice with seawater, it is estimated that it will take about 1,000 years for the sea level to rise fully from this phenomenon *(8)*.

Land ice. Figure 8 *(9)* shows the volume of land ice in Greenland and Antarctica measured by NASA's Gravity Recovery and Climate Experiment (GRACE) satellites since 2002. The rate of loss is 279 km^3 and 148 km^3 per year for Greenland and the Antarctic, respectively. Much of the melting land ice ultimately flows to the oceans, causing ocean levels to rise.

Glaciers. Figure 9 *(10)* shows the loss of ice and snow in reference glaciers around the world. Meltwater from glaciers ultimately flows to the oceans, causing sea levels to rise.

Figure 10 *(11)* shows the Muir Glacier in Alaska, photographed from the same vantage point in 1941 and in 2004. Clearly, a significant loss of ice occurred during this period.

The loss of glaciers has been popularized by the documentary *Chasing Ice*.

Sea levels

Figure 11 *(12)* shows historical changes in sea levels measured by tide gauges starting in 1880. More recently, satellites have measured sea levels as well. Sea levels rise from melting ice, as described previously, but also due to thermal expansion as ocean temperatures increase.

Even in the absence of storms, rising sea levels cause sea-level cities to flood. The term nuisance flooding refers to low levels of inundation that do not pose significant threats to public safety or cause major property damage, but can disrupt routine day-to-day activities, strain infrastructure systems such as roadways and sewers, and cause minor property damage *(13)*.

Such nuisance flooding has increased substantially since the 1950s (Figure 12) *(14)*. Figure 13 *(15)* and Figure 14 *(16)* show nuisance flooding in Washington, DC, and Miami, FL, respectively, during a king tide, a non-scientific term that describes exceptionally high tide events. King tides occur when the moon, sun, and Earth align, making them predictable based on the known motion of these celestial bodies. King tides are even stronger when the moon is closest to the Earth during its perigee (as was the case in the flooding depicted in Figure 13). These nuisance floods portend future flooding as sea levels continue to rise from climate change.

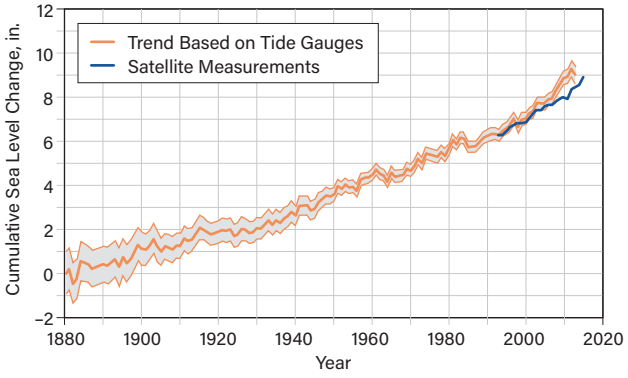

▲ **Figure 11.** Sea levels have been rising since the beginning of the 20th century. Source: *(12)*.

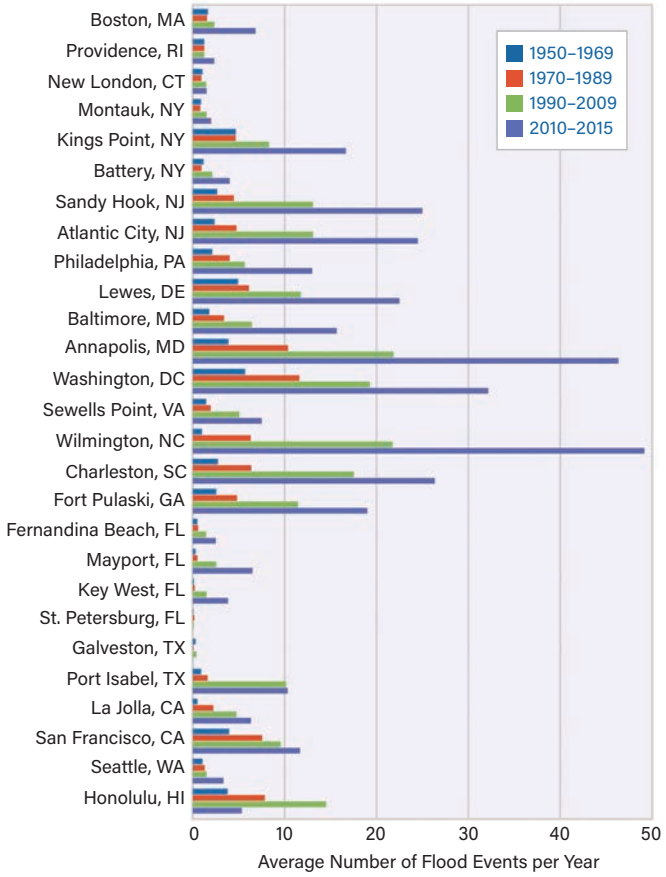

▲ **Figure 12.** Nuisance flooding in U.S. coastal cities has been increasing since the 1950s. Source: *(14)*.

Article continues on next page

Cyclones

In the tropics and subtropics, warm surface waters drive the formation of rotating, organized systems of clouds and thunderstorms called tropical cyclones. Once a tropical cyclone sustains wind speeds over 74 mph, it is classified as a hurricane (in the Atlantic and Northeast Pacific), typhoon (Northwest Pacific), or cyclone (South Pacific and Indian Ocean). Here we use the term cyclone for all of these events.

▲ **Figure 13.** Hains Point, in Washington, DC, experienced nuisance flooding on Sept. 26, 2015, when a perigee moon coincided with high tide. Source: *(15)*.

▲ **Figure 14.** Sunny day tidal flooding occurred in downtown Miami in October 2016. Source: *(16)*.

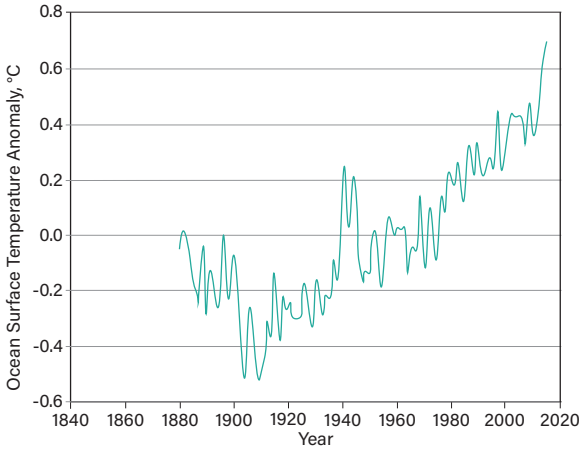

▲ **Figure 15.** Annual mean anomalies of ocean surface temperature relative to 1951–1980. Source: Data from *(17)*.

Figure 15 *(17)* shows that ocean surface temperatures have increased by 1.0°C since 1900. Figure 16 *(18)* shows the intensity of cyclones measured by accumulated cyclone energy (ACE), an index that combines the number of systems, their duration, and their intensity. It is calculated by squaring the maximum sustained surface wind every six hours that the cyclone is a named storm and summing it for all storms over the season. On average, this index appears to have increased by 70% since 1850; however, because early historical data are less complete, it is difficult to make a definitive statement. The impact of global warming on cyclones is an active area of research.

In the U.S., the 2017 hurricane season was particularly intense. Hurricane Harvey caused severe flooding in Houston, TX (Figure 17) *(19)*. Nearly 52 in. of rain fell during that storm, which exceeded the previous record (48 in.) for the contiguous 48 states set by Tropical Storm Amelia in 1978 *(19)*. Some regions experienced a thousand-year rainfall (Figure 18) — *i.e.,* based on historical rain patterns, such rainfall would be expected to occur once every 1,000 years, or, stated differently, in a given year, the probability of this level of rainfall is 0.1%. This record rainfall occurred after 500-yr rainfall events were reported to have occurred in both 2015 and 2016 *(20)*. (Some researchers dispute whether the 2016 occurrence was a 500-yr rainfall event.)

After catastrophic weather events, a common question relates to attribution *(21)*: "The oft-asked question is whether human-caused climate change caused these storms. However, this is the wrong way of looking at it. Climate change reflects a change in the background state in which all weather exists. It does not, by itself, cause hurricanes, but it can certainly make a hurricane's impacts worse. Climate change can warm the waters which hurricanes use for fuel. Climate change can warm the atmosphere allowing for more moisture

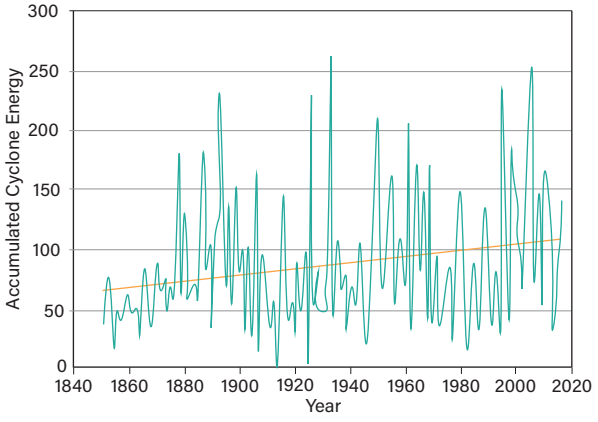

▲ **Figure 16.** The historical intensity of cyclones is characterized by accumulated cyclone energy, an index that combines the numbers of systems, their duration, and their intensity. Source: Data from *(18)*.

to be evaporated and more rain to fall. And climate change can melt land ice and expand ocean waters, leading to sea level rise and making it easier for coastal areas to flood."

Precipitation

As global temperatures rise, more water evaporates from the oceans, lakes, and soil, which increases the moisture content of the atmosphere, which in turn produces more rainfall. Figure 19 *(22)* shows increases in land area of the contiguous 48 states impacted by extreme single-day precipitation events. Figure 20 *(23)* shows how the total annual amount of precipitation in the contiguous 48 states has changed since 1900 — increasing an average of 0.17 in. per decade. Globally, rainfall is increasing on average 0.08 in. per decade (Figure 21) *(23)*. These increases in average precipitation are not distributed uniformly — some regions are experiencing more rainfall and others less *(24)*.

▲ **Figure 17.** Hurricane Harvey caused significant flooding in Houston, TX, in August 2017. Source: *(19)*.

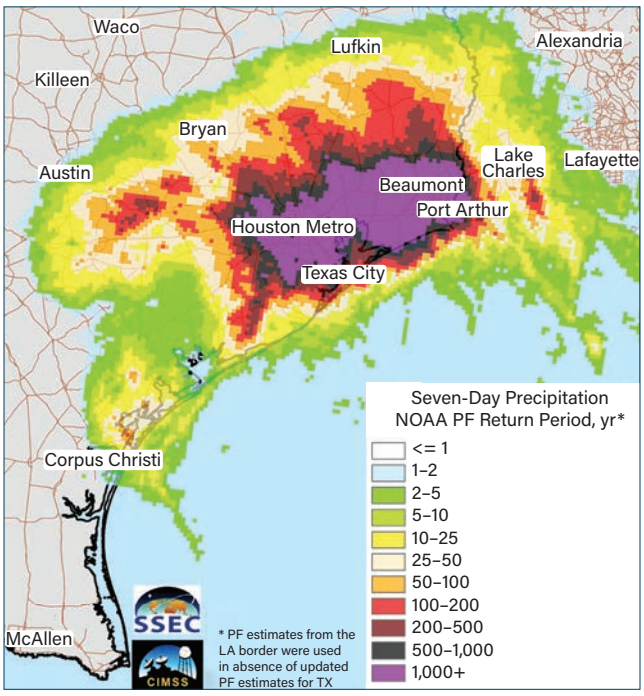

▲ **Figure 18.** The Houston, TX, area experienced a 1,000-year rainfall during Hurricane Harvey. In a given year, the probability of this level of rainfall is 0.1%. Source: Shane Hubbard, Space Science and Engineering Center, Cooperative Institute for Meteorological Satellite Studies, Univ. of Wisconsin–Madison.

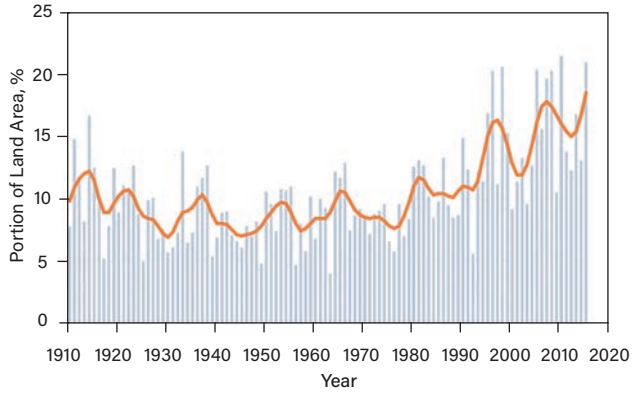

▲ **Figure 19.** Extreme one-day precipitation events in the contiguous states have been increasing. The orange line represents a nine-year weighted average. Source: *(22)*.

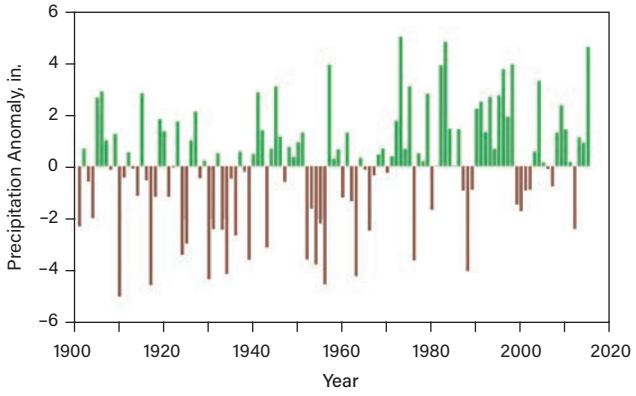

▲ **Figure 20.** Precipitation in the contiguous 48 states has increased by about 0.17 in. per decade since 1900. Source: *(23)*.

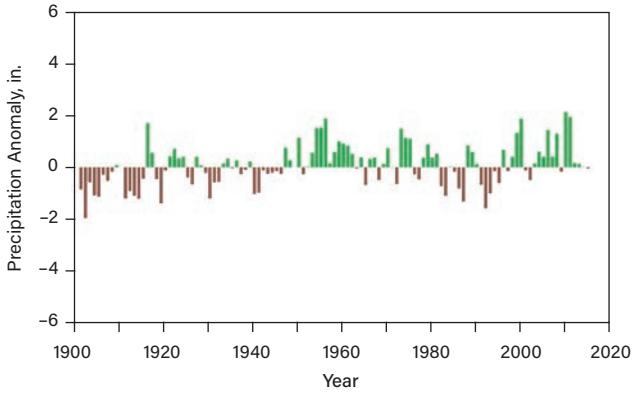

▲ **Figure 21.** Global precipitation has increased by about 0.08 in. per decade since 1900. Source: *(23)*.

Article continues on next page

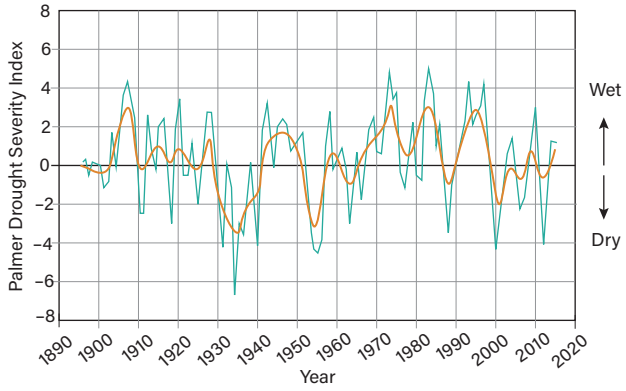

▲ **Figure 22.** Average drought conditions for the contiguous 48 states reveal no long-term trend toward wetness or dryness. The orange line represents a nine-year weighted average. Source: *(26)*.

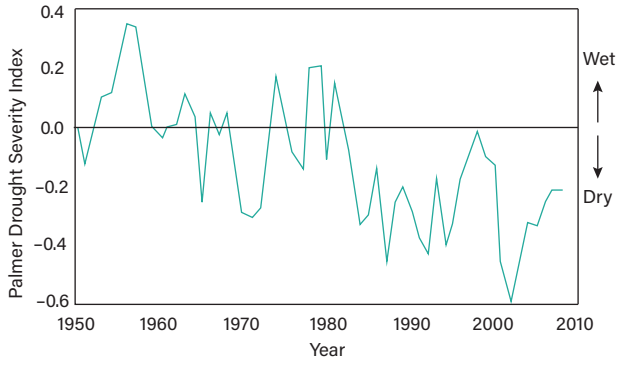

▲ **Figure 23.** Globally, drought conditions have been getting more severe. Source: *(27)*.

Droughts

As temperatures rise, moisture evaporates more rapidly from the soil, which could result in more droughts. On the other hand, this can be offset by more rainfall, as described previously. Drought can be quantified by the Palmer Drought Severity Index (PDSI), which employs temperature and precipitation data to estimate dryness and wetness using a simple physical water balance model. This standardized index ranges from –10 (dry) to +10 (wet). It should be noted that defining drought is difficult, and there is much discussion among experts about the best way to quantify it *(25)*.

Figure 22 *(26)* shows the PDSI for the contiguous 48 states. Positive values represent wetter-than-average conditions, whereas negative values represent drier-than-average conditions. A value between –2 and –3 indicates moderate drought, –3 to –4 is severe drought, and –4 and below indicates extreme drought. The orange line represents a nine-year weighted average.

The long-term trend in the U.S. is neither toward wetness nor toward dryness. However, the global PDSI has been declining since 1950, the first year with reliable global records (Figure 23) *(27)*.

Wildfires

Figure 24 *(28)* indicates that wildfires in the U.S. have increased significantly since 1980. Contributing factors include more plant biomass from carbon dioxide fertilization, regional droughts, and earlier snow melts, all of which can be caused by global warming.

Figure 25 *(29)* shows that the wildfire season — the time between the discovery of the first fire and control of the last fire — has been lengthening since 1970.

Economic damage

The annual cost of U.S. climate-related disasters (drought, freeze, hurricane, wildfire, winter storm, severe storm, flooding) with losses of $1 billion or more have

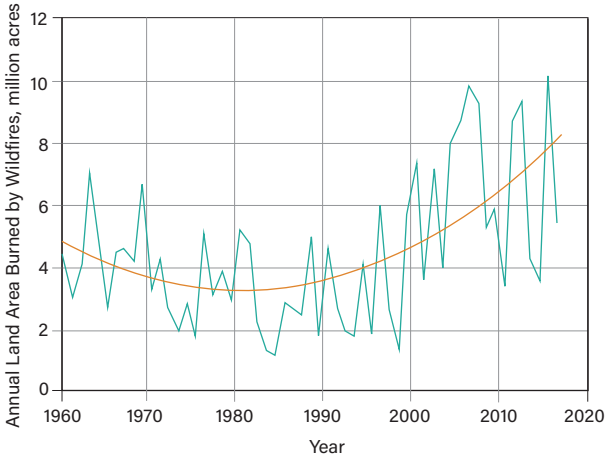

▲ **Figure 24.** The amount of land in the U.S. burned by wildfires has been increasing since the 1980s. Source: Data from *(28)*.

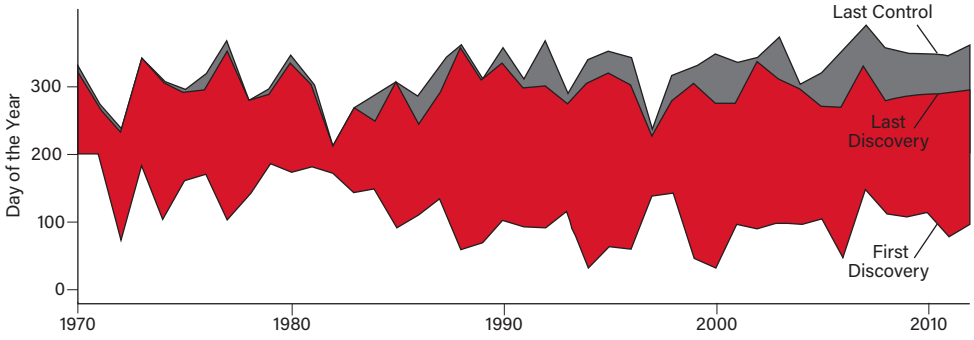

▲ **Figure 25.** The fire season (considering large, >400 ha, wildfires in the western U.S.) has been lengthening. Source: *(29)*.

increased dramatically in recent decades (Figure 26) *(30, 31)*. In 2017, the total cost of U.S. weather-related disasters was $306.2 billion, which set a new record *(30)*. It should be noted that greater economic losses occur not only because of climate change, but also increased human population and more widespread infrastructure.

Oceans

Increasing atmospheric concentrations of carbon dioxide drive more carbon dioxide into the ocean, where it forms carbonic acid and lowers ocean pH (Figure 27) *(32)*. Figure 28 *(33)* shows that small reductions in pH dramatically lower the carbonate concentration in seawater, which affects the ability of sea creatures (*e.g.,* oysters, clams, scallops, conchs, corals), zooplankton (*e.g.,* foraminifera, pteropod), and phytoplankton (*e.g.,* coccolithophores) to form carbonate shells. Zooplankton and phytoplankton (algae) are part of the intricate food web that supports higher life forms, such as fish and mammals.

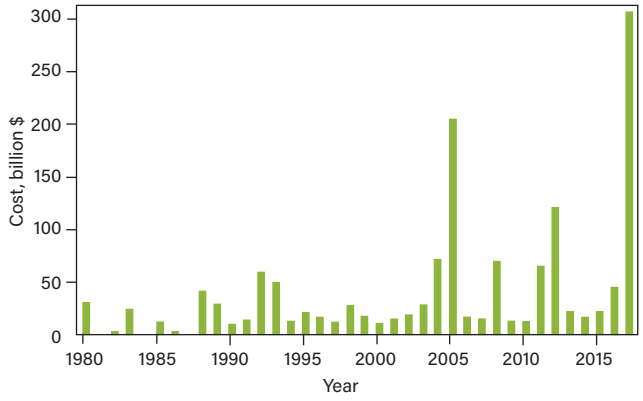

▲ **Figure 26.** The annual cost of U.S. climate-related disasters (drought, freeze, hurricane, wildfire, winter storm, severe storm, flooding) with losses of $1 billion or more is continually increasing. Costs are indicated in inflation-adjusted dollars. Source: Data from *(30, 31)*.

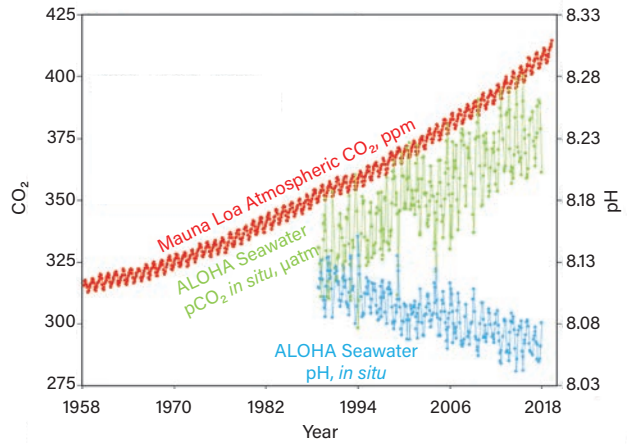

▲ **Figure 27.** Increasing concentrations of carbon dioxide are driving ocean acidification. These measurements were taken in Hawaii. Source: *(32)*.

Increasing ocean temperatures (Figure 15) and lower pH have had dramatic impacts on coral. Corals are small animals that produce carbonate exoskeletons that assemble into reefs, which protect shorelines from erosion and create habitats for marine life. Coral bleaching occurs when the animal is stressed or dies, leaving behind its white exoskeleton, which eventually becomes covered in algae (Figure 29).

Recently, extensive sections of the Australian Great Barrier Reef have been damaged by bleaching caused by warming. Figure 30 *(34)* shows the maximum heat stress during the Third Global Coral Bleaching Event. Regions that experienced high heat stress between June 1, 2014, and May 31, 2017, are displayed. Alert Level 2 heat stress indicates widespread coral bleaching and significant mortality. Alert Level 1 heat stress indicates significant coral bleaching. Lower levels of stress may have caused some bleaching as well. More than 70% of coral reefs around the world experienced the heat stress that can cause bleaching and/or mortality during the three-year-long global event *(34)*. These changes have been documented in the movie *Chasing Coral*.

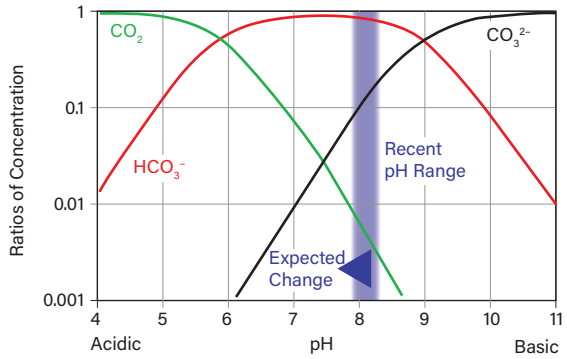

▲ **Figure 28.** This plot shows concentrations of carbon dioxide, bicarbonate, and carbonate as a function of pH. Source: *(33)*.

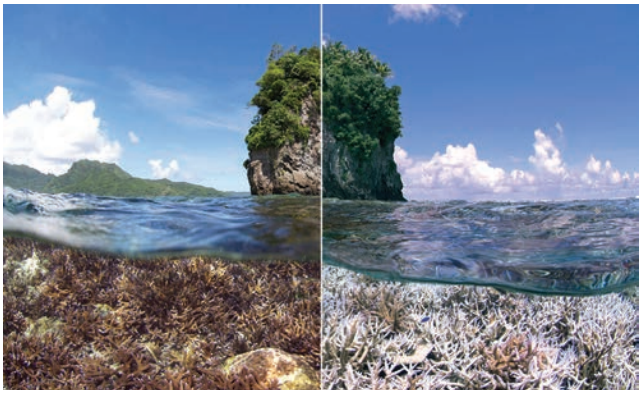

▲ **Figure 29.** Coral in American Samoa before (left) and after (right) bleaching. Source: The Ocean Agency/XL Catlin Seaview Survey (coralreefimagebank.org/before-after).

Article continues on next page

Ecology

Ecology is the branch of biology that deals with the interactions between organisms and their environment, including other organisms. The interactions between plants and animals are exceedingly complex and intertwined. As the complex web changes, many unexpected repercussions can occur. For example, as temperatures increase, some plants flower earlier, which may not be properly timed with natural cycles for pollinating insects. If plants are not properly pollinated, seeds do not form and insects that rely on nectar do not thrive, and in turn birds that eat insects or seeds decline.

In some animals (*e.g.*, alligators, iguanas, silversides fish), gender is determined by temperature. For example, increasing temperatures in the Great Barrier Reef of Australia are causing the birth of 116 female green sea turtles for every one male *(35)*. The dearth of males to fertilize eggs will reduce the long-term survival of this species.

Of course, during the past 500 million years, Earth has been both colder and warmer than current temperatures, and life has continued to thrive at all of these temperatures. The concern is that the rapid pace of the change may accelerate the extinction of modern species. During the 20th century, the rate of temperature increase (0.7°C/century) was about 10 times greater than the temperature increase during the recovery from the last ice age *(36)*. In a business-as-usual scenario, the expected temperature increase during the 21st century could be 4°C to 5°C, which is about 40 to 50 times greater than historical norms.

Figure 31 *(37)* shows the U.S. Dept. of Agriculture (USDA) plant hardiness zones based on average annual minimum winter temperatures for each region of the U.S. The plant hardiness zone map provides a standard definition of climatic conditions relevant to plant growth and survival, and it is used by the agriculture industry to define what plants grow best in what areas. Between 1990 and 2015 — a change of only 25 years — the warmer zones have moved noticeably northward. This rapid warming also has implications for pests and disease. The reduction of hard freezes that kill insects allows more insects to survive

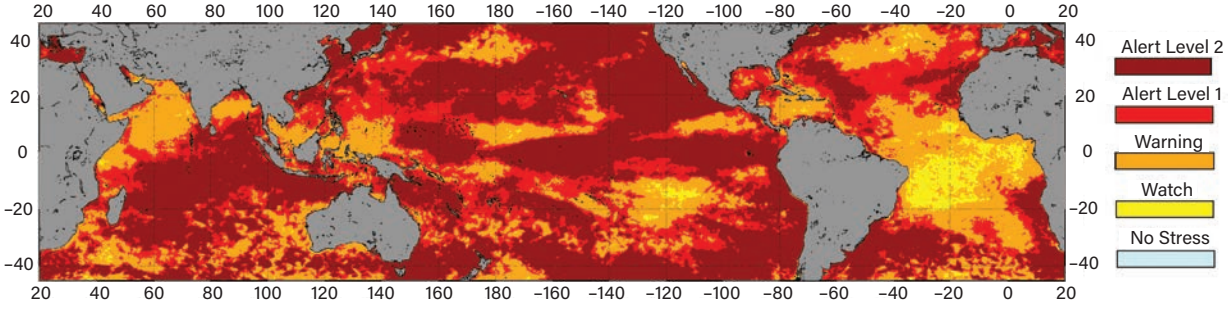

▲ **Figure 30.** The National Oceanic and Atmospheric Administration's (NOAA) Coral Bleaching Alert depicts the maximum heat stress during the Third Global Coral Bleaching Event of 2014–2017. More than 70% of coral reefs around the world experienced the heat stress that can cause bleaching and/or mortality during the three-year long global event. Source: *(34)*.

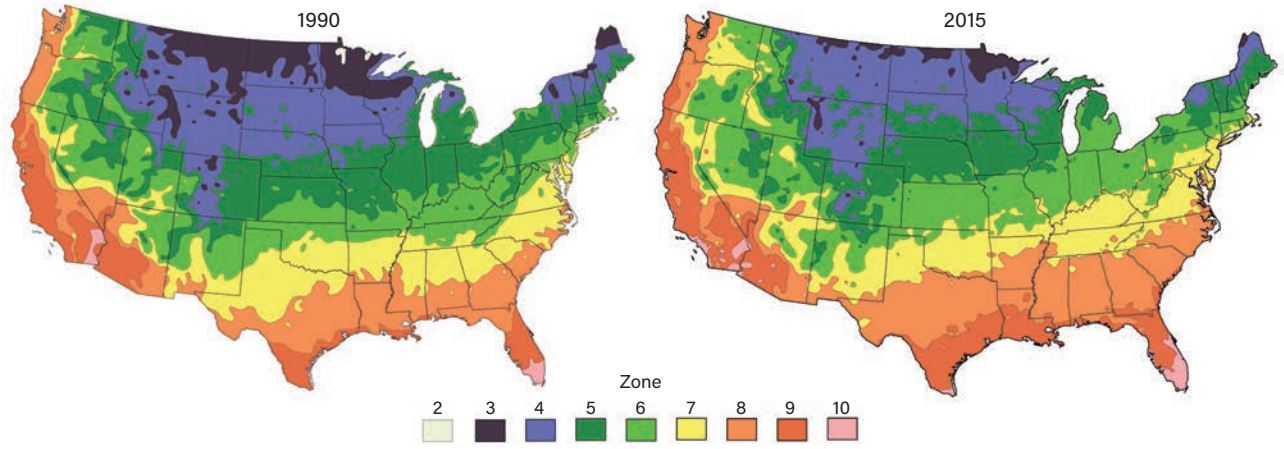

▲ **Figure 31.** The plant hardiness zones map can be used to determine which plants are most likely to thrive at a particular location, based on the average annual minimum winter temperatures. Source: Adapted from *(37)*.

the winter. For example, warmer climate allows pine bark beetles to migrate to higher elevations where the native pine trees have not evolved effective defenses like the lower-elevation pine trees have. In the U.S., pine beetles have destroyed more than 47 million hectares of pine trees, which in effect converted the trees from a (living) carbon sink to a (dead/decaying) carbon source *(38)*. Furthermore, tropical diseases (*e.g.,* dengue fever, malaria, West Nile virus) are moving northward *(39)*.

Deadly heatwaves

Excessively high temperature and humidity make it difficult for humans to dissipate body heat, which is particularly deadly for the elderly and those without access to air conditioning. Currently, about 30% of the global population is exposed to deadly climatic conditions for at least 20 days per year *(40)*.

The most famous examples of deadly heatwaves occurred in Chicago in 1995 (approximately 740 deaths), Paris in 2003 (~4,870 deaths), and Moscow in 2010 (~10,860 deaths); however, numerous other examples are documented in the literature *(40)*. A meta-analysis of the literature describing 783 cases of excess human mortality in 164 cities in 36 countries determined combinations of temperature and humidity that are lethal. Figure 32 *(40)* plots the mean daily surface air temperature and relative humidity during lethal heat events (black crosses) and during periods of equal duration from the same cities but from randomly selected dates (*i.e.,* nonlethal heat events; red to yellow gradient indicates the density of such nonlethal events). The blue line is the threshold that best separates lethal and nonlethal heat events, and the red line is the 95% probability threshold; areas to the right of the thresholds are classified as deadly and those to the left as not deadly.

Because human heat dissipation via perspiration depends both on ambient temperature and humidity, temperature alone does not fully characterize a hot day. In 1979, Robert G. Steadman developed the heat index, a "feels like" temperature that characterizes the impact of humidity on human heat dissipation. The heat index is defined as the dry-bulb temperature that would feel the same if the water vapor pressure were 1.6 kPa. The world-record heat index (178°F, 81°C) occurred in Dhahran, Saudi Arabia, on July 8, 2003, and is shown in Figure 32 as a reference point.

PROJECTED IMPACTS

Figure 33 *(41)* shows projections of future global temperature increases provided to the Congressional Budget Office by the Massachusetts Institute of Technology's (MIT) Integrated Global System Model. This projection is very similar to the high-end business-as-usual emission scenario RCP8.5 in the United Nations (UN) Intergovernmental Panel on Climate Change (IPCC) Fifth Assessment Report (AR5) Synthesis Report *(42)* released in 2014. These business-as-usual scenarios assume that population growth, increases in living standards, and fossil fuel usage continue unabated. By 2100, both MIT and IPCC project a temperature increase of about 4°C to 5°C above current temperatures. To minimize impacts on ecosystems and human economic activity, the UN has recommended that global temperature increase be limited to 2°C above preindustrial temperatures. Both MIT and IPCC project that we will cross this threshold in about 2040, or about 20 years from now.

Figure 34 *(43)* summarizes the potential impacts of climate change that occur with temperature changes up to

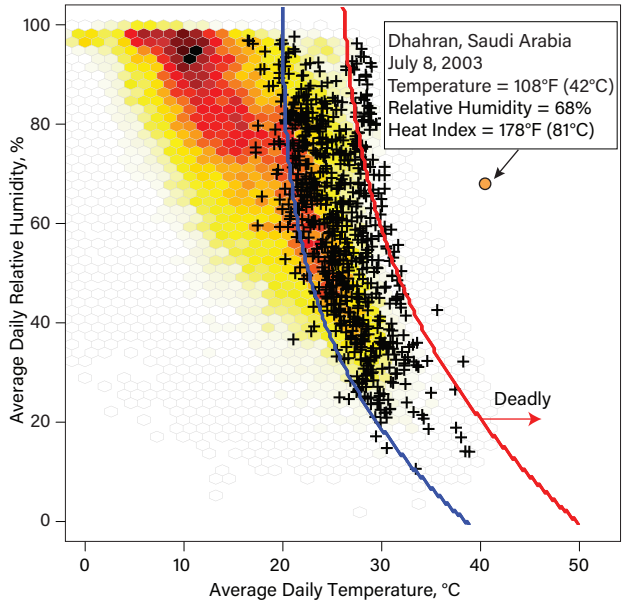

▲ **Figure 32.** Black crosses indicated lethal combinations of temperature and humidity. Conditions to the left of the blue line are considered safe for humans, while regions to the right of the red line are considered deadly. Source: *(40)*.

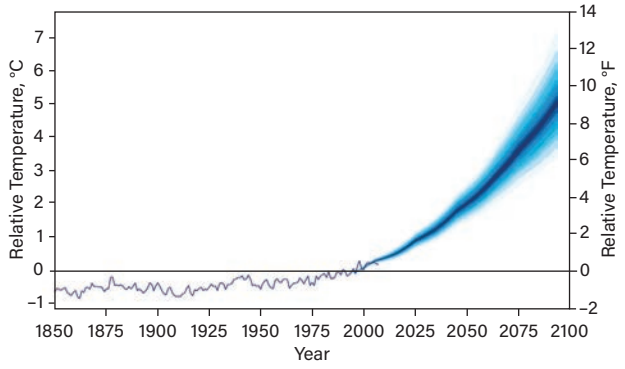

▲ **Figure 33.** Projections of average global temperature relative to the 1981–2000 average. Source: *(41)*.

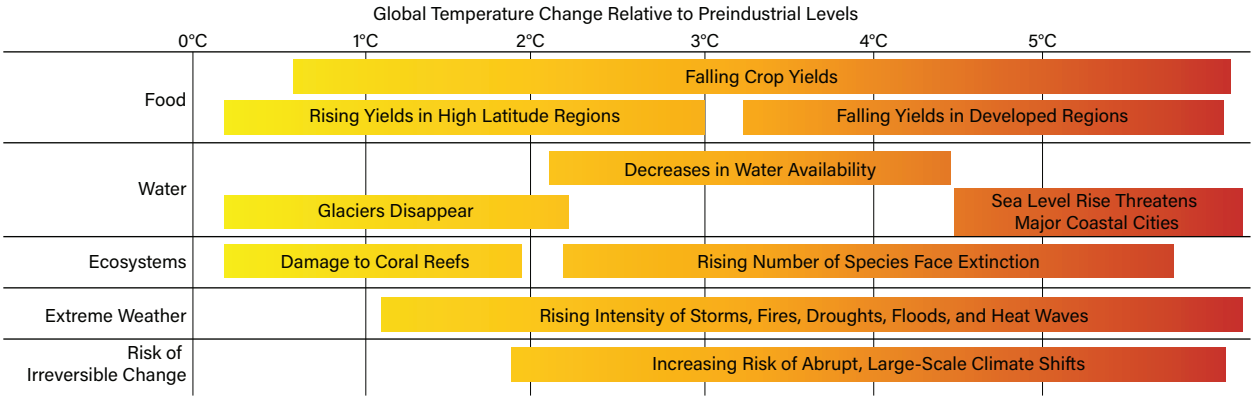

▲ **Figure 34.** Potential impacts from climate change as a function of temperature increase. Source: *(43)*.

5°C. By 2100, if the business-as-usual trajectory continues, about 74% of the global population will be exposed to deadly combinations of temperature and humidity (Figure 32) for at least 20 days per year *(40)*.

Sea level

The IPCC AR5 Synthesis Report *(42)* projects that under the business-as-usual scenario (RCP8.5), by 2100, sea levels will rise by about 0.64 m. (It should be noted that this is only a partial projection and does not include glacial instability in Greenland and Antarctica.) A rise of 0.64 m is sufficient to eliminate about 40% of productive land in Bangladesh *(44)*. To preserve coastal cities, massive civil structures — dikes, dams, floodgates, drainage ditches, canals, and pumping stations — will be required, much like those in the Netherlands. NOAA has a popular website that allows visitors to see how much land will be lost in coastal cities as sea level rises: coast.noaa.gov/slr.

It must be emphasized that the impacts of modern carbon emissions extend far beyond 2100. Much of the carbon dioxide emitted during the next 100 years will remain in the atmosphere for tens to hundreds of thousands of years *(45)*. Because of enormous lags in the climate system, the full impact of modern emissions will not be felt immediately. During the next ten millennia, sea level is projected to rise 25–52 m, depending on the emission scenario *(45)*. Complete loss of the Greenland and Antarctic ice sheets will increase sea levels by about 7 m and 58 m, respectively *(45, 46)*.

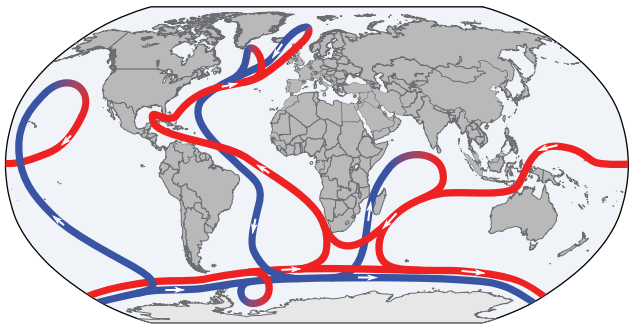

▲ **Figure 35.** Thermohaline circulation is a collection of currents responsible for the large-scale exchange of water masses in the ocean. Source: *(51)*.

Agriculture

Each plant has an optimal temperature. For example, the optimal reproductive temperatures for corn and soybeans are 19°C and 23°C (66°F and 73°F), respectively *(47)*. As global temperatures rise, adaptive responses include shifting agricultural production northward, developing temperature-tolerant varieties of traditional crops, and switching to alternative crops that tolerate higher temperatures.

Climate change can result in mild winters that disrupt the flowering cycles of trees and thereby reduce fruit yields. Mild winters also allow more insect pests to survive, which can negatively impact agricultural productivity *(48)*. A recent study indicates that losses of major grains (corn, wheat, rice) due to insects will increase 10–25% per degree celsius of warming, with the greatest impacts in temperate regions *(49)*.

Farmers will face additional challenges from droughts,

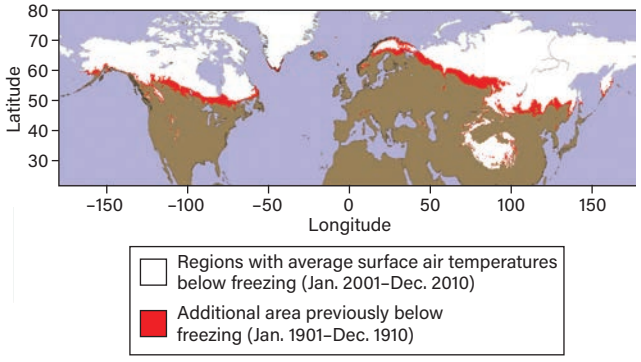

▲ **Figure 36.** The areas in red show permafrost that is thought to have thawed in the past 100 years. Source: *(3)*.

floods, and rising sea levels caused by climate change. For example, Bangladesh, India, and Vietnam produce rice in low-lying regions that will be flooded by rising sea levels, which will stress these countries and their large populations.

To some degree, these negative consequences of climate change can be offset by greater plant productivity that occurs at high CO_2 concentrations. On the other hand, in high-CO_2 environments, plants produce higher concentrations of carbohydrates and lower concentrations of nutrients (*e.g.,* protein, iron, zinc) *(48, 50)*. And, in high-CO_2 environments, insects must consume significantly more leaf area to meet their nutritional requirements *(48)*.

TIPPING POINTS

A tipping point is a critical condition beyond which a significant and often unstoppable change occurs. The following sections describe some potential climate change tipping points.

Thermohaline circulation

Thermohaline circulation is large-scale ocean circulation driven by global density gradients created by water temperature (thermo) and salt concentration (haline) differences. This system of currents transports warm surface water from the tropics to northern latitudes (Figure 35) *(51),* and is referred to as the ocean conveyor belt. Because warm water is less dense, it floats on the surface. As it cools, its density increases and the cooled water sinks, completing the conveyor belt circuit.

Because of its northern latitude, much of Europe should be cold. However, the Gulf Stream thermohaline circulation provides thermal energy that makes it much warmer. If the thermohaline circulation were to stop, Western and Northern European temperatures would be significantly colder, which would negatively impact Europe's ability to grow food. Warm surface temperatures (Figure 15), freshwater from melting ice, and abundant rain reduce the density of surface waters, making it more difficult for water to sink and complete the conveyor belt circuit. Changes in the thermohaline circulation are implicated in historical abrupt climate change events, such as the Younger Dryas (which ended abruptly around 11,500 years ago) *(52)*.

Climate scientists are studying recent changes in the thermohaline circulation and are attempting to understand whether it is likely to play a role in future climate. A recent study determined that the Atlantic meridional overturning circulation (AMOC), a system of ocean currents in the North Atlantic, has declined by 15% compared to the mid-20th century *(53)*. The measured changes are consistent with predictions from climate models.

Permafrost

As discussed previously, thawing permafrost allows microbes to anaerobically digest biomass in the soil and release carbon dioxide and the more potent greenhouse gas methane. This positive feedback mechanism accentuates global warming. Figure 36 *(3)* provides an estimate of the amount of permafrost that has thawed within the past 100 years. Figure 37 *(54)* shows that the amount of carbon estimated to be stored in permafrost is roughly equivalent to the carbon within total fossil fuel reserves, so carbon releases from permafrost have the potential to be very significant.

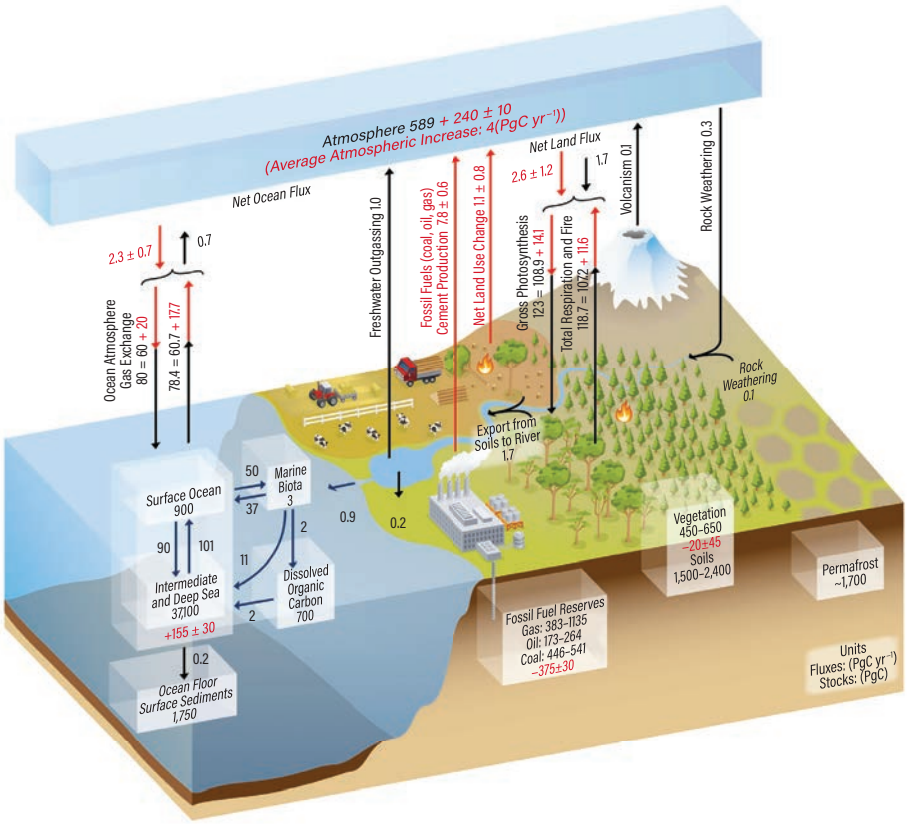

▲ **Figure 37.** Carbon stores and fluxes. Red indicates impact of human activity. Source: climatechange2013.org/images/figures/WGI_AR5_Fig6-1_errata.jpg in *(54)*.

Article continues on next page

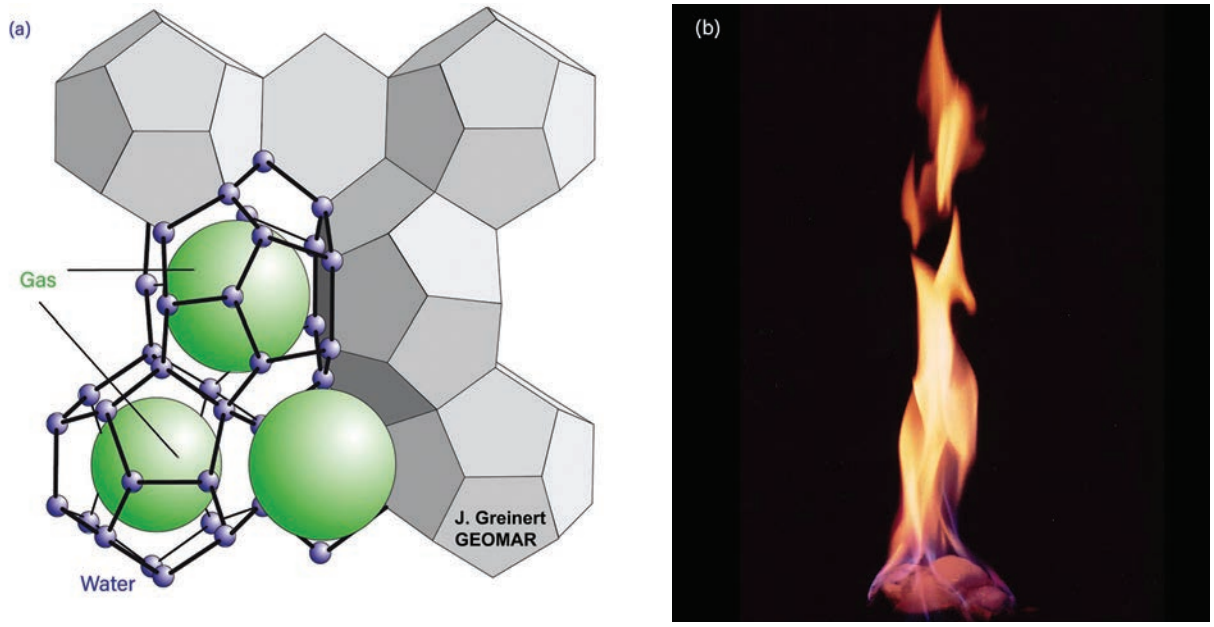

▲ **Figure 38.** (a) Methane hydrates consisting of a gas molecule surrounded by a cage-like structure of ice are found in cold, deep ocean waters. Source: *(55),* Jens Greinert/GEOMAR. (b) As the deep ocean warms, methane hydrates become unstable and release methane gas. Source: usgs.gov/media/images/burning-gas-hydrates.

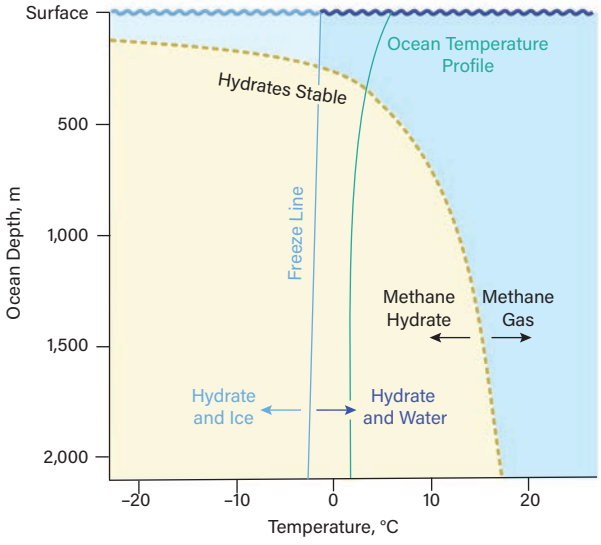

▲ **Figure 39.** Phase diagram for methane hydrates. Source: *(56).*

Methane hydrates

Figure 38 *(55)* shows images of methane hydrates, which consist of a gas molecule surrounded by a cage-like structure of ice. Figure 39 *(56)* is the phase diagram for these structures. For the ocean temperature profile shown, methane hydrates are stable below 350 m. In very cold Arctic waters (–1.8°C), methane hydrates are stable below about 250 m. If the temperature is cold enough, they are also stable in permafrost.

Figure 40 *(54)* shows the amount of methane hydrates found in permafrost and ocean sediments. The amount of carbon in methane hydrates is estimated to be significantly larger than all of the carbon in conventional fossil fuels (coal, natural gas, oil). As the deep ocean warms, some methane hydrates will become unstable and will release methane gas into the water. Because of the large thermal mass of the oceans, warming is very slow. Furthermore, most methane hydrates are deep enough to be stable; therefore, methane release from deep waters is likely to be very slow. Nonetheless, some researchers are concerned about methane hydrates in shallow waters in Arctic Siberia, which is warming at rapid rates (Figure 21 in the article on climate observations, Part 2, p. 22) and has less thermal mass than deep waters. Shakhova *et al.* consider the abrupt release of up to 50 Gt of stored methane hydrate highly probable at any time, which may cause an approximately 12-times increase in the atmospheric methane burden with consequent catastrophic greenhouse warming *(57)*.

Figure 41 *(58)* shows a massive blowhole in Yamal, Siberia, which is believed to have resulted from the sudden release of methane from melting methane hydrates.

Closing thoughts

Climate change is often viewed as a concern only for the future. This view was correct in the 1950s, but that is no longer the case. Numerous datasets indicate measureable impacts from climate change: greater plant growth, more melting ice, rising sea levels, stronger cyclones, greater rainfall, more droughts, longer wildfire seasons, coral bleaching, etc. Some of these impacts may be viewed

as beneficial (*e.g.,* greater plant growth), but most are negative. Many of these negative impacts have direct economic consequences, such as damage to coastal cities, loss of seafood, and destruction of valuable timber. Some consequences impact ecosystems that may not seem to directly impact humans, but may impact us indirectly. For example, coral reefs protect shorelines from erosion and thereby provide economic benefits.

Our understanding of the scientific principles underlying global warming allows us to predict future consequences of fossil fuel combustion and changing land use, such as increasing temperatures and rising sea levels. If population continues to grow at current rates, with increasing standards of living, and primary dependence on fossil fuels, global temperatures are expected to increase by 4°C to 5°C by 2100, which is significant in the context of geological temperatures (Figure 12 in the article on climate observations, Part 2, p. 18). Furthermore, by 2100, sea levels are projected to rise by another 0.64 m, which is 2.8 times greater than the sea level rise that has occurred since 1880. This new sea level will flood low-lying coastal lands (*e.g.,* Bangladesh) and will require the construction of large civil works to protect coastal cities. Because of lags in the climate system, the full impact of sea level rise will not be felt for many millennia and is projected to be 25–52 m, depending on the emission scenario. If carbon dioxide concentrations are not stabilized, at the millennial time scale, modern cities will be submerged and cannot be protected by civil works.

In the U.S., the cost of climate-related disasters has been increasing in recent years, with 2017 setting a new record of $306.2 billion.

Currently, about 30% of the world's population is exposed to deadly combinations of temperature and humidity for at least 20 days per year. If we continue on the business-as-usual trajectory, by 2100 this percentage increases to about 74%.

Climate models are not able to predict discontinuities that occur should we pass tipping points. Thus, the risk of abrupt climate change persists. CEP

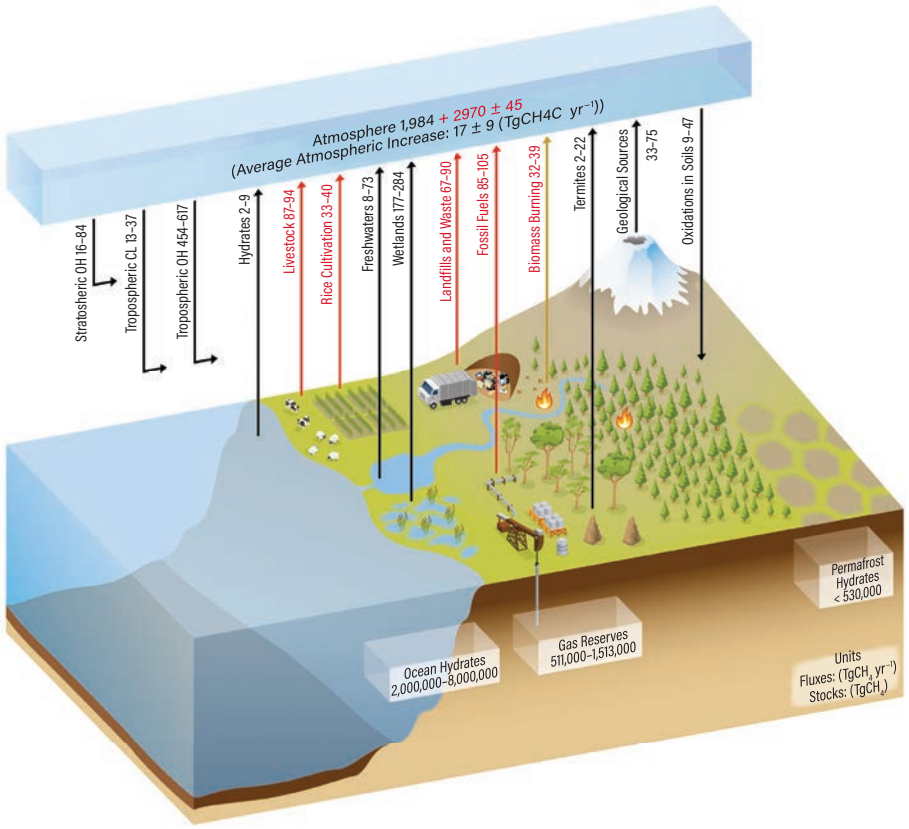

▲ **Figure 40.** Methane stores and fluxes. Red indicates impact of human activity. Source: climatechange2013.org/images/figures/WGI_AR5_Fig6-2.jpg in *(54).*

▲ **Figure 41.** This blowhole in Yamal, Siberia, likely formed when methane hydrates melted. Source: *(58).*

Acknowledgments

The author expresses gratitude to Arthur Humphrey and climate scientists Andrew Dessler, Gunnar Schade, and John Nielsen-Gammon of Texas A&M Univ. for providing helpful critiques.

Article continues on next page

Key Findings of the IPCC

The United Nations (UN) Intergovernmental Panel on Climate Change (IPCC) Fifth Assessment Report's (AR5) Summary for Policy Makers *(46)* provides a succinct discussion of current and future impacts of climate change. Its key findings regarding future anthropogenic climate change include:

- Species with limited adaptive response (*e.g.,* coral) are most vulnerable.
- Impacts that have already been demonstrated (*e.g.,* ice melting, permafrost thawing, ocean acidification, rising sea levels) will be accentuated.
- Biodiversity is expected to be significantly impacted at temperature increases above 3°C.
- Low-lying coastal zones are most vulnerable.
- Extreme events (*e.g.,* floods, hurricanes, wildfires) will disrupt infrastructure.
- Competition for potable water will become more severe.
- Forests are vulnerable.
- The potential for human conflict is amplified.
- Negative impacts on health will disproportionately fall on the poor.
- Food systems are at risk, particularly for the poor.

Interested readers are encouraged to download the 34-page summary report (ipcc.ch/pdf/assessment-report/ar5/wg2/ar5_wgII_spm_en.pdf) to explore these and other points (including the degree of confidence that these impacts will occur) in more depth.

Literature Cited

1. **Sage, R. F.,** "C3 versus C4 Photosynthesis in Rice: Ecophysiological Perspectives," *Studies in Plant Science*, **7,** pp. 13–35 (2000).
2. **Reiny, S.,** "Carbon Dioxide Fertilization Greening Earth, Study Finds," NASA, nasa.gov/feature/goddard/2016/carbon-dioxide-fertilization-greening-earth (Apr. 26, 2016).
3. **Berkeley Earth,** "Graphics: Physical Effects of Warming," berkeley-earth.org/physical-effects-of-warming-new (accessed Sept. 9, 2020).
4. **Jurvetson, S.,** "Permafrost Thaw Ponds in Hudson Bay Canada near Greenland," commons.wikimedia.org/wiki/File:Permafrost_thaw_ponds_in_Hudson_Bay_Canada_near_Greenland.jpg, Creative Commons Attribution 2.0 Generic License (CC BY 2.0) (accessed Oct. 21, 2020).
5. **National Snow and Ice Data Center,** "Arctic Sea Ice Minimum," NSIDC/NASA, climate.nasa.gov/vital-signs/arctic-sea-ice (accessed Sept. 9, 2020).
6. **Starr, C.,** "September Arctic Minimum Arctic Sea Ice 2012," NASA/Goddard Space Flight Center Scientific Visualization Studio, svs.gsfc.nasa.gov/vis/a000000/a003900/a003998/index.html (accessed Sept. 9, 2020).
7. **NASA,** "Antarctica, Sea Ice Trend," climate.nasa.gov/interactives/global-ice-viewer/#/4/12 (accessed Sept. 9, 2020).
8. **Noerdlinger, P. D., and K. R. Bower,** "The Melting of Floating Ice Raises the Ocean Level," *Geophysical Journal International,* **170** (1), pp. 145–150, doi.org/10.1111/j.1365-246X.2007.03472.x (July 2007).
9. **NASA,** "Ice Sheets," climate.nasa.gov/vital-signs/land-ice (accessed Sept. 9, 2020).
10. **U.S. Environmental Protection Agency,** "Climate Change Indicators: Glaciers," epa.gov/climate-indicators/climate-change-indicators-glaciers (accessed Sept. 9, 2020).
11. **NASA,** "Graphic: Dramatic Glacier Melt," Jet Propulsion Laboratory, California Institute of Technology, climate.nasa.gov/climate_resources/4 (accessed Sept. 9, 2020).
12. **U.S. Environmental Protection Agency,** "Climate Change Indicators: Sea Level," epa.gov/climate-indicators/climate-change-indicators-sea-level (accessed Sept. 9, 2020).
13. **Moftakhari, H. R., *et al.,*** "What Is Nuisance Flooding? Defining and Monitoring an Emerging Challenge," *Water Resources Research,* **54** (7), pp. 4218–4227, doi.org/10.1029/2018WR022828 (July 2018).
14. **U.S. Environmental Protection Agency,** "Climate Change Indicators: Coastal Flooding," epa.gov/climate-indicators/climate-change-indicators-coastal-flooding#ref3 (accessed Sept. 9, 2020).
15. **National Ocean Service,** "What is High Tide Flooding?," NOAA, oceanservice.noaa.gov/facts/nuisance-flooding.html (accessed Sept. 9, 2020).
16. "Oct. 17, 2016 Sunny Day Tidal Flooding at Brickell Bay Drive and 12 Street Downtown Miami," commons.wikimedia.org/wiki/File:October_17_2016_sunny_day_tidal_flooding_at_Brickell_Bay_Drive_and_12_Street_downtown_Miami,_4.30_MLLW_high_tide_am.jpg, Creative Commons Attribution-ShareAlike 4.0 International license (CC BY-SA 4.0) (accessed Dec. 2, 2020).
17. **NASA,** "Mean Surface Air Temperature over Ocean or Land Areas (C), Annual Mean Anomalies with respect to 1951–1980," data.giss.nasa.gov/gistemp/graphs/graph_data/Temperature_Anomalies_over_Land_and_over_Ocean/graph.txt (accessed Sept. 9, 2020).
18. **Hurricane Research Div.,** "North Atlantic Hurricane Basin (1851–2018), Comparison of Original and Revised HURDAT," NOAA, aoml.noaa.gov/hrd/hurdat/comparison_table.html (accessed Sept. 9, 2020).
19. **National Weather Service,** "Hurricane Harvey Info," weather.gov/hgx/hurricaneharvey (accessed Oct. 23, 2020).
20. "Hurricane Harvey is Third '500-year' Flood in Houston in Three Years. How Is That Possible?," washingtonpost.com/news/wonk/wp/2017/08/29/houston-is-experiencing-its-third-500-year-flood-in-3-years-how-is-that-possible/?utm_term=.87d6b67c4bb8 (Aug. 29, 2017).
21. **Di Liberto, T.,** "Reviewing Hurricane Harvey's Catastrophic Rain and Flooding," climate.gov/news-features/event-tracker/reviewing-hurricane-harveys-catastrophic-rain-and-flooding (Sept. 18, 2017).
22. **U.S. Environmental Protection Agency,** "Climate Change Indicators: Heavy Precipitation," epa.gov/climate-indicators/climate-change-indicators-heavy-precipitation (accessed Sept. 9, 2020).
23. **U.S. Environmental Protection Agency,** "Climate Change Indicators: U.S. and Global Precipitation," epa.gov/climate-indicators/climate-change-indicators-us-and-global-precipitation (accessed Sept. 9, 2020).
24. **U.S. Global Change Research Program,** "Precipitation Change," nca2014.globalchange.gov/report/our-changing-climate/precipitation-change (accessed Sept. 9, 2020).
25. "Topical Collection on Climate Change and Drought," link.springer.com/journal/40641/topicalCollection/AC_dd1d-b992682b0b202124cd69e1c4d95b/page/1 (accessed Sept. 10, 2020).
26. **U.S. Environmental Protection Agency,** "Climate Change

Literature Cited continues on next page

Literature Cited (continued)

Indicators: Drought," epa.gov/climate-indicators/climate-change-indicators-drought (accessed Sept. 9, 2020).

27. **Dai, A., and T. Zhao,** "Uncertainties in Historical Changes and Future Projections of Drought. Part I: Estimates of Historical Drought Changes," *Climatic Change*, **144** (3), pp. 519–533 (Oct. 2017).
28. **National Interagency Fire Center,** "Total Wildland Fires and Acres (1926–2019)," nifc.gov/fireInfo/fireInfo_stats_totalFires.html (accessed Sept. 9, 2020).
29. **Westerling, A. L. R.,** "Increasing Western U.S. Forest Wildfire Activity: Sensitivity to Changes in the Timing of Spring," *Philosophical Transactions of the Royal Society B, Biological Sciences*, **371** (1696), 20150178, doi: org/10.1098/rstb.2015.0178 (June 5, 2016).
30. **National Oceanic and Atmospheric Administration,** "Billion-Dollar Weather and Climate Disasters: Overview," National Centers for Environmental Information, NOAA, ncdc.noaa.gov/billions (accessed Sept. 9, 2020).
31. **Smith, A. B.,** "2016: A Historic Year for Billion-Dollar Weather and Climate Disasters in U.S.," NOAA, climate.gov/news-features/blogs/beyond-data/2016-historic-year-billion-dollar-weather-and-climate-disasters-us (accessed Sept. 9, 2020).
32. **NOAA,** "Hawaii Carbon Dioxide Time-Series," pmel.noaa.gov/co2/file/Hawaii+Carbon+Dioxide+Time-Series (accessed Sept. 9, 2020).
33. "Carbonate System of Seawater," commons.wikimedia.org/wiki/File:Carbonate_system_of_seawater.svg (accessed Sept. 9, 2020).
34. **NOAA Coral Reef Watch,** "Coral Bleaching During and Since the 2014–2017 Global Coral Bleaching Event," NOAA Satellite and Information Service, National Environmental Satellite, Data, and Information Service (NESDIS), coralreefwatch.noaa.gov/satellite/analyses_guidance/global_coral_bleaching_2014-17_status.php (accessed Nov. 2, 2020).
35. **Welch, C.,** "Rising Temperatures Cause Sea Turtles to Turn Female," news.nationalgeographic.com/2018/01/australia-green-sea-turtles-turning-female-climate-change-raine-island-sex-temperature (Jan. 8, 2018).
36. **NASA Earth Observatory,** "How is Today's Warming Different from the Past?," earthobservatory.nasa.gov/features/GlobalWarming/page3.php (accessed Sept. 10, 2020).
37. **Arbor Day Foundation,** "Differences between 1990 USDA Hardiness Zones and 2015 Arborday.org Hardiness Zones," arborday.org/media/map_change.cfm, Creative Commons Attribution-NoDerivs 2.5 Generic License (CC BY-ND 2.5) (accessed Nov. 2, 2020).
38. **Raffa, K. F.,** "Temperature-Driven Range Expansion of an Irruptive Insect Heightened by Weakly Coevolved Plant Defenses," *Proceedings of the National Academy of Sciences,* **110** (6), pp. 2193–2198, doi.org/10.1073/pnas.1216666110, pnas.org/content/110/6/2193 (Feb. 5, 2013).
39. **Scheer, R., and D. Moss, eds.,** "Mosquito-Borne Diseases on the Uptick — Thanks to Global Warming," scientificamerican.com/article/mosquito-borne-diseases-on-the-uptick-thanks-to-global-warming (Sept. 27, 2013).
40. **Mora, C., *et al.,*** "Global Risk of Deadly Heat," *Nature Climate Change*, **7,** pp. 501–506 (June 19, 2017).
41. **Congressional Budget Office,** "Potential Impacts of Climate Change in the United States," The Congress of the United States, Congressional Budget Office, cbo.gov/sites/default/files/111th-congress-2009-2010/reports/05-04-climatechange_forweb.pdf (May 2009).
42. **Pachauri, R. K., and L. Meyer, eds.,** "Climate Change 2014: Synthesis Report," Contribution of Working Groups I, II, and III to the Fifth Assessment Report of the Intergovernmental Panel on Climate Change, IPCC, Geneva, Switzerland, ar5-syr.ipcc.ch/ipcc/resources/pdf/IPCC_SynthesisReport.pdf (2014).
43. **Stern, N.,** "The Economics of Climate Changes: The Stern Review," Cambridge Univ. Press, Cambridge, U.K. (2007).
44. **World Bank,** "Turn Down the Heat: Climate Extremes, Regional Impacts, and the Case for Resilience," International Bank for Reconstruction and Development, Washington, DC, worldbank.org/content/dam/Worldbank/document/Full_Report_Vol_2_Turn_Down_The_Heat_%20Climate_Extremes_Regional_Impacts_Case_for_Resilience_Print%20version_FINAL.pdf (June 19, 2013).
45. **Clark, P. U., *et al.,*** "Consequences of Twenty-First-Century Policy for Multi-Millennial Climate and Sea-Level Change," *Nature Climate Change*, **6,** pp. 360–369 (Feb. 8, 2016).
46. **Field, C. B., *et al.,*** "Summary for Policymakers," in "Climate Change 2014: Impacts, Adaptations, and Vulnerability. Part A: Global and Sectoral Aspects," Contribution of Working Group II to the Fifth Assessment of the Intergovernmental Panel on Climate Change," Cambridge Univ. Press, Cambridge, U.K. and New York, NY, ipcc.ch/pdf/assessment-report/ar5/wg2/ar5_wgII_spm_en.pdf (2014).
47. **U.S. Global Change Research Program,** "Global Climate Change Impacts in the United States, 2009 Report," nca2009.globalchange.gov/agriculture/index.html (accessed Sept. 9, 2020).
48. **DeLucia, E. H., *et al.,*** "Climate Change: Resetting Plant-Insect Interactions," *Plant Physiology,* **160,** pp. 1677–1685, doi.org/10.1104/pp.112.204750, plantphysiol.org/content/160/4/1677 (Dec. 2012).
49. **Deutsch, C. A., *et al.,*** "Increase in Crop Losses to Insect Pests in a Warming Climate," *Science*, **361** (6405), pp. 916–919 (Aug. 31, 2018).
50. **Dietterich, L. H., *et al.,*** "Impacts of Elevated Atmospheric CO_2 on Nutrient Content of Important Food Crops," *Scientific Data,* **2,** Article No. 150036, nature.com/articles/sdata201536 (July 21, 2015).
51. "Thermohaline Circulation," commons.wikimedia.org/wiki/File:Thermohaline_Circulation.svg, Creative Commons Attribution-ShareAlike 3.0 Unported license (CC BY-SA 3.0) (accessed Nov. 2, 2020).
52. **National Centers for Environmental Information,** "The Younger Dryas," ncdc.noaa.gov/abrupt-climate-change/The%20Younger%20Dryas (accessed Sept. 10, 2020).
53. **Caesar, L., *et al.,*** "Observed Fingerprint of a Weakening Atlantic Ocean Overturning Circulation," *Nature*, **556,** pp. 191–196 (2018).
54. **Stocker, T. F., *et al.,*** "Climate Change 2013: The Physical Science Basis," Contribution of Working Group I to the Fifth Assessment Report of the Intergovernmental Panel on Climate Change, Cambridge Univ. Press, Cambridge, U.K., and New York, NY, www.climatechange2013.org (2013).
55. "Gas Hydrate Research: Advanced Knowledge and New Technologies," GEOMAR Helmholtz Centre for Ocean Research Kiel, geomar.de/en/discover/articles/gas-hydrate-research-advanced-knowledge-and-new-technologies (accessed Sept. 9, 2020).
56. "Undersea Methane Hydrate Phase Diagram," commons.wikimedia.org/wiki/File:Undersea_methane_hydrate_phase_diagram.svg, Creative Commons Attribution-ShareAlike 4.0 International License (CC BY-SA 4.0) (accessed Sept. 9, 2020).
57. **Shakhova, N., *et al.,*** "Anomalies of Methane in the Atmosphere over the East Siberian Shelf: Is There Any Sign of Methane Leakage from Shallow Shelf Hydrates?," *Geophysical Research Abstracts,* cosis.net/abstracts/EGU2008/01526/EGU2008-A-01526.pdf (2008).
58. **Northern Forum Secretariat,** "Scientists Have Solved the Mystery of the Craters in Yamal Peninsula, Russia," northernforum.org/en/news/811-scientists-have-solved-the-mystery-of-the-craters-in-yamal-peninsula-russia (accessed Oct. 23, 2020).

Solutions to Climate Change

Mark Holtzapple ▪ **Faruque Hasan** ▪ Texas A&M Univ.

A wide array of technologies will be needed to deal with the impacts of climate change.

The preceding articles in this issue discussed climate observations (pp. 14–23), climate modeling (pp. 24–35), and impacts of climate change (pp. 36–51). This article discusses society's response and explores some of the technologies that have the potential to mitigate or reverse climate change.

Risk

Risk is defined as the probability of an event occurring multiplied by the loss should it occur:

$$\text{Risk} \equiv \text{Probability} \times \text{Loss}$$

For example, a chemical plant located on the Gulf of Mexico is exposed to risk during the hurricane season. Meteorologists monitor satellite data and use weather models to determine whether a tropical storm will develop into a hurricane and make landfall. The engineers who operate the plant must assess the probability that the hurricane will actually hit their plant and estimate the potential losses that might occur. Based on their risk assessment, the engineers' response would range from doing nothing (no response) to shutting down the plant and implementing protective measures (maximum response).

This same process must occur as society decides how it will respond to the risks posed by climate change. To predict future temperatures, rain patterns, inland flooding, and sea levels, climate scientists use global climate models (GCMs). This information is used to assess the probability that losses will occur and the resulting financial impact. Insurance companies have a particular incentive to assess climate risk because they must charge appropriate premiums that ensure their future profitability. Society must decide whether to pay higher insurance premiums or to take prudent protective measures that reduce risk.

Values

Society's response to climate change goes beyond assessments of risk and financial impacts. Do we care that millions of poor people living in low-lying coastal Bangladesh will be displaced by rising sea levels, even though they did not contribute to the problem? Do we care that if the current trajectory continues, sea levels will rise by 25–52 m over the next 5,000 years *(1)* and thereby flood coastal cities and destroy cultural artifacts? Do we care that climate change will doom many species of plants and animals to extinction? How we answer these questions reflects the values of our society.

Civil infrastructure projects

As society decides how to respond to the challenge of climate change, it must take immediate remedial action in coastal cities that are already feeling its impacts. For

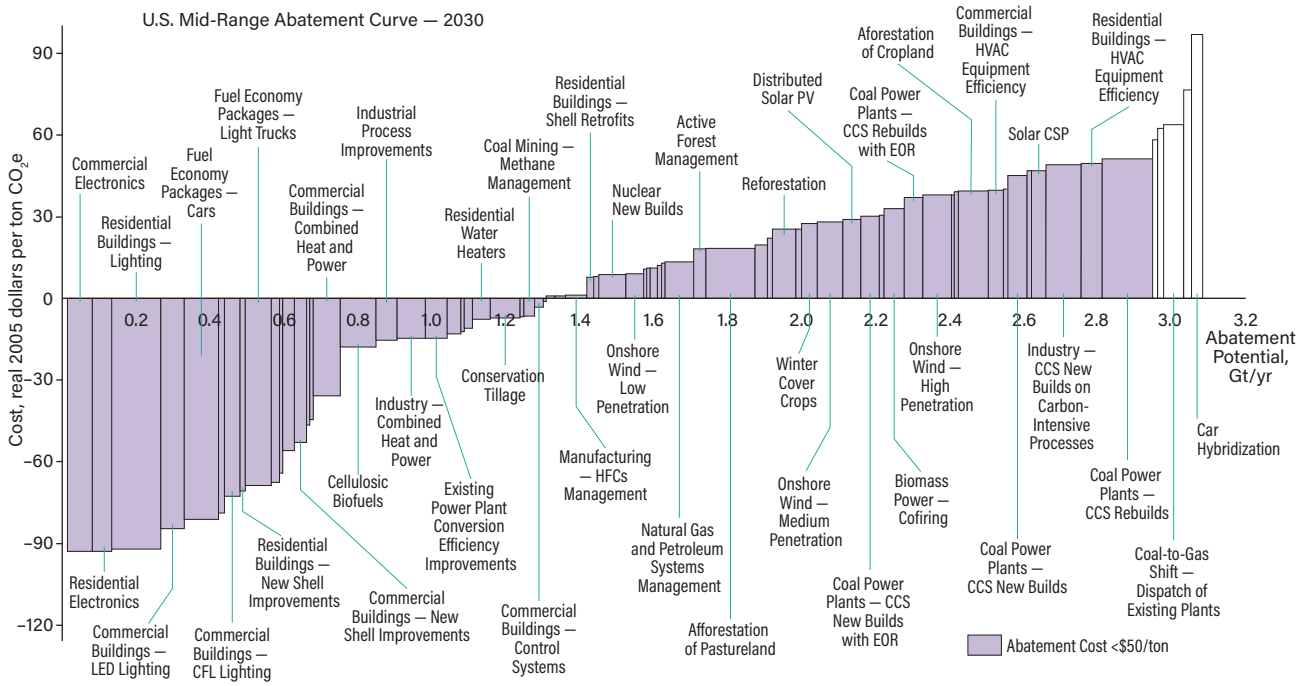

▲ **Figure 1.** This mid-range abatement cost curve for reducing carbon dioxide equivalent (CO_2e) emissions indicates that almost 40% of the approximately 3.0 Gt/yr potential emission reduction by 2030 could be achieved at a negative cost. Source: *(3)*.

example, Charleston, SC, and Miami, FL, must spend $200 million and $400 million, respectively, to address nuisance flooding in which high tides cause flooding even in the absence of rain or storms *(2)*.

To protect coastal cities from rising sea levels, large investments in dikes, dams, floodgates, drainage ditches, canals, and pumping stations will be required, much like those in Holland. Even inland cities will require higher levees to protect them from flooding caused by extreme rain events.

Improved efficiency

Most strategies for addressing climate change focus on reducing the accumulation of carbon dioxide — the dominant greenhouse gas (GHG) — in the atmosphere. Figure 1 *(3)* shows an abatement cost-curve analysis performed by the consulting company McKinsey. Abatement potential is the magnitude of potential carbon dioxide reductions that are technologically and economically feasible to achieve. Abatement opportunities are spread across the economy, and abatement potentials and costs vary across geographies.

Almost 40% of the abatement that could be accomplished by 2030 could be achieved at negative marginal costs — *i.e.,* the abatement technology pays for itself. Many of the low-cost methods to reduce carbon emissions involve improving the efficiency of lighting, motors, compressors, engines, and heating, ventilation, and air conditioning (HVAC) systems.

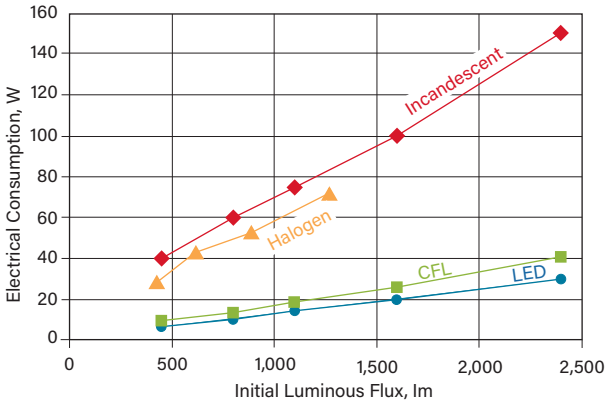

▲ **Figure 2.** Compact fluorescent lamp (CFL) and light-emitting diode (LED) bulbs are significantly more efficient than traditional incandescent lightbulbs. Source: *(5)*.

Lighting. Improving lighting efficiency is one of the most cost-effective measures for reducing carbon emissions. Lighting accounts for 5% of U.S. electricity consumption *(4)*. Figure 2 *(5)* shows that compact fluorescent lamps (CFLs) and light-emitting diodes (LEDs) are up to seven and nine times more efficient, respectively, than traditional incandescent light bulbs. The energy savings are so great and the capital investment so little that the cost of carbon abatement is negative — *i.e.,* it is profitable to replace incandescent bulbs with more efficient lighting.

Motors. Electric motors account for 40% of global electricity consumption *(6)*. Large electric motors can approach 100% efficiency; for example, ABB reported achieving a record 99.05% efficiency for a 44-MW electric motor *(7)*. Figure 3 *(8–11)* illustrates the efficiency of smaller electric motors. Induction motors are inefficient, particularly at partial load and small scale. New standards are being implemented that require manufacturers to increase motor efficiency. Permanent magnet motors are more efficient, but they tend to be more expensive.

Compressors. Many electric motors drive compressors for air conditioning, refrigeration, and gas compression for manufacturing or pipelines. High-efficiency compressors reduce the energy required to operate these processes, thereby reducing carbon dioxide emissions.

An example of a high-efficiency compressor is the rotary gerotor compressor, a type of positive-displacement compressor. Figure 4 compares the efficiency of gerotor compressors to conventional compressors (*e.g.,* centrifugal, screw, reciprocating) and turboexpanders. Gerotor compressors are very efficient even at small scale, making distributed processing more economically viable. Furthermore, gerotor compressors maintain their efficiency over a wide range of speeds (Figure 5), thus providing excellent turndown ratios. (*Disclosure:* Author Holtzapple is a co-inventor of gerotor compressors, expanders, and engines being developed by StarRotor Corp.)

Engines. Compressors and expanders may be combined to form Brayton cycle engines, which may be used in wide-ranging applications such as powering vehicles and generating electricity. Adding a recuperator reduces fuel consumption in the combustor, which improves energy efficiency. Furthermore, spraying atomized liquid water into the compressor inlet allows the compressor to approximate isothermal compression (Figure 6). When implemented in large-scale gas turbines, these humid recuperated Brayton

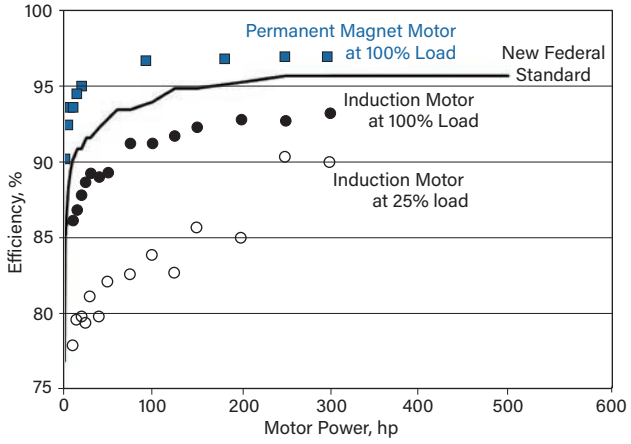

▲ **Figure 3.** Efficiencies for induction motors (black) are lower than the efficiencies of permanent magnet motors (blue). Source: Data from *(8–11)*.

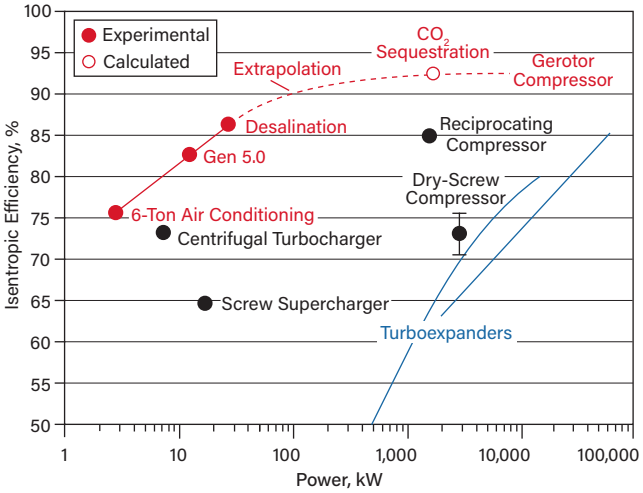

▲ **Figure 4.** A gerotor compressor is more efficient than conventional compressors and turboexpanders. Source: StarRotor Corp.

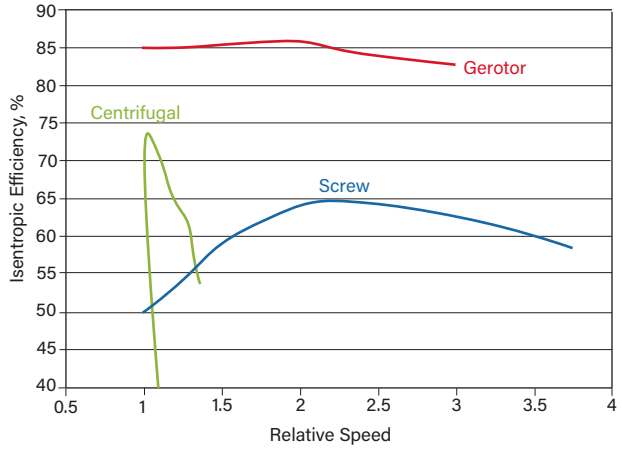

▲ **Figure 5.** A 25-kW gerotor compressor is more efficient than comparably sized centrifugal and dry screw compressors. Source: StarRotor Corp.

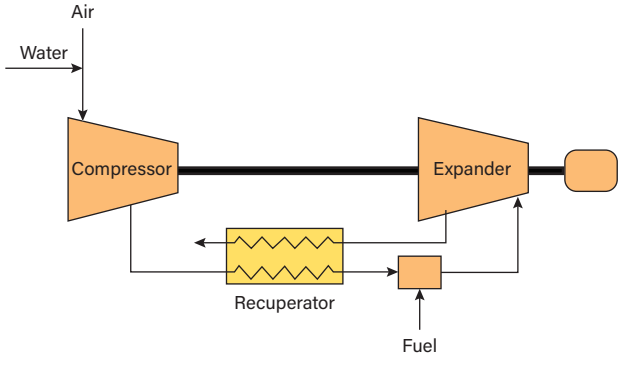

▲ **Figure 6.** Adding a recuperator and spraying atomized water into the compressor inlet improves the efficiency of a Brayton cycle engine.

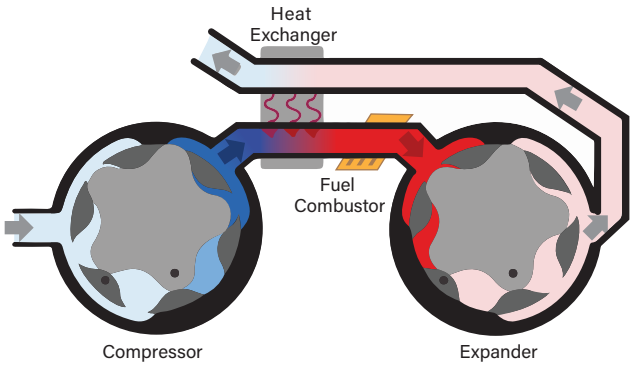

▲ **Figure 7.** A gerotor engine is a humid recuperated Brayton cycle with a gerotor compressor and expander. Source: StarRotor Corp.

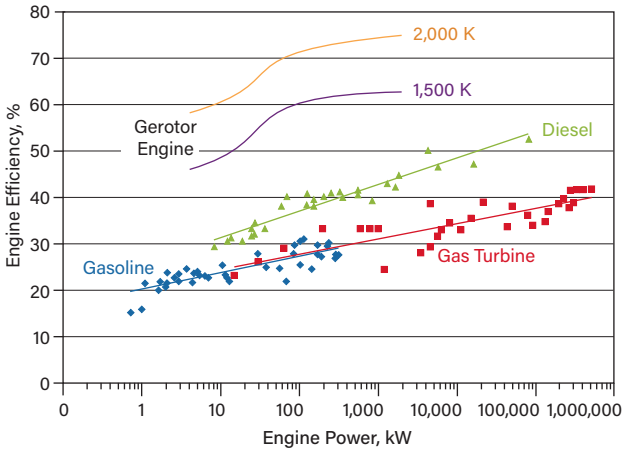

▲ **Figure 8.** The calculated efficiency of a gerotor engine, which uses a humid recuperated Brayton cycle with 6:1 pressure ratio and 25 K approach temperature in the recuperator, exceeds other engines' efficiencies. Gas turbines are from Capstone, Solar Turbines, and General Electric; gasoline engines are from Honda (lawn care and marine) and Volvo (marine); diesel engines are from Caterpillar and Wärtsilä. Source: StarRotor Corp.

cycle engines are 58.2% efficient *(12)*. Such high efficiencies are possible because these engines approximate the Ericsson cycle, which has the same efficiency as a Carnot heat engine, the maximum allowed by nature *(13)*.

Humid recuperated Brayton cycles may be implemented with gerotor compressors and expanders to create a gerotor engine (Figure 7). Although a gerotor engine has yet to be constructed, in theory, it would consume much less energy than a traditional engine and would hence contribute to lowering GHG emissions. The cycle efficiency of such an engine can be estimated using the component efficiencies reported in Figure 4. Figure 8 shows the estimated cycle efficiency at two combustor temperatures (1,500 K and 2,000 K). At all power levels, the projected efficiency of the gerotor engine far exceeds the efficiency of conventional gasoline engines, diesel engines, and simple-cycle gas turbines.

Combined-cycle gas turbines use a Rankine steam cycle to capture waste heat from the exhaust. The record efficiency for a combined-cycle gas turbine is 63.08%, which was achieved at 1,188-MW scale *(14)*. The gerotor engine efficiency is projected to exceed this efficiency at much smaller scales of about 100 kW, which is suitable for many transportation applications.

HVAC systems. Currently, air conditioners and cooling fans consume about 10% of global electricity *(15)*. By 2050, demand is expected to increase by 350% *(15)*. Thus, improving air conditioner efficiency can dramatically lower energy consumption.

The atmospheric temperature varies widely with seasons and often is too hot or cold for human comfort. In contrast, soil and groundwater temperatures (Figure 9) *(16)* reflect the average temperature of the atmosphere and have a value close to human comfort. Because the groundwater temperature is similar to the temperature of a comfortable building, it is a convenient source or sink of heat. Figure 10 *(17)* shows a ground-source heat pump that functions as an air conditioner during the summer by absorbing heat from the home and rejecting it to the Earth. During the winter, it functions as

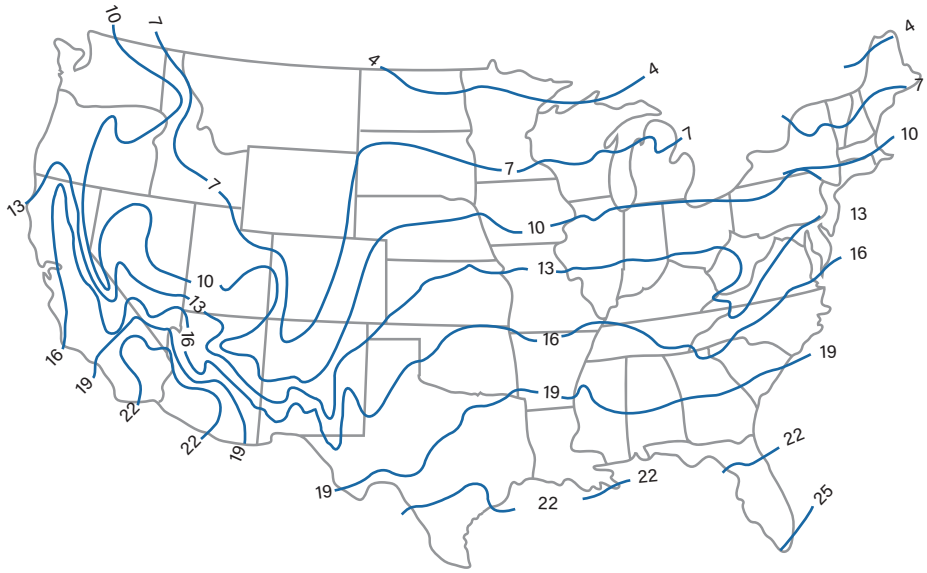

▲ **Figure 9.** The estimated mean groundwater temperature (°C) in the continental U.S. at a 10–5-m depth (annual variation is 5–10°C). Source: *(16)*.

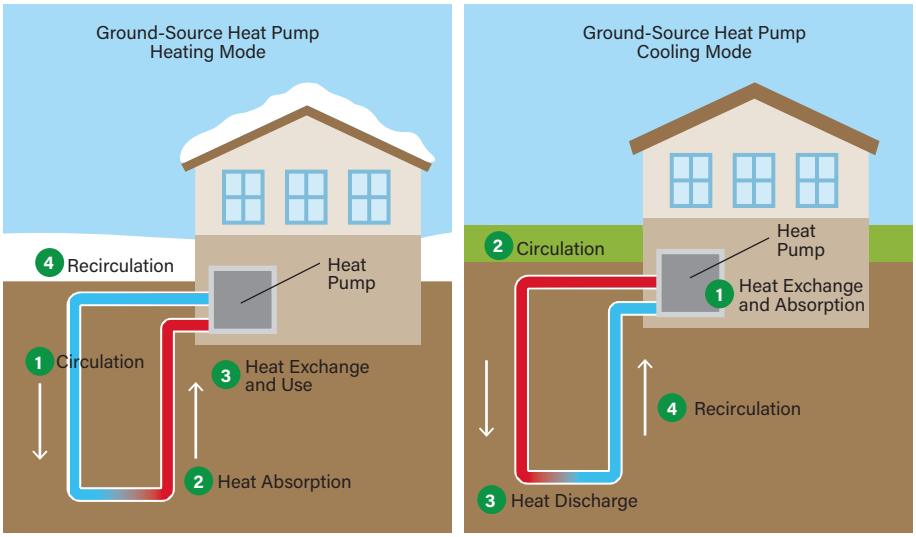

▲ **Figure 10.** A ground-source heat pump can provide heating and cooling. Source: *(17)*.

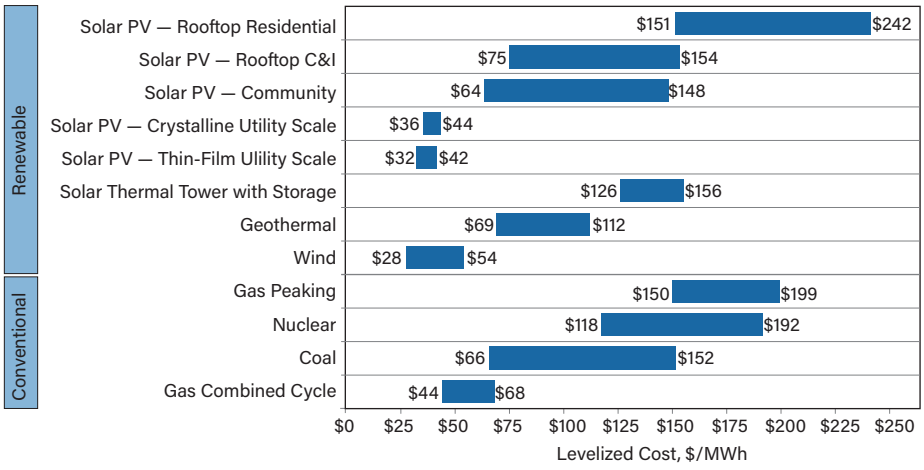

▲ **Figure 11.** Unsubsidized levelized cost of electricity from various sources. Source: *(19)*.

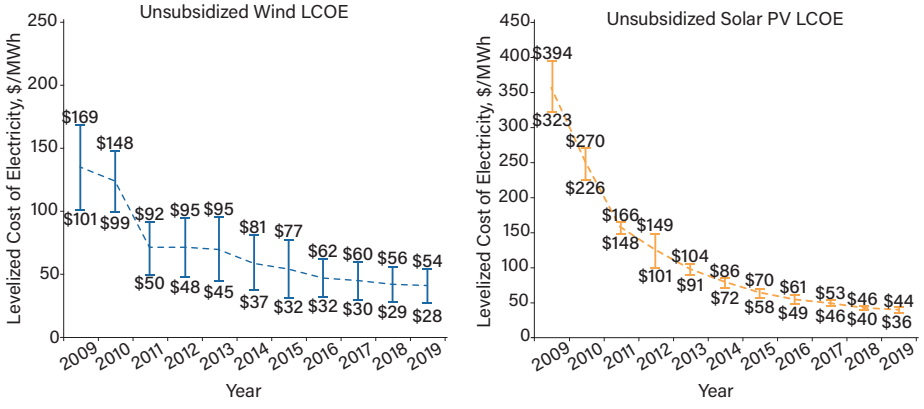

▲ **Figure 12.** Unsubsidized levelized cost of electricity (LCOE) for wind and utility-scale solar photovoltaic (PV) energy in the U.S. Source: *(19)*.

a heater by absorbing heat from the Earth and rejecting it into the home. Because the Earth temperature is similar to the interior temperature of the home, the temperature differences are low, allowing heat to be pumped with modest electricity input. Widespread implementation of such systems would greatly reduce the amount of fossil fuels burned for home heating and cooling.

Using aquifer thermal energy storage (ATES), the efficiency of ground-sourced heat pumps can be further improved by coupling them to two groundwater zones, each serving as an energy storage system *(18)*. *Charging phase:* During the summer, Zone 1 is heated by circulating aquifer water through a solar collector. During the winter, Zone 2 is cooled by circulating aquifer water through a cooling tower. *Discharging phase:* During the winter, Zone 1 is used to warm the home, and during the summer, Zone 2 is used to cool the home.

Carbon-neutral electricity

Figure 11 *(19)* shows the levelized cost of electricity (LCOE) for various electricity-generating technologies. LCOE is the net present value of electricity during the life of an electricity-generating technology and is considered the breakeven price of electricity for each technology.

Nuclear fission. The first commercial nuclear power plants were built in the mid-1950s. Most commercial plants use enriched ^{235}U, which provides energy from fission reactions that break large nuclei into smaller nuclei. Unfortunately, only 0.72% of the uranium in natural ores is ^{235}U, with ^{238}U accounting for most of the remainder. At current consumption rates, conventional uranium ores

can supply uranium for about 230 years, while the uranium in the oceans can supply uranium for 60,000 years *(20)*. Using breeder reactors, which create fissile fuels from ^{238}U, uranium supplies are sufficient for 30,000 years (conventional ore) and 7.8 million years (oceans).

Breeder reactors can also produce fissile materials from ^{232}Th. Thorium ores are three times more abundant than uranium ores and can provide over 1,000 years of energy while generating less waste than uranium fission.

When introducing nuclear power to the market in the 1950s, Lewis Strauss (chairman of the U.S. Atomic Energy Commission) claimed that it would be too cheap to meter; however, his prediction did not materialize. Other forms of energy are less expensive than nuclear power, as shown in Figure 11. The development of small modular reactors (SMRs) may reduce the cost of nuclear power by achieving economies of scale through mass production techniques.

Nuclear fusion. The preferred nuclear fusion reaction produces helium from the fusion of deuterium and tritium. Deuterium is found in essentially infinite quantities in seawater and tritium can be bred from lithium, an abundant element. So far, an economical method for controlled nuclear fusion has not been identified. However, the federal government and private industry (*e.g.,* Lockheed Martin, Commonwealth Fusion Systems, General Fusion) continue to research this possibility *(21)*.

In the 1970s, Project PACER proposed to detonate two 50-kiloton nuclear bombs per day in steam-filled salt domes, which would produce about 2 GW of electricity through conventional steam turbines.

Famously, in 1989, Pons and Fleishman claimed to perform nuclear fusion in a tabletop electrochemical reactor, a process they termed cold fusion. Their claims were highly controversial and were discredited by many; however, research continues as rebranded low-energy nuclear reactions (LENR).

Wind. Wind is among the least expensive sources of electricity. Figure 12 *(19)* shows that the cost has decreased recently, and it is now competitive with fossil energy. Figure 13 *(22)* shows that this energy resource is located primarily in the central U.S. and along the coasts. Wind power is proportional to the cube of velocity, so the economics strongly depend on wind velocity.

Solar. At grid scale, solar energy is produced by photovoltaics (PV) and so-called power towers, in which a field of mirrors concentrates solar energy onto a tower that heats a working fluid in a Rankine cycle. Figure 12 shows that the cost of solar PV has decreased dramatically, and it is now competitive with fossil energy. Figure 14 *(23)* shows that solar resources are concentrated mainly in the southwestern

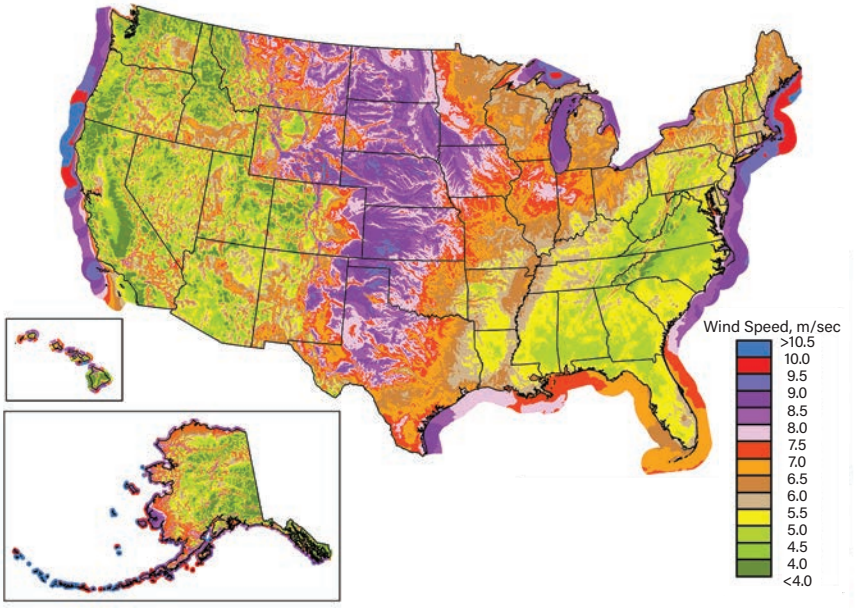

▲ **Figure 13.** The highest wind speeds occur in the central U.S. and along the coasts. Source: *(22)*.

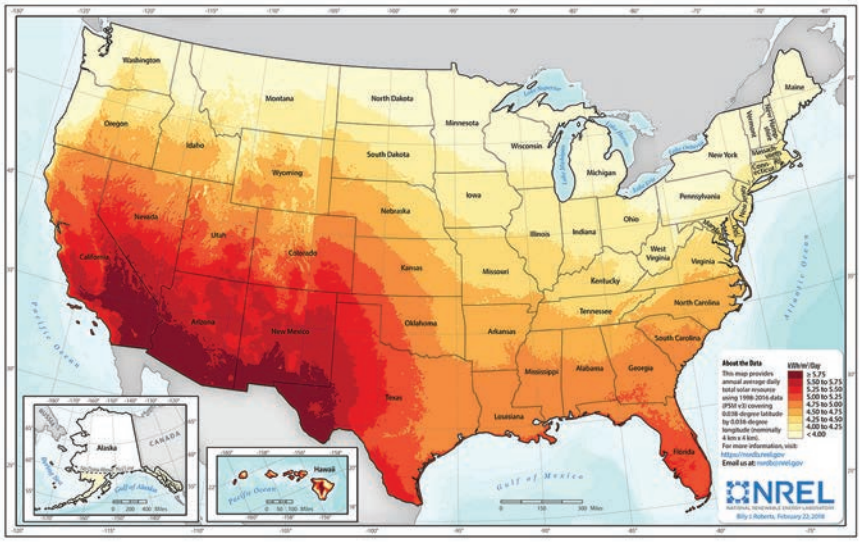

▲ **Figure 14.** The southwestern U.S. receives the highest levels of solar radiation. Source: *(23)*.

U.S. The yellow box in Figure 15 represents the amount of land area that could meet current U.S. electricity demand if it were completely covered in PV cells, assuming that 10% of the solar energy is delivered to the consumer.

Geothermal. A few regions of the U.S. have abundant geothermal energy that can be converted to electricity using the Rankine cycle. Typically, geothermal energy is practical only near tectonic plates (*e.g.*, California) where the heat is available at shallower depths. Among nations, Iceland produces the greatest percentage (30%) of its electricity from geothermal sources. Because the temperatures are low, the conversion of heat to electricity is fairly low (10–23%).

Biomass. Wood waste and black liquor from paper pulping is combusted to make heat for Rankine cycle engines. In 2018, the combustion of woody and waste biomass accounted for one-quarter of all U.S. renewable energy.

Distribution. Generally, solar, wind, and geothermal resources are distant from population centers, requiring transportation for their use. The most economical method to transport electricity long distances is via high-voltage direct-current (HVDC) transmission lines. At 800 kV, only 2.6% losses occur over a distance of 800 km *(24)*.

Electricity storage

Currently, wind and solar energy provide only 7.3% and 1.8% of U.S. electricity, respectively *(25)*. Figure 16 *(26)* shows that electricity generation from these energy sources has been increasing rapidly, a trend that is projected to continue. Wind and solar energy are available intermittently, so conventional gas turbines are used as backup power to match electricity production with demand. This is an acceptable interim solution; however, it is expensive to invest capital in both gas turbines and wind/solar power, each of which is used intermittently. Furthermore, gas turbines typically burn natural gas, which contributes to carbon dioxide emissions. Ideally, the future grid will employ increasing amounts of electricity storage to match intermittent production with demand.

Pumped hydraulic storage. This method pumps low-elevation water to a high-elevation lake. During the charge cycle, the equipment functions as a motor/pump, and during the discharge cycle it functions as a generator/turbine. These systems have large capacity and good round-trip efficiency of approximately 80%; however, they are limited to hilly geographies *(27)*. Pumped hydraulic storage comprises about 95% of current energy storage systems *(28)*.

Compressed-air energy storage. During the charge cycle, a motor/compressor is used to store compressed air in sealed caverns. During the discharge cycle, the compressed air is combined with fuel, combusted, and expanded in a gas turbine to drive a generator. Alternatively, it is possible that a motor/compressor (charge) can also function as a generator/expander (discharge) and recover energy without the need to combust fuel.

Batteries. Numerous battery technologies can store electrical energy. However, they often contain toxic materi-

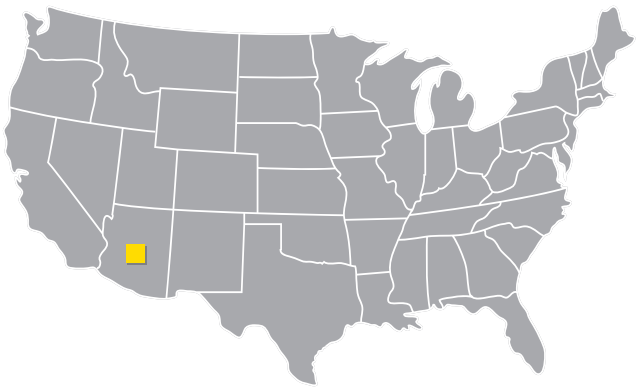

▲ **Figure 15.** The entire U.S. electricity demand could be supplied by photovoltaic (PV) cells covering the area in the desert Southwest represented by the yellow box (assuming 10% of incident solar energy is delivered to the consumer).

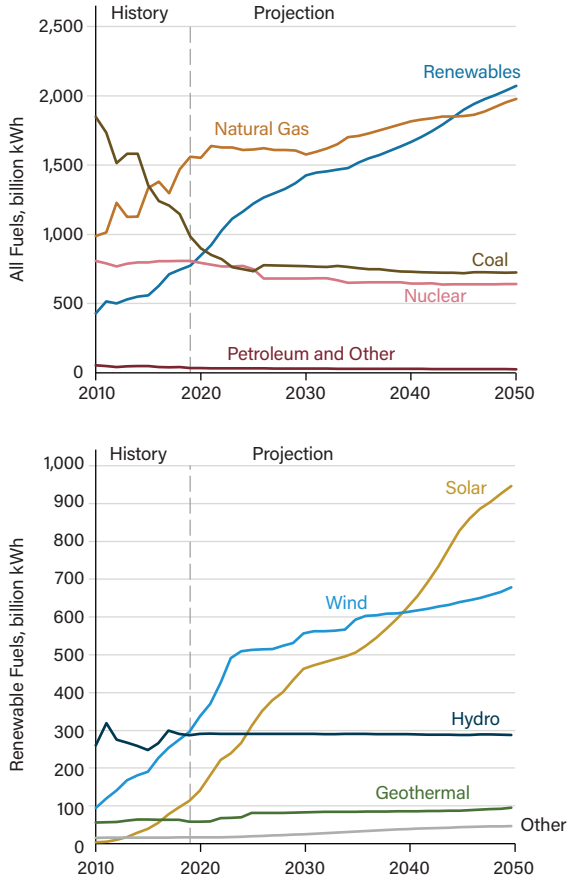

▲ **Figure 16.** In the U.S., electricity from renewable sources is expected to soon exceed that from nuclear and coal. Source: *(26)*.

als and have several challenges: low energy densities, low power capacity, high maintenance costs, and short cycle life *(27)*. Flow batteries have a fixed electrode area that is sized to provide a given amount of power; the electrolyte is stored in large tanks, and increasing the tank volume increases the amount of energy storage. Molten metal batteries employ two molten metals with dissimilar densities and a layer of molten salt between them; they are designed to use inexpensive Earth-abundant elements and cycle repeatedly with little degradation in performance *(29)*. (For an in-depth treatment of battery electric storage, see the special section on that topic in the May 2020 issue of *CEP*. — Editor)

Fuel cells. Water can be electrolyzed to hydrogen and oxygen (charge) and then reacted to form water and electricity (discharge). Unfortunately, the cycle efficiency is low *(27)*. (For an in-depth treatment of fuel cells, see the special section on that topic in the July 2016 issue of *CEP*. — Editor)

Liquid air. During the charge cycle, liquid air is created and stored in an insulated tank. During the discharge cycle, the air is gasified using thermal energy from the surroundings *(27)*. This method tends to be inefficient because of temperature differences in heat exchangers needed to drive heat transfer. Although all thermodynamic cycles are negatively impacted by temperature differences in heat exchangers, the problem is exacerbated at cryogenic temperatures.

Thermal storage. Thermal energy — which could be supplied from a concentrating solar collector — can be stored in molten salts, concrete, or phase-change materials and later recovered as electricity through heat engines *(27)*.

Heat pump storage. During the charge cycle, a heat pump transfers heat from a low-temperature source (T_1) to a high-temperature sink (T_2). During the discharge cycle, a heat engine withdraws thermal energy from the high-temperature sink (T_2) to produce electricity while rejecting heat to the environment (T_3). If the low-temperature source is waste heat from an industrial process, then $T_1 > T_3$. In this scenario, thermodynamics allows the output of electricity to be greater than the input of electricity *(30)*.

Flywheels, superconductors, and supercapacitors. These technologies have high power densities and are efficient, but energy densities are low *(27)*. They are best suited for instantaneous power conditioning, but are not practical for long-term energy storage.

Electrification of transportation

Carbon-neutral electricity can be produced by numerous technologies, as discussed previously. This potentially abundant resource can be used to directly power portions of the transportation sector and thus avoid the combustion of traditional fossil fuels.

Automobiles. Increasingly, automobiles are being electrified. Mild hybrids have a conventional engine, but the starter and alternator are replaced with a single device (~10 kW) that assists the powertrain. Fuel economy improves modestly (by about 10%) by allowing for regenerative braking and for the engine to turn off at stoplights. Hybrids use smaller engines that operate closer to peak efficiency. The electric device is more powerful (~50 kW) and provides a larger efficiency improvement (by about 25%). Plug-in hybrids have a large battery that allows for electric-only power during short commutes (less than about 40 miles). An engine powers the vehicle during long trips. All-electric automobiles operate exclusively with stored electricity and therefore require large batteries.

Trucking. The Texas Transportation Institute is actively developing a freight shuttle system in which freight-laden trailers ride autonomous transporters powered by linear-induction electric motors embedded in guideways similar to train tracks *(31)*. It is envisioned that this system will greatly reduce diesel truck traffic on highways and reduce the associated air pollution.

Trains. Traditionally, electric-powered trains transport people over short distances in population-dense regions. This paradigm may be broken by electric-powered hyperloop trains, which are being developed to transport people and cargo between distant cities at speeds comparable to the speed of airplanes. The train is located in an evacuated tube that greatly reduces drag (Figure 17). Theoretically, this technology would transport a person from Los Angeles to San Francisco in about 45 minutes while using about $0.50 of electricity, whereas an airplane would require about $30 of jet fuel. Hyperloop pods containing about 30 people would leave every two minutes during peak traffic periods. The technology is being developed by two startup companies: Virgin Hyperloop One and Hyperloop Transportation Technologies.

Planes. As batteries become lighter, there is increasing interest in electric-powered airplanes. However, currently only short distances are feasible.

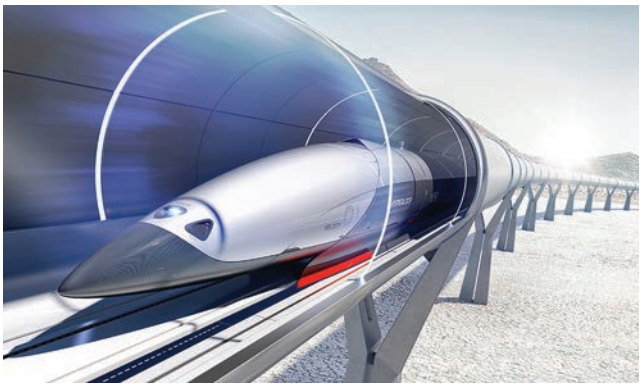

▲ **Figure 17.** Hyperloop trains are being developed to transport people and cargo over long distances at high speeds. Source: PriestmanGoode.

Article continues on next page

Carbon-neutral fuels

Although electricity is an excellent form of energy, there will always be a need for fuels, a form of stored chemical energy that can be released on demand.

Hydrogen. Electrical energy is readily converted to hydrogen fuel via water electrolyzers, which are about 82% efficient *(32)*. Alternatively, water can be split thermally through a variety of chemistries, such as the sulfur-iodine cycle:

$$I_2 + SO_2 \rightarrow 2HI + H_2SO_4 \quad (120°C)$$
$$2H_2SO_4 \rightarrow 2SO_2 + 2H_2O + O_2 \quad (830°C)$$
$$2HI \rightarrow I_2 + H_2 \quad (450°C)$$
$$2H_2O \rightarrow 2H_2 + O_2$$

It is commonly assumed that hydrogen will be employed by fuel cells, which convert hydrogen back to electricity with about 50–70% efficiency *(33)*. Using an electric motor, this electricity can be converted to shaft power that propels a vehicle. Alternatively, the vehicle can be propelled by shaft power from a conventional internal combustion engine. These two scenarios can be compared using the following assumptions:

- grid price of electricity = $0.05/kWh
- electrolyzer efficiency = 82%
- fuel cell efficiency = 60%
- electric motor/controller efficiency = 92%
- fuel heating value = 115,000 Btu/gal
- automotive engine efficiency = 25%.

The equivalent cost of hydrogen that produces the same shaft power as gasoline is $0.93/gal, which is attractive compared to the current cost of gasoline at the refinery gate (~$1.40/gal).

For transportation purposes, a significant challenge is the storage of hydrogen, which has a lower energy density than gasoline (Figure 18) *(34)*. To overcome this challenge, hydrogen energy can be incorporated into liquid fuels that are easier to transport. (For an in-depth treatment of hydrogen deployment, see the special section on that topic in the August 2019 issue of *CEP*. — Editor)

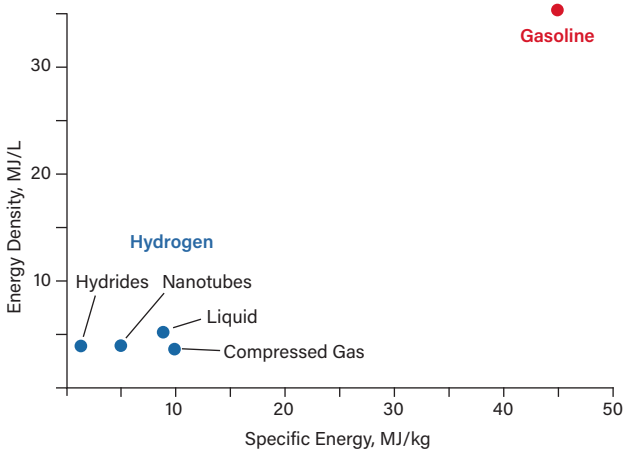

▲ **Figure 18.** Hydrogen has a much lower energy density than gasoline. Source: *(34)*.

Using the reverse shift reaction, carbon dioxide can be reduced to carbon monoxide:

$$CO_2 + H_2 \rightarrow CO + H_2O$$

A mixture of carbon monoxide and hydrogen is synthesis gas, which is readily converted to liquid fuels, such as methanol, mixed alcohols, or hydrocarbons. The U.S. Navy is developing technology to extract carbon dioxide from seawater and produce hydrogen by nuclear-powered electrolyzers *(35)*. The resulting hydrocarbons will be used to power jet aircraft. A civilian sunlight-to-fuels variant of this technology extracts carbon dioxide from the air and produces hydrogen by solar-powered electrolyzers *(36)*. Carbon dioxide is absorbed directly from the air by a dry quaternary amine ion exchange resin that is regenerated when water washes the resin.

Biomass. In the U.S., motor gasoline contains about 10% ethanol, which is derived primarily from corn. Of the

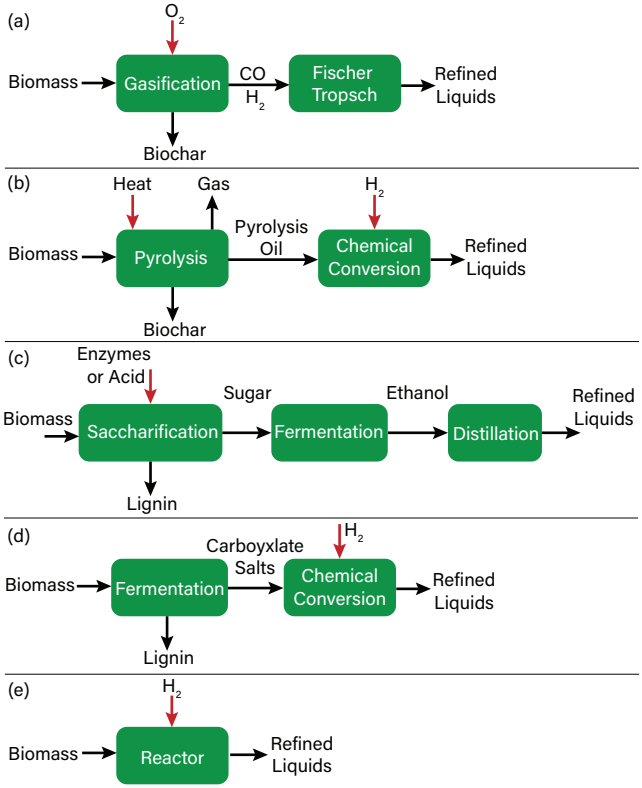

▲ **Figure 19.** Lignocellulosic biomass can be converted to liquid transportation fuels by (a) gasification, (b) pyrolysis, (c) the sugar platform, (d) the carboxylate platform, and (e) direct hydrogenation.

2019 U.S. corn crop, 29.5% was devoted to ethanol production, which required 26 million acres to be planted *(37)*. In Brazil, motor gasoline contains about 25% ethanol, which is derived primarily from sugarcane. Some Brazilian cars can also operate on 100% hydrous ethanol. The U.S. and Brazil account for about 85% of global ethanol production. Both countries use feedstocks that compete with food.

Biodiesel is produced by reacting fats and oils with alcohol (*e.g.,* methanol) to produce a fatty acid ester (product) and glycerol (byproduct). In the tropics, palm oil is commonly used as the feedstock, while in temperate regions, common feedstocks are waste frying oil, animal tallow, rapeseed oil, and soybean oil.

Lignocellulosic biomass (*e.g.,* wood, grass, agricultural residues) is extremely abundant and does not compete with food. It is estimated that 1 billion tons per year can be obtained for $80/ton or less *(38)*. It can be converted to liquid transportation fuels using the following approaches:

• *Gasification* (Figure 19a) partially oxidizes the biomass to form synthesis gas ($CO + H_2$), which can be catalytically converted to liquid transportation fuels (alcohols, hydrocarbons). The technology is similar to coal gasification practiced in South Africa and natural-gas-to-liquids technology practiced in Qatar.

• *Pyrolysis* (Figure 19b) heats biomass in the absence of oxygen to form gas, biochar, and pyrolysis oil. Although pyrolysis oil appears similar to crude oil, it has a high oxygen content and is acidic. To be used as a liquid hydrocarbon for transportation, it must be upgraded with hydrogen.

• The *sugar platform* (Figure 19c) uses enzymes or acids to catalytically convert cellulose and hemicellulose into free sugars (*e.g.,* glucose, xylose) that can be fermented by microorganisms that are selected based on the desired final product. For example, yeast ferments glucose to ethanol, which can be recovered using conventional distillation.

• The *carboxylate platform* (Figure 19d) uses a mixed culture of microorganisms typically found in the soil or cattle rumen to produce carboxylate salts (*e.g.,* acetate, propionate, butyrate) that are recovered and chemically converted to refined transportation fuels (alcohols, hydrocarbons). (*Disclosure:* Author Holtzapple is a co-inventor of the carboxylate platform.)

Table 1. Economic comparison of lignocellulosic biomass conversion processes.

Platform	Capital Cost, $/GGE	Selling Price, $/GGE	Reference
Gasification	16	4.50	*(39)*
Pyrolysis	4–8	2.60	*(39)*
Sugar	10.40	3.27	*(40)*
Carboxylate	2.60–3.70	1.00–2.50	*(41)*

GGE = gallon of gasoline equivalent

Table 1 *(39–41)* compares the estimated costs of these four lignocellulosic biomass conversion technologies.

Figure 20 is a photograph of sorghum, a drought-resistant high-yield crop that grows in 35 U.S. states. The green box labeled 1× in Figure 21 represents the land area required to grow the sorghum needed to supply current U.S. (2019) gasoline consumption *(42)* of 143 billion gal/yr by the carboxylate platform, assuming current automobile efficiencies, a sorghum yield of 15 dry ton/acre-yr, and 70 gal of hydrocarbon per dry ton of biomass. This would require 136 million acres — five times the amount of land currently devoted to corn ethanol production.

▲ **Figure 20.** This forage sorghum crop in Texas was grown from seeds planted in March and reached a height of about 15 ft by November.

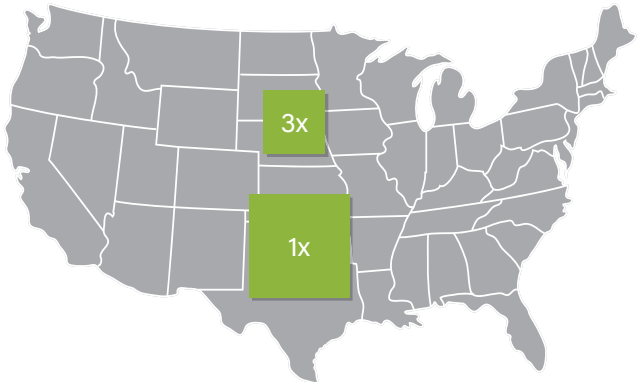

▲ **Figure 21.** The amount of land represented by the green box labeled 1× (136 million acres) would be required to grow enough sorghum to supply the total 2019 U.S. gasoline demand of 143 billion gal/yr, assuming current automobile engine efficiencies. If automobiles could be made three times more efficient, the land requirement could be reduced to 45 million acres, depicted by the green box labeled 3×.

Article continues on next page

Automobiles have the potential to be three times more efficient by increasing engine efficiency, electrification, reducing mass, reducing rolling resistance, and reducing drag. In that scenario, the required land area (the green box labeled 3×) would be 45 million acres, or about 1.7 times the land area currently planted in corn for ethanol.

Even with these improvements, the required land area to grow fuels is substantially greater than the land area needed to produce electricity. This reflects the fact that biomass production is about 1% efficient (sorghum) whereas photovoltaics are about 20% efficient. Biofuel processes that can take advantage of hydrogen input — which can be derived from carbon-neutral sources — reduce the acreage required to grow biomass.

• *Direct hydrogenation* (Figure 19e) converts biomass oxygen to water and biomass carbon to hydrocarbons. Approaches include the use of hydrogen-donor solvents *(43)* and hydrodeoxygenation catalysts *(44)*. The following reaction uses Douglas fir as an example biomass and hexane as an example hydrocarbon:

$$6\ CH_{1.45}O_{0.581} + 6.136\ H_2 \rightarrow C_6H_{14} + 3.486\ H_2O$$

This reaction achieves a theoretical mass yield of 0.630 g hexane per gram of wood (229 gal hexane per ton of wood). In practice, mass yields of 0.25–0.28 g hydrocarbon per gram of wood have been achieved *(44)*.

Annually, the U.S. produces about 147 million tons of waste biomass (*e.g.,* municipal solid waste, agricultural residues, forestry residues) that have the theoretical potential to produce about 33 billion gal/yr of hydrocarbons through direct hydrogenation. Assuming automotive mileage improves threefold as previously discussed, these wastes could provide about 70% of U.S. gasoline consumption.

Algae are being explored as a potential source of liquid hydrocarbons. Under appropriate growth conditions, about 40% of algae is lipid, which can be extracted and upgraded to refined liquid fuels. Algae are highly productive when grown with enriched carbon dioxide, and they do not require prime agricultural land. However, cultivation is expensive, and raw algae costs $500 to $3,000 per ton *(38)*.

Carbon capture

Several different strategies may be employed to capture carbon dioxide.

Biomass. Biomass naturally captures carbon dioxide from the atmosphere and sequesters it in the form of wood or other plant materials. When plants die, they decompose and release the carbon back to the atmosphere. This cycle is broken when biomass is gasified or pyrolyzed to produce biochar, a form of carbon that resists biodegradation. Biochar (which is similar to charcoal) remains in the soil for hundreds or thousands of years, sequestering the carbon while simultaneously improving soil fertility. Thousands of years ago, Amazon natives used slash-and-burn to convert trees to biochar that was incorporated into the soil to create *terra preta de indio* — rich black Earth with fertility substantially greater than that of the surrounding poor soils. Figure 22 shows that adding biochar to soil can greatly enhance its productivity. Typical addition rates are 1.5–4.0 ton/acre. At a price of $100/ton, the market size for agricultural biochar is estimated to be 43.5 million ton/yr *(41)*.

▲ **Figure 22.** Researchers from the Univ. of Tennessee, Knoxville grew soybeans on sands deposited after a flood without (left) and with (right) the application of biochar. Credit: Forbes Walker.

Carbon capture and sequestration. Carbon dioxide can be captured from stationary emission sources, such as cement kilns, ethanol plants, sugar mills, paper mills, steel mills, refineries, chemical plants, and power plants. Then, the recovered carbon dioxide can be pressurized and sequestered in the deep ocean, oil and gas wells, coal seams, or saline aquifers. Sequestering carbon dioxide from biological sources (*e.g.,* ethanol plants, sugar mills, paper mills) depletes carbon dioxide from the atmosphere and is a potentially impactful method to help reduce atmospheric carbon dioxide concentrations.

To create economic value, high-pressure carbon dioxide can be used in enhanced oil recovery. Currently, the carbon dioxide is sourced from natural formations, such as carbon dioxide wells in Colorado. In the future, it is possible that the carbon dioxide could be sourced from carbon-capture facilities along the Gulf Coast *(45)*.

Low-pressure separation (Figure 23a) employs various technologies to recover carbon dioxide from other gases (*e.g.,* nitrogen, oxygen) in a waste stream. Separation methods typically involve reversible absorption in liquids (*e.g.,* methanol, amines, ionic liquids), reversible adsorption on zeolites or metal-organic frameworks (*e.g.,* pressure, vacuum, or temperature swing), membranes, or cryogenics *(46)*.

Several combustion techniques may be employed to eliminate the need to separate combustion products (carbon dioxide, water) from inerts (nitrogen, argon). Oxy-fuel combustion performs the combustion with pure oxygen rather than air. Chemical looping combustion employs a two-reactor system — in one reactor, fuel and metal oxide form combustion products and reduced metal, and in the other reactor, the reduced metal is oxidized with air, which regenerates the metal oxide.

In the U.S., the cost of carbon capture and storage is estimated to be $57–$66/m.t. (coal) and $88–$99/m.t. (natural gas) *(47)*. Using $60/m.t. as a reference price, carbon capture and storage adds about $27/bbl oil, $3/MMBtu natural gas, $150/ton coal, and $0.018/kWh electricity (assuming natural-gas-fired combined cycle at 60% efficiency).

High-pressure separation (Figure 23b) compresses the entire waste gas stream, which increases the partial pressure of carbon dioxide and enhances its separation. In this approach, high-efficiency compressors and expanders are essential for economical operation. The conventional separation methods described above may be employed in the separation process, which is intensified because of the higher pressure.

Carbon capture and utilization. To avoid the cost of sequestration, the captured carbon dioxide can be converted to useful products. For example, reacting carbon dioxide with excess hydrogen produces synthesis gas ($CO + H_2$), which can be converted to many products (*e.g.,* methanol, hydrocarbons). Alternatively, feeding the captured carbon dioxide to algae ponds enables the production of biodiesel.

Fuels produced from captured carbon dioxide derived from combusted fossil fuels do not permanently mitigate global warming, because the combustion of the fuels releases carbon dioxide back into the atmosphere. To address this issue, some researchers are exploring the conversion of carbon dioxide to building materials or polymers that permanently sequester the carbon. However, the quantities of these materials are small relative to the volume of carbon dioxide released and therefore will have little impact on global warming. Even so, many researchers consider carbon utilization as a valuable first step toward achieving carbon neutrality. The cost of carbon utilization varies widely, from –$90/m.t. (providing a net profit) to $920/m.t., depending on the technology *(48)*.

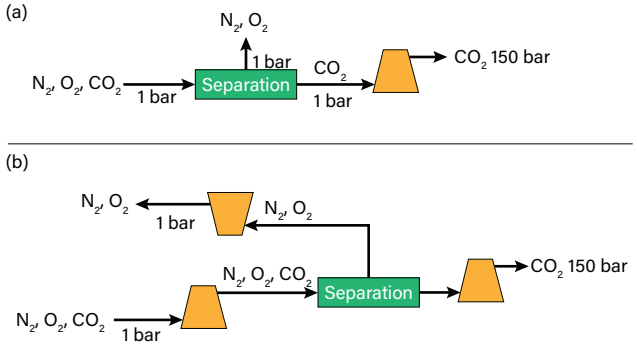

▲ **Figure 23.** Processes for capturing and sequestering carbon dioxide can use (a) low-pressure separation or (b) high-pressure separation.

Energy return on investment

Energy return on investment (EROI) is the output energy produced divided by the input energy invested to produce the energy. Clearly, for an energy technology to be viable, the EROI must be significantly greater than 1.0. Table 2 *(49, 50)* compares the EROI of various energy technologies.

Among fossil fuels, coal has the highest EROI (46)

Table 2. Energy return on investment (EROI) must be significantly greater than 1 for a technology to be viable.

Energy Source	EROI
Fossil Fuels *(49)*	
Coal	46
Oil and gas, non-U.S.	20
U.S. oil and gas	11
Shale oil	7
Tar sands	4
Carbon-Neutral Electricity *(49)*	
Hydro	84
Wind	18
Nuclear	14
Photovoltaic solar	10
Geothermal	9
Biofuels *(50)*	
Lignocellulose — carboxylate platform	19
Lignocellulose — sugar platform	15
Lignocellulose — gasification	15
Sugarcane ethanol	9
Biodiesel	2
Corn ethanol	1.3–3.3

followed by non-U.S. oil and gas (20). In the U.S., oil and gas have a lower EROI (11). As time passes, the EROI of fossil fuels tends to decline as the easy-to-recover resources become exhausted and the resources that are more difficult to recover must be exploited. For example, shale oil (7) and tar sands (4) have significantly lower EROI. The EROI is lower if carbon capture systems must be added.

Carbon-neutral electricity has excellent EROI. Hydro (84) has the highest EROI of any energy source. Wind (18) and nuclear (14) are higher than U.S. oil and gas (11), whereas PV solar (10) and geothermal (9) are only slightly less. The EROI is lower if energy storage systems are added.

Among biofuels, lignocellulose has the highest EROI (15–19). Brazilian sugarcane ethanol has a high EROI (9), whereas the EROIs for biodiesel (2) and corn ethanol (1.3–3.3) are very low.

Geoengineering

Geoengineering *(51)* involves purposeful large-scale intervention in the global climate.

Removal of atmospheric greenhouse gases. Trees remove carbon dioxide from the atmosphere, so planting trees would increase the sequestration of carbon in the wood. Similarly, proper management of rangelands can enhance carbon sequestration in soil *(52)*. Producing biochar from biomass sequesters carbon in the soil and enhances soil fertility. Capturing and sequestering carbon dioxide from biobased processes (*e.g.,* the production of ethanol) also removes carbon dioxide from the atmosphere.

The startup company Climeworks (climeworks.com) has developed a filter that captures carbon dioxide from the atmosphere and, when heated to 100°C, releases the carbon dioxide for utilization or sequestration.

Fertilizing oceans with iron or other limiting nutrients promotes algae growth, which sequesters carbon temporarily. A long-term concern about this approach is that the algae will die and deplete oxygen from the ocean as they decompose. This technique remains controversial.

Solar management. Painting roofs or roads with reflective colors increases albedo and mitigates warming. Spraying fine mists of seawater into the atmosphere provides nuclei that promote the formation of reflective marine clouds. Releasing sulfate aerosols into the stratosphere simulates natural volcanic processes that provide nucleation sites for reflective cloud formation; however, these aerosols destroy ozone, promote acid rain, and accelerate ocean acidification. Scattering fine white particles (*e.g.,* $CaCO_3$) into the atmosphere reflects some radiation back into space, but raises concerns about potential ozone depletion. NASA has even proposed shading the Earth with orbiting "parasols."

Although solar management has the potential to mitigate rising temperatures, it does not address ocean acidification.

Mitigating risk

The broad themes of this special issue of *CEP* are:

- Global warming and associated climate change are occurring.
- Human activities, particularly since the 1960s, are substantially responsible for climate change.
- The majority of consequences from climate change will negatively impact human civilization.
- The public, business leaders, and politicians are increasingly aware that human-caused climate change is occurring.

Climate change poses substantial risk to many traditional industries that employ chemical engineers, including the oil and gas, petrochemicals, and electricity production sectors. Business as usual is not a rational response to these risks; an appropriate response is essential. Too drastic a response may disrupt the economic engine needed to meet the challenge. Too little response will ensure that long-term consequences of climate change will negatively impact civilization.

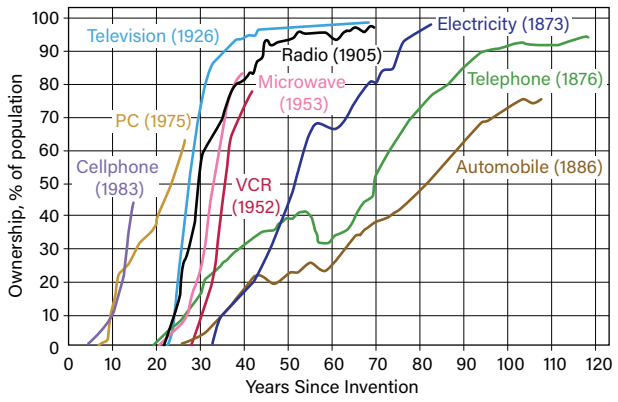

▲ **Figure 24.** The adoption of new technologies takes many years, often decades. Source: *(55)*.

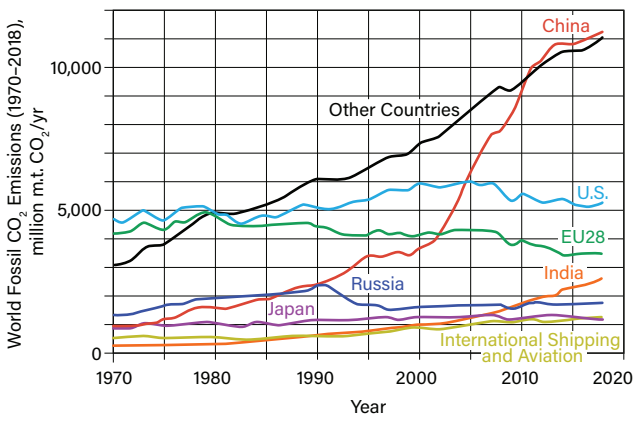

▲ **Figure 25.** Fossil carbon dioxide emissions from major emitters. Source: *(56)*.

Addressing climate change is the largest technical, economic, and political challenge that civilization faces. Technologies must function economically and reliably at a scale that can make an impact. Governments must ensure that the burdens of addressing climate change are met globally in a politically acceptable manner.

To address climate change, the International Energy Agency estimates that current global energy-sector investments must double to about $3.5 trillion per year for the next 35 years *(53)*. Although this level of investment seems daunting — and it is — it represents 4.0% of the $87.7 trillion global gross domestic product (GDP) in 2019 *(54)*. (As a reference point, the 2019 U.S. defense budget was 3.4% of U.S. GDP.) It should be noted that much of this investment will provide opportunities to engineers who will lead the restructuring of the energy economy.

The energy sector is extremely capital-intensive, so change is necessarily slow. Figure 24 *(55)* shows the adoption rate of various technologies. In all cases, the incubation period was 20–30 years. The very capital-intensive industries (electricity, telephone, automobiles) took many additional decades before full adoption was achieved.

The United Nations recommends that we limit global temperature change to 2°C above preindustrial levels, which will occur in about 2040 (Figure 32 in the previous article, on the impacts of climate change, p. 45), or about 20 years from now. Given the enormity of the lags in technology development and large-scale capital deployment, we cannot wait until then to address the problem. We must address climate change now with a sense of urgency.

In the near term, we should focus on implementing "no-regrets" technologies that make sense purely from an economic perspective. Examples include the use of energy-efficient technologies (*e.g.,* lighting, HVAC systems, and engines), the conversion of environmental wastes (*e.g.,* manure, sewage sludge, municipal solid waste) to industrial chemicals and fuels, the planting of more trees, proper management of rangelands, and the sequestration of carbon as biochar to improve soil fertility. Eventually, as the public demands solutions to climate change and appropriate laws are enacted — such as a carbon tax — then other technologies (*e.g.,* carbon capture and sequestration) can be implemented.

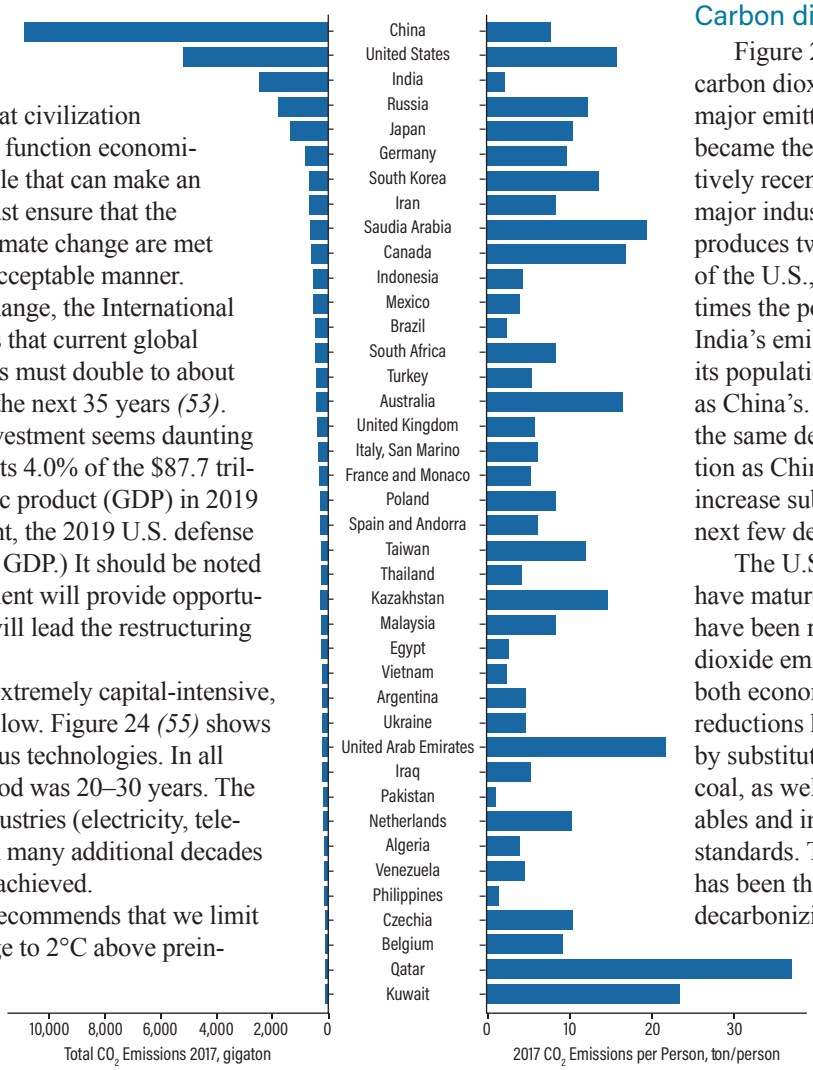

▲ **Figure 26.** Carbon dioxide emissions per country and on a per-capita basis in 2017. Source: *(57)*.

Carbon dioxide emissions

Figure 25 *(56)* shows fossil carbon dioxide emissions from major emitting nations. China became the largest emitter relatively recently as it has undergone major industrialization. China produces twice the emissions of the U.S., but also has four times the population. Currently, India's emissions are small, but its population is nearly the same as China's. Should India undergo the same degree of industrialization as China, its emissions will increase substantially within the next few decades.

The U.S. and European Union have mature economies, and both have been reducing their carbon dioxide emissions even though both economies are growing. U.S. reductions have been achieved by substituting natural gas for coal, as well as installing renewables and increasing efficiency standards. The European Union has been the most successful at decarbonizing its economy, motivated by aggressive government policies.

As represented by the black line in Figure 25, the emissions trajectory of the other countries is strongly upward. If this trend continues, carbon dioxide emissions will increase significantly into the foreseeable future.

Figure 26 *(57)* shows the total carbon emissions for the top 40 emitters, as well as the carbon dioxide emissions on a per-capita basis.

Figure 27 *(58)* shows that the carbon intensity of electricity production varies widely among the major economies. Because of their dependence on coal to produce electricity, China and India produce electricity with very high carbon intensity. In contrast, many European Union nations have low-carbon-intensity electricity because they produce electricity through hydropower (Norway) or nuclear (France). Overall, the European Union produces electricity with about half the carbon intensity of China and India. India is not reducing its carbon intensity, whereas the other three major economies are.

Article continues on next page

Progress

Although fossil fuels continue to be the dominant source of energy, some progress is being made toward reducing carbon emissions. As shown in Figure 25, European carbon dioxide emissions peaked in 1979 and have declined by 30%, and U.S. carbon dioxide emissions peaked in 2005 and have declined by 13%. The U.S. is retiring high-carbon electricity from coal and is adding low-carbon electricity from renewables and natural gas (Figure 28) *(59)*. Germany has an aggressive program to reduce carbon dioxide emissions and in 2019 produced 46.3% of its electricity from renewables *(60)*.

Since 2010, China's carbon dioxide emissions have stabilized, largely the result of efforts to increase the efficiency of its coal-fired power plants. Furthermore, China has an aggressive solar energy program. In 2008, China set a target of 2 GW from solar photovoltaics by 2020 *(61)* — however, it has already exceeded that target by 100 times *(62)*.

Figures 29 and 30 *(63)* show global investments in renewable energy. China is the largest investor, followed by Europe collectively and then the U.S. Although the size of the investments and the trends are encouraging, the current investment represents 8% of the $3.5 trillion per year required to achieve a carbon-neutral economy in 35 years *(53)*.

Closing thoughts

Our current energy infrastructure — which is based on the combustion of fossil fuels — has brought enormous prosperity. Unfortunately, staying on this path threatens our future prosperity. Because change must occur at an unprecedented scale, the transformation to a carbon-neutral economy is the greatest technical, economic, and political challenge yet faced by humankind. All engineering professions will play a role in this transformation; however, chemical engineers will play a particularly important role because fundamentally the problem originates with chemistry. CEP

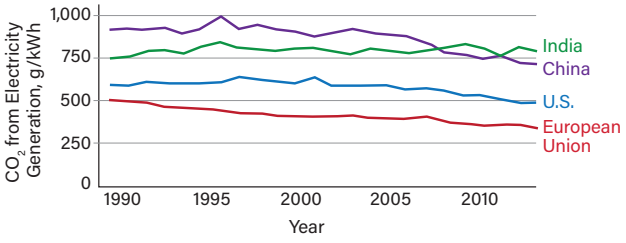

▲ **Figure 27.** Carbon intensity of electricity production varies among the major economies. Source: Created at *(58)*.

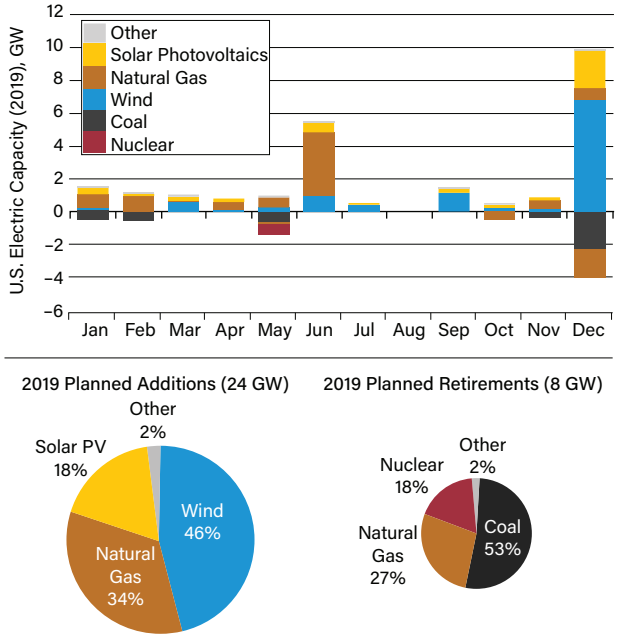

▲ **Figure 28.** The U.S. is retiring high-carbon generating plants and adding lower-carbon electricity generation. Source: *(59)*.

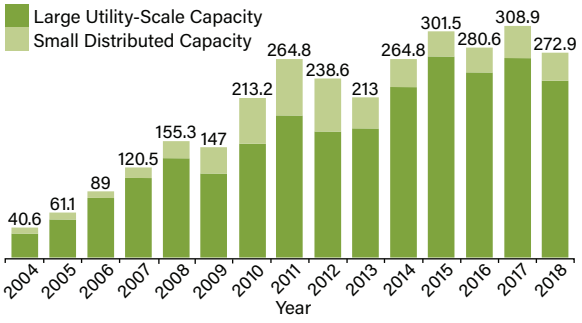

▲ **Figure 29.** Global capital investment ($ billion) in renewable energy. Source: *(63)*.

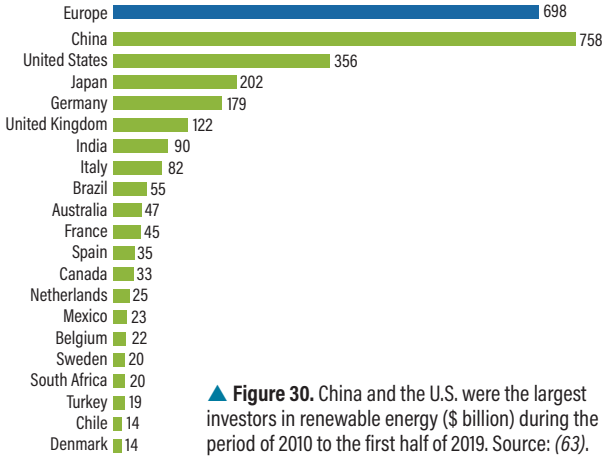

▲ **Figure 30.** China and the U.S. were the largest investors in renewable energy ($ billion) during the period of 2010 to the first half of 2019. Source: *(63)*.

Acknowledgments

The authors are grateful for the helpful suggestions provided by John Nielsen-Gammon, Regents Professor of Texas A&M Univ. and Texas State Climatologist, as well as Liz Fisher, a chemical engineer with Citizens Climate Lobby.

Literature Cited

1. **Clark, P. U., *et al.,*** "Consequences of Twenty-First-Century Policy for Multi-Millennial Climate and Sea-Level Change," *Nature Climate Change*, **6,** pp. 360–369 (Feb. 8, 2016).
2. **Corum, J.,** "A Sharp Increase in 'Sunny Day' Flooding," *New York Times,* nytimes.com/interactive/2016/09/04/science/global-warming-increases-nuisance-flooding.html (Sept. 3, 2016).
3. **Creyts, J., *et al.,*** "Reducing U.S. Greenhouse Gas Emissions: How Much at What Cost?," U.S. Greenhouse Gas Abatement Mapping Initiative, Executive Report by McKinsey & Co., mckinsey.com/business-functions/sustainability-and-resource-productivity/our-insights/reducing-us-greenhouse-gas-emissions (Dec. 2007).
4. **U.S. Energy Information Administration,** "How Much Electricity Is Used for Lighting in the United States?," Frequently Asked Questions, EIA, Washington, DC, eia.gov/tools/faqs/faq.php?id=99&t=3 (accessed Sept. 11, 2020).
5. **Esham, B. D.,** "Energy Usage for Different Types of Light Bulbs Operating at Different Light Outputs," in "Compact Fluorescent Lamp," en.wikipedia.org/wiki/Compact_fluorescent_lamp (accessed Sept. 11, 2020).
6. **Waide, P., and C. U. Brunner,** "Energy-Efficiency Policy Opportunities for Electric Motor-Driven Systems," International Energy Agency, Paris, France, iea.org/reports/energy-efficiency-policy-opportunities-for-electric-motor-driven-systems (2011).
7. **Rosberg, J.,** "Pioneering Technology Leader ABB Sets World Record Efficiency for Synchronous Motor," *ABB Conversations,* abb-conversations.com/2017/07/abb-motor-sets-world-record-in-energy-efficiency (July 12, 2017).
8. **U.S. Dept. of Energy,** "Determining Electric Motor Load and Efficiency," DOE Motor Challenge, DOE/GO-10097-517, DOE, Washington, DC, energy.gov/sites/prod/files/2014/04/f15/10097517.pdf (accessed Sept. 11, 2020).
9. U.S. Code of Federal Regulations, "Table 5 — Nominal Full-Load Efficiencies of NEMA Design A, NEMA Design B, and IEC Design N Motors (Excluding Fire Pump Electric Motors) at 60 Hz," in Title 10: Energy, Part 431 — Energy Efficiency Program for Certain Commercial and Industrial Equipment, ecfr.gov/cgi-bin/retrieveECFR?gp=&SID=15b31a3387b5986938f3520712bfa06c&mc=true&n=pt10.3.431&r=PART&ty=HTML#sp10.3.431.b (accessed Sept. 11, 2020).
10. **Bistak, S., and S. Y. Kim,** "AC Induction Motors vs. Permanent Magnet Synchronous Motors," Empowering Pumps & Equipment, empoweringpumps.com/ac-induction-motors-versus-permanent-magnet-synchronous-motors-fuji (accessed Sept. 11, 2020).
11. **U.S. Dept. of Energy,** "Premium Efficiency Motor Selection and Application Guide," DOE, Office of Energy Efficiency and Renewable Energy, Advanced Manufacturing Office, Washington, DC, DOE/GO-102014-4107, energy.gov/sites/prod/files/2014/04/f15/amo_motors_handbook_web.pdf (Feb. 2014).
12. **Jonsson, M.,** "Humidified Gas Turbines — A Review of Proposed and Implemented Cycles," *Energy,* **30** (7), pp. 1013–1078, doi: org/10.1016/j.energy.2004.08.005 (June 2005).
13. **Holtzapple, M.,** "StarRotor Engine for Military Applications," *Journal of Defense Management*, **6** (1), doi: 10.35248/2167-0374.19.142, longdom.org/open-access/starrotor-engine-for-military-applications-2167-0374-1000142.pdf (2016).
14. **GE Power,** "Breaking the Power Plant Efficiency Record … Again!," General Electric Power, ge.com/power/about/insights/articles/2018/03/nishi-nagoya-efficiency-record (Mar. 27, 2018).
15. **International Energy Agency,** "The Future of Cooling: Opportunities for Energy-Efficient Air Conditioning," IEA, Paris, France, iea.org/news/air-conditioning-use-emerges-as-one-of-the-key-drivers-of-global-electricity-demand-growth (2018).
16. **Heath, R. C.,** "Basic Ground-Water Hydrology," Water Supply Paper 2220, U.S. Geological Survey, pubs.usgs.gov/wsp/2220/report.pdf (1983).
17. **Blodgett Supply,** "Geothermal Heat Pump Tax Credits Reinstated," blodgettsupply.com/company_news_and_announcements.html?news_id=79761&year=2018&month=2&newspaper_id=74587 (accessed Sept. 11, 2020).
18. **Harris, W. B., and R. R. Davison,** "Liquid Aquifer Energy Storage Method," U.S. Patent No. 3,931,851A (1976).
19. **Lazard,** "Lazard's Levelized Cost of Energy Analysis — Version 13.0," lazard.com/media/451086/lazards-levelized-cost-of-energy-version-130-vf.pdf (2019).
20. **Fetter, S.,** "How Long Will the World's Uranium Supplies Last?," *Scientific American,* scientificamerican.com/article/how-long-will-global-uranium-deposits-last (Jan. 26, 2009).
21. **Berry, J., *et al.,*** "Bringing a Star to Earth," *Chemical Engineering Progress,* **105** (4), pp. 26–32 (Apr. 2009).
22. **National Renewable Energy Laboratory,** "United States — Land-Based and Offshore Annual Average Wind Speed at 100 m," File:Awstwspd100onoff3-1.jpg, at "List of NREL Map Files," openei.org/wiki/List_of_NREL_Map_Files (accessed Oct. 23, 2020).
23. **Sengupta, M., *et al.,*** "The National Solar Radiation Data Base (NSRDB)," Renewable and Sustainable Energy Reviews, **89,** pp. 51–60 (June 2018).
24. **Siemens,** "Fact Sheet: High-Voltage Direct Current Transmission (HVDC)," Siemens, assets.new.siemens.com/siemens/assets/api/uuid:d5c5f4ae-d9f6-49e9-b68b-85bb7ceb4f41/factsheet-hvdc-e.pdf (May 2014).
25. **U.S. Energy Information Administration,** "What is U.S. Electricity Generation by Energy Source?," Frequently Asked Questions, EIA, Washington, DC, eia.gov/tools/faqs/faq.php?id=427&t=3 (accessed Sept. 11, 2020).
26. **U.S. Energy Information Administration,** "EIA Expects U.S. Electricity Generation from Renewables to Soon Surpass Nuclear and Coal," EIA, Washington, DC, eia.gov/todayinenergy/detail.php?id=42655 (Jan. 30, 2020; accessed Sept. 11, 2020).
27. **Chen, H., *et al.,*** "Progress in Electrical Energy Storage System: A Critical Review," *Progress in Natural Science*, **19** (3), pp. 291–312 (Mar. 2009).
28. **U.S. Dept. of Energy,** "Grid Energy Storage," DOE, Washington, DC, energy.gov/sites/prod/files/2014/09/f18/Grid%20Energy%20Storage%20December%202013.pdf (Dec. 2013).
29. **Crawford, M.,** "Liquid Metal Batteries May Revolutionize Energy Storage," asme.org/topics-resources/content/liquid-metal-batteries-may-revolutionize-energy (June 14, 2017).
30. **Cahn, R. P., and E. W. Nicholson,** "Thermal Energy Storage by Means of Reversible Heat Pumping Using Industrial Waste Heat," U.S. Patent No. 4,110,987 (1978).
31. **Texas A&M Transportation Institute,** "Freight Shuttle System," tti.tamu.edu/freight-shuttle (accessed Sept. 11, 2020).

Literature Cited continues on next page

Literature Cited (continued)

32. **Kotowicz, J., *et al.,*** "Analysis of Hydrogen Production in Alkaline Electrolyzers," *Journal of Power Technologies,* **96** (3), pp. 149–156 (2016).
33. **U.S. Dept. of Energy,** "Fuel Cells," DOE, Energy Efficiency and Renewable Energy, Fuel Cell Technologies Office, Washington, DC, energy.gov/sites/prod/files/2015/11/f27/fcto_fuel_cells_fact_sheet.pdf (accessed Sept. 11, 2020).
34. **Thomas, G., and J. Keller,** "Hydrogen Storage — Overview," Sandia National Labortories, https://www1.eere.energy.gov/hydrogenandfuelcells/pdfs/bulk_hydrogen_stor_pres_sandia.pdf (May 13, 2003).
35. **DiMascio, F., *et al.,*** "Extraction of Carbon Dioxide and Hydrogen from Seawater and Hydrocarbon Production Therefrom," U.S. Patent Application US20160215403 A1 (July 28, 2016).
36. **Lackner, K. S., *et al.,*** "Closing the Carbon Cycle: Liquid Fuels from Air, Water and Sunshine" Columbia Univ., New York, NY wordpress.ei.columbia.edu/lenfest/files/2012/11/SunlightToFuels_WhitePaper.pdf (accessed Sept. 11, 2020).
37. **National Corn Growers Association,** "World of Corn 2020," worldofcorn.com/# (accessed Sept. 11, 2020).
38. **U.S. Dept. of Energy,** "2016 Billion-Ton Report: Advancing Domestic Resources for a Thriving Bioeconomy," Vol. I, DOE, Washington, DC, energy.gov/sites/prod/files/2016/12/f34/2016_billion_ton_report_12.2.16_0.pdf (July 2016).
39. **Brown, R. C., *et al.,*** "Producing Biofuels via the Thermochemical Platform," *Chemical Engineering Progress*, **111** (3), pp. 41–44 (Mar. 2015).
40. **Wyman, C. E., *et al.,*** "Producing Biofuels via the Sugar Platform," *Chemical Engineering Progress*, **111** (3), pp. 45–51 (Mar. 2015).
41. **Holtzapple, M., *et al.,*** "Producing Biofuels via the Carboxylate Platform," *Chemical Engineering Progress*, **111** (3), pp. 52–57 (Mar. 2015).
42. **U.S. Energy Information Association,** "Short-Term Energy Outlook: U.S. Liquid Fuels," EIA, Washington, DC, eia.gov/outlooks/steo/report/us_oil.php (accessed Sept. 11, 2020).
43. **Isa, K. M., *et al.,*** "Hydrogen Donor Solvents in Liquefaction of Biomass: A Review," *Renewab e and Sustainab e Energy Reviews*, **81** (1), pp. 1259–1268, doi: org/10.1016/j.rser.2017.04.006 (2018).
44. **Zia, Q., *et al.,*** "Direct Hydrodeoxygenation of Raw Woody Biomass into Liquid Alkanes," *Nature Communications*, **7,** Article Number: 11162, doi: 10.1038/ncomms11162 (Mar. 30, 2016).
45. **Blum, J.,** "Oil Sector Climate Initiatives Target Texas Coast and Gulf of Mexico," *Houston Chronicle,* chron.com/business/energy/article/Oil-sector-climate-initiatives-target-Texas-coast-14463529.php (Sept. 24, 2019).
46. **Metz, B., *et al.,*** "Carbon Dioxide Capture and Storage," Special Report Prepared by Working Group III of the Intergovernmental Panel on Climate Change," IPCC, Cambridge Univ. Press, Cambridge, U.K., ipcc.ch/report/carbon-dioxide-capture-and-storage (2005).
47. **Schmelz, W. J., *et al.,*** "Total Cost of Carbon Capture and Storage Implemented at a Regional Scale: Northeastern and Midwestern United States," *Interface Focus,* **10** (5), https://doi.org/10.1098/rsfs.2019.0065 (Aug. 14, 2020).
48. **Adlen, E., and C. Hepburn,** "10 Carbon Capture Methods Compared: Costs, Scalability, Permanence, Cleanness," *Energy Post,* energypost.eu/10-carbon-capture-methods-compared-costs-scalability-permanence-cleanness (Nov. 11, 2019).
49. **Hall, C. A. S., *et al.,*** "EROI of Different Fuels and the Implications for Society," *Energy Policy*, **64,** pp. 141–152 (Jan. 2014).
50. **Granda, C. B., *et al.,*** "Sustainable Liquid Biofuels and Their Environmental Impact," *Environmental Progress*, **26** (3), pp. 233–250 (2007).
51. "Climate Engineering," en.wikipedia.org/wiki/Climate_engineering (accessed Sept. 12, 2020).
52. **Flynn, A. J., *et al.,*** "Soil Carbon Sequestration in United States Rangelands," Chapter IV in Grassland Carbon Sequestration: Management, Policy, and Economics," Proceedings of the Workshop on the Role of Grassland Carbon Sequestration in the Mitigation of Climate Change, Rome, Italy, fao.org/docrep/013/i1880e/i1880e03.pdf (Apr. 2009).
53. **International Energy Agency and International Renewable Energy Agency,** "Perspectives for the Energy Transition: Investment Needs for a Low-Carbon Energy System, irena.org/publications/2017/Mar/Perspectives-for-the-energy-transition-Investment-needs-for-a-low-carbon-energy-system (2017).
54. **World Bank,** "GDP (Current US$)," data.worldbank.org/indicator/NY.GDP.MKTP.CD (accessed Sept. 12, 2020).
55. **Brimelow, P.,** "The Silent Boom," *Forb s,* pp. 170–171 (July 7, 1997).
56. **Tomastvivlaren,** "World Fossil Carbon Dioxide Emissions Six Top Countries and Confederations," en.wikipedia.org/wiki/List_of_countries_by_carbon_dioxide_emissions#/media/File:World_fossil_carbon_dioxide_emissions_six_top_countries_and_confederations.png, Creative Commons Attribution-ShareAlike 4.0 International (CC BY-SA 4.0) (accessed Sept. 12, 2020).
57. **Mgcontr,** "Total CO_2 Emissions by Country in 2017 vs. per capita Emissions (Top 40 Countries)," en.wikipedia.org/wiki/List_of_countries_by_carbon_dioxide_emissions#/media/File:Total_CO2_emissions_by_country_in_2017_vs_per_capita_emissions_(top_40_countries).svg, in "List of Countries by Carbon Dioxide Emissions," en.wikipedia.org/wiki/List_of_countries_by_carbon_dioxide_emissions, Creative Commons Attribution-ShareAlike 4.0 International (CC BY-SA 4.0) (accessed Sept. 12, 2020).
58. **Organisation for Economic Co-operation and Development,** "Compare Your Country," compareyourcountry.org/climate-policies?cr=oecd&lg=en&page=2 (accessed Sept. 11, 2020).
59. **U.S. Energy Information Administration,** "New Electric Generating Capacity in 2019 Will Come from Renewables and Natural Gas," eia.gov/todayinenergy/detail.php?id=37952 (Jan. 10, 2019; accessed Sept. 12, 2020).
60. "Renewable Energy in Germany," en.wikipedia.org/wiki/Renewable_energy_in_Germany (accessed Sept. 11, 2020).
61. **Tollefson, J.,** "Can the World Kick its Fossil-Fuel Addiction Fast Enough?," *Nature,* **556,** pp. 422–425 (2018).
62. **Hove, A.,** "Current Direction for Renewable Energy in China," Oxford Institute for Energy Studies, Oxford, U.K., oxfordenergy.org/wpcms/wp-content/uploads/2020/06/Current-direction-for-renewable-energy-in-China.pdf (June 2020).
63. **Frankfurt School of Finance & Management,** "Global Trends in Renewable Energy Investment," wedocs.unep.org/bitstream/handle/20.500.11822/29752/GTR2019.pdf (2019; accessed Sept. 12, 2020).

AIChE Updates its Climate Change Policy Statement

Phil Westmoreland ▪ Past Chair, PAIC
Mary Ellen Ternes ▪ Chair, PAIC Climate Change Task Force

Our world is being affected by climate change. As the changes become more significant, we will have to adapt. Chemical engineers are in a special position to explain what is happening with our climate and to create and guide technological responses. That is the essence of AIChE's updated Climate Change Policy (aiche.org/aiche_climate).

Climate change is likely to disrupt manufacturing, agriculture, supply chains, biodiversity, coastlines, cities, and entire populations, and it is strongly influenced by anthropogenic emissions of greenhouse gases like CO_2 and methane. That conclusion was already accepted by many people when AIChE's Board of Directors set our first Climate Change Policy in 2014, yet there was not a sufficient consensus among our members about the predicted changes. Choosing to act in areas where we did agree, and in the context of the former U.S. policy and developing regulations to mitigate climate change leading up to the Paris Agreement, the 2014 policy focused on AIChE's commitment to be a forum for members about climate change, a resource for policy makers, and a source of reliable information for the public.

That policy was suitable until the changes in federal climate policy described in *CEP*'s January 2017 ChE in Context column, "Adjusting to Policy Changes: Full Reversal in Washington, DC." The AIChE Board then charged the Public Affairs and Information Committee (PAIC) to lead an AIChE-wide assessment of the "consensus science" that there is climate change occurring because of human activities. As described in the October 2018 ChE in Context column, the PAIC's Climate Change Task Force invited AIChE members to critique the U.S. Environmental Protection Agency's (EPA's) Endangerment and Cause or Contribute Findings of 2009 (the "Endangerment Findings"). That assessment's technical foundations were the data and climate modeling by U.S. agencies and the Intergovernmental Panel on Climate Change (IPCC). Its legal foundations were the U.S. Clean Air Act (CAA), the EPA's statutory scope of administrative discretion, and the 2007 Supreme Court case, Massachusetts v. EPA.

The PAIC received AIChE members' input through the ChEnected blog and AIChE Engage (engage.aiche.org). Members took up the challenge to identify and test criticisms of the Endangerment Findings' assumptions, models, and conclusions. The resulting analyses are posted at www.aiche.org/paic-climate-discussions. Several flaws and uncertainties were identified, but none changed the substantive conclusions about climate change, ultimately supporting the consensus science.

Based on this participation, the AIChE Board of Directors approved an updated policy in March 2019, with three new parts. First, AIChE recognizes our collective and individual responsibilities to society as professionals:

As a professional society, AIChE must be a source of sound information and analysis for its members, for government policy makers, and for the public. AIChE is also committed to helping its members and stakeholders create and maintain resilient, sustainable processes, products, and facilities.

Second, AIChE's policy now explicitly affirms the consensus about climate change based on the member review and analysis:

Scientific analysis finds that non-natural climate change is occurring and has been strongly influenced by human-caused releases of greenhouse gases. Using an open, moderated process in 2017–18, AIChE members were provided an opportunity to critique the current consensus climate science as captured in the U.S. EPA's Endangerment Findings. After listening to all points of view and challenges, assessing the climate science based on documented evidence, their analysis supported the credibility of this science.

Third, the policy draws from the prior two items to state our professional responsibilities as chemical engineers toward climate change:

Adverse climate change poses threats to all of us, both individually and as a society. These threats fall squarely in the realm of the chemical engineer, who is well-positioned to assess the issues and develop solutions through well-founded engineering and economic approaches.

Moving ahead, AIChE will tackle the tough questions about acting on these visions. How can we best mitigate greenhouse gas emissions? How can we, as chemical engineers, help engineer solutions to grand societal challenges with climate change as a factor? How can we adapt our manufacturing sites and ports for sea-level rise and extreme weather events to mitigate risk? More broadly, how do we build sustainability and resilience into our resources, processes, products, and supply chains, and at what costs? How do we help shape the multidisciplinary actions that are needed, both technical and nontechnical?

If you want to help answer and act on those questions, please join the work of AIChE's new Climate Solutions Community (aiche.org/climate-solutions), which is discussed in the article on the next page.

Excerpted from *CEP*, The ChE in Context, July 2019, p. 40.

AIChE's Climate Solutions Community

Climate change is one of the greatest challenges society faces today. It is a complex global problem with multiple dimensions — social, economic, political, and ethical. Responding to climate change will require multidisciplinary efforts involving all fields of engineering and science working with businesses, governments, academia, and the public.

It is important that chemical engineers and AIChE engage in dialogue across traditional boundaries and be open to understanding risks and creative new solutions. Toward that end, in October 2018, the AIChE Board of Directors approved the formation of The Climate Solutions Community (TCSC) within the Institute for Sustainability.

Tom Rehm, a process safety specialist and past chair of the South Texas Local Section, spearheaded the formation of the community. In discussing TCSC, Rehm noted that chemical engineers' versatility and formidable problem-solving skills make them well-suited to help address many of the world's foremost challenges, including climate change. "It is incumbent on AIChE and its member stakeholders to apply their unique insights and technical abilities to identify viable solutions to mitigate, adapt, and become resilient to the effects of climate change," he said.

Engineers and industrial scientists from across disciplines are invited to participate in the Climate Solutions Community. Its goal is to lead efforts to develop a portfolio of technical and government policy solutions to address both industrial and societal challenges.

"Time is of the essence. We encourage you to join this multidisciplinary community to solve this pressing global problem," Rehm says.

For information and to join, visit aiche.org/community/sites/climate-solutions-community.

TCSC Vision

To promote technically feasible and economically viable solutions that mitigate and/or adapt to climate change.

TCSC Mission

To collaborate with applicable fields of engineering and science to develop solutions.

TCSC Objectives

- To engage chemical engineers to improve their versatility and formidable problem-solving skills with respect to climate change, the world's foremost technical challenge.
- To apply chemical engineers' unique insights and technical abilities to identify viable solutions that address climate change through mitigation, adaptation, and resilience.
- To develop partnerships with other scientific and engineering entities to develop the multidisciplinary responses required to address climate change.
- To develop a portfolio of technical and government policy solutions necessary to address both industrial and societal challenges resulting from climate change.

The Climate Solutions Community
An AIChE Initiative

THE PEOPLE BEHIND THE PAGES

MARK HOLTZAPPLE, PhD,

is a professor in the Artie McFerrin Dept. of Chemical Engineering at Texas A&M Univ. (College Station, TX; Phone: 979-845-9708; Email: m-holtzapple@tamu.edu; video portfolio: https://tinyurl.com/ycymdey2). He received his chemical engineering degrees from Cornell Univ. (BS, 1978) and the Univ. of Pennsylvania (PhD, 1981). After his formal education, he served as a captain in the U.S. Army, working at the Natick R&D Center to develop a miniature air conditioner for soldiers wearing chemical protective clothing. He joined the faculty of Texas A&M Univ. in 1986. His research focuses on sustainability, including the conversion of waste biomass to fuels, chemicals, and animal feed; high-efficiency engines and air conditioners; conversion of waste heat to electricity; high-torque electric motors; and water desalination. He has received many awards for teaching and research, including the Presidential Green Chemistry Challenge Award from the president and vice president of the U.S.

FARUQUE HASAN, PhD,

coauthor of Part 5, "Solutions to Climate Change," is an associate professor and the Kim Tompkins McDivitt '88 and Phillip McDivitt '87 Faculty Fellow in the Artie McFerrin Dept. of Chemical Engineering at Texas A&M Univ. (College Station, TX; Phone: 979-862-1449; Email: hasan@tamu.edu; Website: http://people.tamu.edu/~hasan.) He received a BSc in chemical engineering from Bangladesh Univ. of Engineering and Technology in 2005, a PhD from the National Univ. of Singapore in 2010, and postdoctoral training at Princeton Univ. before joining Texas A&M in 2014. He leads a research group that is now being recognized for developing fundamental process systems engineering and optimization methods for the design, intensification, and analysis of sustainable chemical processes. He has received several awards, including the NSF CAREER award, the *I&EC Research* 2019 Class of Influential Researchers Award, and the World Technology Network Award in the Environmental Category.

PHILLIP R. WESTMORELAND, PhD,

coauthor of "AIChE Updates its Climate Change Policy Statement," is a professor of chemical and biomolecular engineering at North Carolina State Univ. He holds chemical engineering degrees from North Carolina State Univ. (BS), Louisiana State Univ. (MS), and the Massachusetts Institute of Technology (PhD). He was the 2013 president of AIChE, was the founding chair of the Computational Molecular Science and Engineering Forum, is a Fellow of AIChE, and is a trustee and past president of CACHE (Computer Aids for Chemical Engineering Education). He received the 2017 AIChE Institute Award for Excellence in Industrial Gases Technology for his experimental and computational achievements in the chemistry of fire suppressants and air-pollutant prevention. He also received AIChE's 2007 George Lappin Award and shared the 2009 AIChE Gary Leach Award.

MARY ELLEN TERNES, ESQ.,

coauthor of "AIChE Updates its Climate Change Policy Statement,"is a partner in the Oklahoma City office of D.C.-based Earth & Water Law, LLC, serving industrial, energy, and municipal clients on regulatory and enforcement defense strategies, environmental remediation, litigation, and more. She holds a BE (ChE) from Vanderbilt Univ. and a JD from the Univ. of Arkansas Little Rock School of Law and is a Fellow and Life Member of AIChE. She received the 2020 Environmental Div. Dr. Peter B. Lederman Service Award, chaired the Public Affairs and Information Committee's (PAIC) Legal Developments Subcommittee, and led the Climate Change Task Force and Policy Review Project. She is also a Fellow and president of the American College of Environmental Lawyers and past chair of the Climate Change, Sustainable Development, and Ecosystems Committee of the American Bar Association.

MEET THE EDITORS

The editorial staff of *CEP* is proud to present this special digital issue, Thinking About Climate.

CYNTHIA MASCONE
Editor-in-Chief

EMILY PETRUZZELLI
Managing Editor

ELIZABETH PAVONE
Senior Editor

GORDON ELLIS
Assistant Editor

EVAN PFAB
Assistant Editor

NIDHI SHARMA
Assistant Editor, News

KAREN SIMPSON
Production Manager

DEBBIE SLOTT
Art Director